Molecular Characterisation of *sneezy*, a Notochord Mutation

A Thesis submitted to the University of London

For the degree of Doctor of Philosophy

By Pedro João de Carvalho e Saraiva Coutinho

N.I.M.R./ University College London

2001

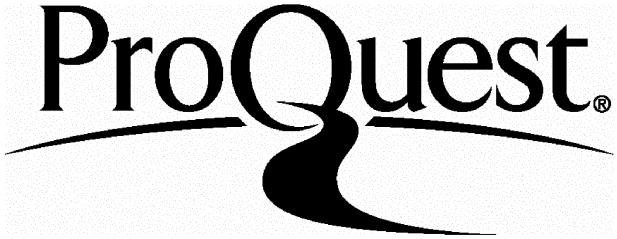

To Ana, Inês and "little one" with love.

Acknowledgments

I thank my supervisor, Derek Stemple, for giving me the opportunity to work on this project. I am very grateful to Derek for his support and good advice. I would also like to specially thank Leonor Saúde, Isabel Campos, Mike Parsons, Carl-Philipp Heisenberg, Liz Hirst, Steve Pollard, Ben Feldman and Ana Coutinho. Leonor collaborated with me on the ADMP project and helped me with the transplants. Liz helped with the electron microscopy. Isabel helped me with the *copa in situs*. Mike collaborated with me on the *sleepy* project and helped me with the *sneezy* mapping. C-P collaborated with me on the *masterblind* project and read the introduction to this thesis. Steve read the thesis. Ben read the discussion to this thesis. I thank Ana for all her patience and for reading my thesis.

I would like to thank all the members of the Developmental Biology Division, in particular Jackie Smith for being so helpful and making our work much easier.

I thank the Fundação para a Ciência e Tecnologia for funding me and supporting my decision of changing from Mathematics to Developmental Biology.

Finally, I would like to thank all my family and in particular my wife, Ana, my father, António and my daughter Inês for their love and support.

Abstract

Mutant alleles of *sneezy* were identified during the first Tübingen and Boston large-scale systematic screens for recessive-zygotic mutations affecting embryogenesis in zebrafish. It affects differentiation of the notochord, pigmentation, fin formation and leads to widespread degeneration of the embryo in the mid hatching period at about 60 hpf.

Using a positional cloning approach, I have identified *coatomer subunit α (copa)* as the gene mutated in *sneezy*. The coatomer complex, together with the small GTPase ARF1, constitutes the protein coat of COPI vesicles, an essential component of the early secretory pathway.

In zebrafish, *copa* is expressed maternally and during the first 24 hpf shows ubiquitous zygotic expression. This maternal wild-type component is responsible for absence of defects prior to ± 24 hpf. By tissue transplantation, I show that α-COP function is required within the shield derivatives for normal notochord differentiation. In addition, we find that α-COP activity is required within the neural tube for normal melanophore development.

At 24 hpf *sneezy* mutant embryos display an abnormal maintenance of early chordamesoderm marker gene expression. This correlates with a failure of the chordamesoderm to differentiate into notochord. EM studies of notochord cells in *sneezy* mutants and wild-type siblings show that the early secretory pathway is blocked in *sneezy*. This results in disruption of formation or maintenance of the perinotochordal basal lamina. This general block in transport, which may affect the elaboration of integral membrane receptors, leads to a failure in notochord differentiation and subsequent apoptosis. In addition, abnormally high levels of apoptosis occur in the floorplate and posterior dorsal neural tube. Apoptosis in the posterior dorsal neural tube correlates with the lack of pigmentation, in the posterior trunk of mutant embryos. At more anterior levels, where melanophores may survive, the failure to become pigmented probably arises from a failure of the Golgi apparatus, which normally generates the melanosomes.

Table of contents

List of figures

List of tables

Chapter 1 General Introduction

1.1 Introduction

The notochord is a rod-like skeletal element of chordate embryos located at the midline just ventral to the neural tube. The notochord is derived from the dorsal organiser, an embryonic structure that acts as a source of signals that pattern the vertebrate axis. In teleost fish the dorsal organiser is called the embryonic shield (Oppenheimer, 1936).

During gastrulation, the cells of the embryonic shield converge, involute and extend anteriorly, narrowing along the dorsal midline of the hypoblast to form the chordamesoderm (the notochord precursor). The chordamesoderm can be identified from the onset of gastrulation initially by the expression of molecular markers such as *floating head* (Talbot et al., 1995), *shh* (Krauss et al., 1993), *α1-collagen Type II (col2a1)* (Yan et al., 1995) and *Brachyury* (*no tail* in zebrafish) (Schulte-Merker et al., 1994). At later stages the chordamesoderm is easily identified by morphology.

During the segmentation period, the chordamesoderm differentiates into the notochord ultimately to comprise large vacuolated cells surrounded by a basal lamina sheath. After differentiation, the expression of *shh, α1-collagen Type II (col2a1)* or *Brachyury* (*no tail* in zebrafish) in the notochord is down-regulated and virtually undetectable by *in situ* hybridisation. In higher vertebrates, later in development, the notochord becomes integrated into structures of the adult spinal column. Within the forming vertebrae, notochord cells are replaced by bone. Between the vertebrae notochord cells become part of the tissue at the centre of the intervertebral discs, called the nucleus pulposus.

During development the notochord plays two important roles. First, the notochord is responsible for patterning adjacent tissues such as the neural tube and somites. Second, the notochord serves as the primary skeletal element of vertebrates such as zebrafish. In this role the function of the extracellular sheath and vacuoles becomes apparent. The sheath provides a mechanical barrier against which the vacuolated cells can exert turgor pressure. This provides the notochord with rigidity while maintaining flexibility. Without a mechanically sound notochord young fish cannot feed or escape predation.

The notochord is essential to early development of vertebrates. In addition the notochord provides a model system to study organogenesis. The notochord is composed of only one cell type, which greatly simplifies some problems. Importantly the notochord undergoes all of the key developmental processes such as specification, proliferation, differentiation, extracellular matrix formation and morphogenesis. These features of the notochord combined with the genetics and embryology of zebrafish provide a rich set of tools to study organogenesis.

Two zebrafish large-scale systematic genetic screens identified a large number of mutations affecting notochord development (Driever et al., 1996; Haffter et al., 1996) (Fig.1.1). This set of mutations has been partitioned into subsets of mutations affecting specific stages of notochord development, including: specification of the chordamesoderm; notochord differentiation and notochord morphology.

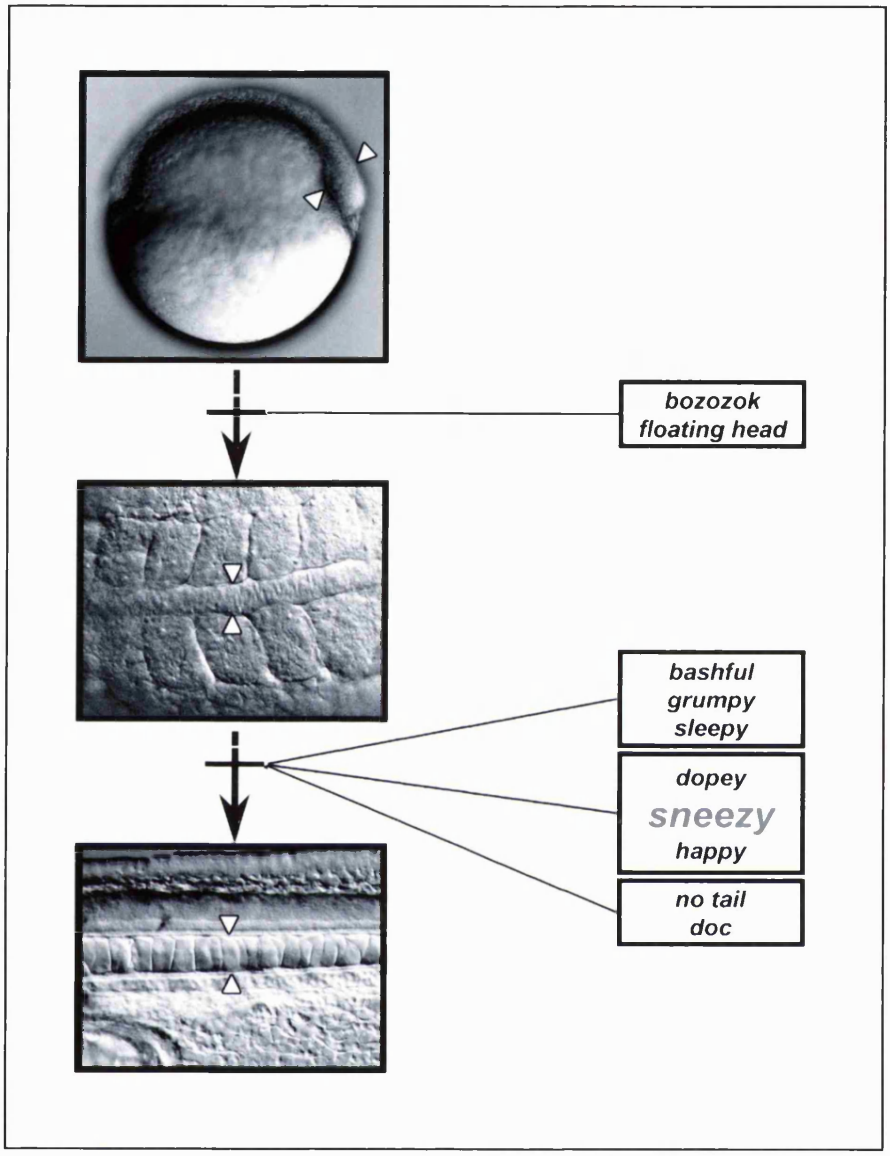

Figure 1.1. Zebrafish mutations help to dissect notochord development. While some notochord mutations like *floating head* or *bozozok* affect the specification of the chordamesoderm, others like *sneezy*, *dopey* or *happy* affect the differentiation of the chordamesoderm into notochord.

To better understand the mechanisms involved in notochord development, we were interested in identifying the genes whose functions are disrupted in the notochord mutations and in further characterising their notochord defects. Since very little is known about the molecular mechanisms of notochord differentiation, I decided to focus my studies on the differentiation mutants, in particular on the process of differentiation of the notochord in the mutation *sneezy*.

At around 24 hpf, a wave of differentiation starts with the rostral-most notochord cells and moves caudally. As notochord cells differentiate, expression genes such as *no tail*, *collagen2α1* and *sonic hedgegog* are down regulated in the notochord. Interestingly, all known notochordal genes expressed prior to differentiation follow this pattern.

Prior to the differentiation event, *sneezy* mutant embryos do not exhibit any defects. At 24 hpf, while wild-type sibling notochord cells become vacuolated, *sneezy* mutant notochord cells fail to vacuolate properly. Although some cells acquire a large vacuole, the dimensions of these vacuoles are variable and always smaller than in wild-type notochord cells. In addition, genes expressed in the notochord prior to differentiation continue to be expressed at 32 hpf in *sneezy* mutant notochords, while their expression has disappeared from the notochord of wild-type siblings (Fig.3.1). The maintenance of expression of undifferentiated notochord-specific genes and the morphology of the *sneezy* notochord cells are indications that it has failed to differentiate properly. From 24 hpf onward *sneezy* embryos are also shorter than wild-type siblings and develop an abnormal body shape (the body bends ventrally). At later stages there is severe reduction in pigmentation (anterior to the trunk a few melanocytes are visible) and absence of developing fins. Finally *sneezy* mutant embryos die during the 3 day post

fertilisation (dpf). Prior to death and beginning at 48 hpf, there is generalised degeneration.

All of the notochord differentiation mutations lead to a reduction in overall body length and fail to form properly vacuolated notochord cells. Other phenotypes allow a distinction between two classes. One class comprises *sleepy*, *grumpy* and *bashful* mutants that also display brain defects. Another class of notochord differentiation mutations consists of *sneezy*, *dopey*, *happy* and *mikry*. Complementation tests have shown that *sneezy*, *dopey* and *happy* (Stemple et al., 1996) and *sneezy*, *dopey* and *mikry* (Odenthal et al., 1996) encode distinct genes, but complementation tests between *happy* and *mikry* have not been performed, so it is possible that they represent alleles of the same gene.

Of all the notochord mutations affecting notochord differentiation, for only five mutations has the gene disrupted been identified, *no tail*, *sleepy*, *grumpy*, *bashful* and now *sneezy*. The *no tail* gene is a zebrafish *brachyury* homologue (Schulte-Merker et al., 1994), but its role in notochord differentiation is still unknown. The *bashful*, *grumpy* and *sleepy* genes encode the laminin chains $\alpha 1$, $\beta 1$ and $\gamma 1$, respectively (M. Parsons, S.Pollard, D.Stemple; in preparation). Laminin-1 is the major component of the perinotochordal basal lamina. In this thesis I present data demonstrating that the *sneezy* gene encodes the α subunit of the zebrafish coatomer complex and that the *sneezy* gene product is essential for proper formation of the perinotochordal sheath and notochord differentiation. In the remainder of this chapter I will discuss notochord development, the genomic tools I used to clone *sneezy*, and finally some details of the early secretory pathway.

1.2 The role of the notochord in development

1.2.1 Dorsoventral and mediolateral patterning by the notochord

1.2.1.1 Patterning the neural tube

The notochord produces signals that control differentiation of ventral fates in the neural tube, in particular the notochord is thought to induce formation of the floorplate. The floorplate is a structure made up of a small group of cells, located at the ventral midline of the neural tube, just dorsal to the notochord. There are two views about the role of the notochord in floorplate formation. One view holds that secretion of the protein Sonic hedgehog (Shh) from the notochord, in a cell contact-dependent way, induces floorplate differentiation (Placzek et al., 2000). In support of this model, mice that lack *Shh* do not develop a floorplate even in the presence of the notochord (although there is not a complete notochord) (Chiang et al., 1996; Ding et al., 1998; Matise et al., 1998), furthermore, removal of a portion of the notochord from chicken embryos results in absence of differentiated floorplate in the overlying regions of the neural tube (Placzek et al., 1990; van Straaten and Hekking, 1991; Yamada et al., 1991). In addition, grafts of notochord or floorplate lateral to the neural tube (and in contact) can induce ectopic floorplate structures (Placzek et al., 1990; Placzek et al., 1991; Pourquie et al., 1993; van Straaten et al., 1988; Yamada et al., 1991). Moreover, it has been demonstrated that caudal midline neural tube cells transiently express motor neuron markers (Placzek et al., 2000; Ruiz i Altaba, 1996), which suggest that prospective floor plate cells are not induced until signals from the notochord are seen. Finally, fate mapping studies in avians

have shown that some cells which contribute to the floorplate are not derived from the node (Fraser et al., 1990; Schoenwolf et al., 1989).

The second model, based on chicken and zebrafish studies, holds that floorplate differentiation begins in the organiser and that the notochord's function is to maintain the floorplate in a differentiated state. The arguments supporting this model are several as well. The zebrafish *floating head* mutants lack a notochord but still develop some floorplate cells (Halpern et al., 1997; Schulte-Merker et al., 1994; Strahle et al., 1996; Talbot et al., 1995), while *cyclops* and *one-eyed pinhead* mutants have a notochord but the floorplate is almost absent (Rebagliati et al., 1998; Sampath et al., 1998; Strahle et al., 1997; Zhang et al., 1998). Furthermore, perturbations of *delta A* (*dlA*) have consequences on the relationship between the numbers of floorplate cells and notochord cells (Appel et al., 1999; Le Douarin and Halpern, 2000). Overexpression of *dlA* leads to an increase in notochord cell numbers and a decrease of floorplate cell numbers. Reciprocally, mutation or misexpression of a dominant negative construct leads to the opposite phenomenon (Appel et al., 1999). In chicken embryos, there are reports that ablation of a portion of the notochord does not result in absence of differentiated floorplate in the overlying regions of the neural tube and experiments in which a quail Hensen's node is isotopically grafted and later ablated gave identical results (Le Douarin and Halpern, 2000; Teillet et al., 1998). The striking differences between these results and the results from other groups may be due to technical differences or to errors of interpretation. Another possible explanation for these divergent models is that the mechanisms of floorplate differentiation may be different between amniotes and teleosts. The floorplate of zebrafish embryos has two distinct cell populations, in contrast to what is known for other vertebrates. The induction of the medial population does not require

shh like the lateral population, instead appears to be dependent on nodal signalling (Brand et al., 1996; Odenthal et al., 2000; Schauerte et al., 1998; Sirotkin et al., 2000).

The notochord, in conjunction with the floorplate is also responsible for the induction of interneurons, motoneurons and oligodendrocytes in the spinal cord, via secretion of Shh (Beattie et al., 1997; Briscoe and Ericson, 1999; Ericson et al., 1997; Maier and Miller, 1997; Poncet et al., 1996; Pringle et al., 1996). Distinct concentration thresholds give rise to different types of neurons. The floorplate also has a chemotropic function in development. It directs the axonal trajectories of the commissural interneurons (by attraction) and of trochlear motor axons, that grow dorsally away from the floor plate *in vivo* (by repulsion). A key molecule involved in this role of the floorplate is Netrin-1 (Colamarino and Tessier-Lavigne, 1995; Colamarino and Tessier-Lavigne, 1995). In addition to inducing the differentiation of ventral fates, the notochord also supresses dorsal fates in the neuroectoderm (Bovolenta and Dodd, 1991; Goulding et al., 1993).

1.2.1.2 Patterning the somites

Tissues patterned by the notochord, such as the neuroectoderm, are involved in the patterning of the somites in conjunction with the notochord. Thus the notochord acts directly and also indirectly in the patterning of the somites.

After somitogenesis, each somite is a sphere of epithelial cells, enclosing some mesenchymal remnants in the somitocoel (Christ and Ordahl, 1995; Stickney et al., 2000). In amniotes, cells of the ventral half of the epithelial somite become mesenchymal and together with somitocoel cells give rise to the mesenchymal sclerotome (Stockdale et al., 2000). The sclerotome contains precursor cells for the axial skeleton and ribs (Christ and Wilting, 1992; Huang et al., 2000; Olivera-Martinez et al.,

2000). The dorsal half of the somite remains epithelial and forms the dermomyotome. The lateral dermomyotome contains precursor cells for limb muscle, muscle of the ventral body wall and dermis (Dietrich et al., 1998). These types of muscle are called the hypaxial musculature. The medial dermomyotome contains precursor cells for back and intercostal muscles, i.e., the epaxial musculature (Denetclaw et al., 1997). The principal differences between amniotes and teleosts are anatomical. Whilst in amniotes the sclerotome is adjacent to the notochord, in teleosts, it is the myotome. The other two major differences are that there has been no report of dermatome in teleosts and that teleosts somites are predominantly myotome, instead of sclerotome (Stockdale et al., 2000).

The induction and maintenance of the sclerotome requires signals from either the notochord or the floorplate, as shown in mouse notochord mutants (Brand-Saberi et al., 1993; Goulding et al., 1994; Pourquie et al., 1993), ablation and heterotopic grafting experiments in chick embryos (Brand-Saberi et al., 1993; Goulding et al., 1994; Pourquie et al., 1993) and coculture experiments (Fan and Tessier-Lavigne, 1994). In amniotes, Hedgehog from the axial structures (including the notochord) seems to play a key role in the induction of the sclerotome (Dockter, 2000). In zebrafish, there is some evidence that Hedgehog may play a similar role. Distinct concentration thresholds of Hedgehog signalling give rise to distinct numbers of sclerotome cells. Misexpression of RNA encoding pertussis toxin, a specific inhibitor of G-proteins, induces a mild inhibition of Hh signalling in all somites but the first five. While pertussis toxin inhibition leads to expansion of the sclerotome, a strong inhibition by PKA or hyper activation of Hh by a dominant negative PKA (dnPKA) leads to reduction (Hammerschmidt and McMahon, 1998).

In amniotes, the notochord is involved in patterning the dermomyotome. It controls the determination and survival of epaxial muscle (Asakura and Tapscott, 1998; Borycki et al., 1999; Dietrich et al., 1999; Teillet et al., 1998) and the establishment and maintenance of the borders between the epaxial and the hypaxial muscle (Borycki et al., 1999; Marcelle et al., 1997). Hedgehog has been shown to be a key player in this function.

In zebrafish, the slow muscle precursors are initially found adjacent to the notochord (Devoto et al., 1996), which suggest a role of the notochord in the induction of slow muscle, which is equivalent to epaxial muscles in amniotes. The zebrafish notochord mutants, *floating head* (*flh*), *no tail* (*ntl*) and *bozozok* (*boz*) (Fekany et al., 1999) have variable degrees of deficiencies in slow muscle formation, muscle pioneers and horizontal myosepta, that result from abnormalities in notochord development (Blagden et al., 1997; Halpern et al., 1993; Odenthal et al., 1996; Stemple et al., 1996; Talbot et al., 1995). In *flh* and *boz* mutant embryos, the notochord precursors are not formed, while in *ntl* mutant embryos the notochord precursors are present, but do not differentiate. In addition, at least for some of the mutations, wild-type notochord cells transplanted into mutant hosts are able to rescue the deficiency in the muscle pioneers (Halpern et al., 1993).

There is some evidence that the Hedgehog signalling pathway is a crucial element in the patterning role of the notochord in the myotome, in zebrafish. Two *hedgehog* genes are expressed in the zebrafish notochord, *sonic hedgehog* (*shh*) and *echidna hedgehog* (*ehh*) (Currie and Ingham, 1996), and a third one *tiggy winkle hedgehog* (*tghh*) (Ekker et al., 1995) is expressed in the floorplate. The functions of these genes are thought to overlap. In wild-type embryos, overexpression of *hedgehog* RNA leads to expansion of slow muscle and reduction of fast muscle and possibly of sclerotome. In particular, the

combination of *shh* and *ehh* overexpression results in the increase of the number of muscle pioneer cells in the middle of the somite, i.e., normal slow muscle territories (Currie and Ingham, 1996). In notochord mutants, like *bozozok* or *no tail*, slow muscle development can be rescued by *shh* overexpression (Blagden et al., 1997; Du et al., 1997; Hammerschmidt et al., 1996) , while muscle pioneer development can be rescued in *floating head* and *no tail* mutant embryos by *ehh* overexpression (Currie and Ingham, 1996). Reciprocally, the disruption of hedgehog signalling by treatment with forskolin (a Protein kinase A (PKA) agonist), by overexpression of constitutively active PKA or overexpression of Patched leads to defects in the slow muscle and in the case of Patched it results in slow muscle elimination, too (Barresi et al., 2000; Du et al., 1997). Furthermore, mutations in genes encoding proteins involved in the Hedgehog signalling pathway also lead to slow muscle defects (Barresi et al., 2000; Lewis et al., 1999; Schauerte et al., 1998).

The specification of a particular type of slow muscle, the muscle pioneers, appears to be the result of competing signals, the Hhs from the axial midline and BMPs from the most dorsal and most ventral portions of the somite. Ectopic expression of *dorsalin-1* in the notochord inhibits the adaxial cells close to the notochord from developing into muscle pioneers. Furthermore, the muscle pioneer cells evolve from a subset of adaxial cell that stay adjacent to the notochord while all the others migrate radially in direction to the surface. This longer exposure to higher concentration of Hhs may override the BMP negative signals in order to allow the muscle pioneers to develop (Stickney et al., 2000).

In conclusion, signals from the notochord are essential for symmetric patterning of the neuroectoderm and the paraxial mesoderm along the medio-lateral and dorso-ventral axes of the vertebrate embryo.

1.2.2 Left-right asymmetry

During vertebrate development, along the anteroposterior axis, the early symmetry is broken and most internal organs, like the brain, heart, the stomach, the liver and the intestine are asymmetric and occupy asymmetric positions in the embryo. Abnormal left-right development of any of these organs in relation to the others, called heterotaxia, may lead to severe states of illness and death (Bowers et al., 1996).

Work in several vertebrates has shown that left-right asymmetry is dependent on the midline, in particular the notochord. Extirpation of the axial midline during open neural plate stages, reduction of the dorsoanterior development of the midline or bilateral expression of nodal in the lateral plate mesoderm lead to cardiac reversals (Danos and Yost, 1995; Danos and Yost, 1996; Lohr et al., 1997). Furthermore, conjoined embryos show that while signals from one side of the embryo cannot cross the midline and affect the other side, they can affect another neighbouring embryo (Levin et al., 1996; Nascone and Mercola, 1997).

Mice and zebrafish midline mutant models have also been generated and discovered allowing the study of the role of the midline in left-right asymmetry. Two mutant mice examples are the *no turning* and the *Mgat-1*$^{-/-}$. Mice homozygous mutants for *no turning* have degeneration of the notochord and floorplate and as a consequence, the cardiac looping is randomised (Melloy et al., 1998). *Mgat-1* $^{-/-}$ homozygous mutant embryos generated by inactivation by homologous recombination of *Mgat-1*, a gene that encodes an enzyme involved in the biosynthesis of complex N-linked oligosaccharides, die by day 10 of gestation and have several defects, including dorsal midline defects and inversion of the heart looping (Metzler et al., 1994). In zebrafish, mutations in more than 20 genes that affect development of the midline also affect the left-right asymmetry of the heart (Metzler et al., 1994). Among those are three notochord mutants *no tail*, *floating head*

and *bozozok*. In this context, the midline seems to function as a barrier to contain the symmetrical signals to one side. The nature of this barrier can be either physical or molecular.

Another potential role for the notochord in left-right specification is the realignment of extra cellular matrix (ECM) proteins along the anteroposterior axis, driven by the notochord's mechanical elongation of the embryo. The realigned ECM proteins may serve in transduction of information for left-right positioning of the cells. The experimental results that support this idea are the following: pertubation of ECM deposition during gastrula stages either by microsurgery or microinjection of Arg-Gly-Asp peptides or heparinase into the blastocoel randomises heart and gut left-right orientation, and inhibition of proteoglycan synthesis by p-nitrophenyl-beta-D-xylopyranoside during late gastrula and early neurula stages leads to bilaterally symmetric hearts (Yost, 1990; Yost, 1992).

1.2.3 Other roles for the notochord

The notochord also plays important roles in several other aspects of development. For example: guidance and organ formation. One of the organs that depends on signals from the notochord for its formation is the hypochord. The hypochord is a transient embryonic rod-like structure, a mesendodermal derivative, positioned ventrally to the notochord. It consists of a row of single cells and it exists in embryos of fish, lampreys and amphibians (Cleaver et al., 2000; Eriksson and Lofberg, 2000; Lofberg and Collazo, 1997). The hypochord seems to be involved in patterning of the dorsal aorta, since it expresses *vascular endothelial growth factor* (*VEGF*), a growth factor that mediates migration of angioblasts to the dorsal midline, where they organise to form the dorsal aorta (Cleaver and Krieg, 1998). In *Xenopus* embryos, removal of the notochord during

early neurulation leads to absence of the hypochord, while in reciprocal experiments, where notochord grafts were ectopically positioned adjacent to the endoderm, the hypochord developed and was larger than in untreated siblings (Cleaver et al., 2000). These experiments suggest that signals from the notochord are necessary for hypochord formation.

Another organ whose formation is under notochord regulation is the pancreas. In chick embryos, notochord ablation, at stages when the notochord comes into contact with the endoderm, leads to loss of expression of several molecular markers of dorsal pancreas bud development. Reciprocally, *in vitro* studies where pre-pancreatic endoderm was cultured with notochord tissue, it initiates and maintains expression of pancreatic molecular markers, while similar experiments with non-pancreatic endoderm instead of pre-pancreatic endoderm do not result in expression of those markers (Kim et al., 1997). The model proposes that the notochord expresses the genes encoding activin-βB and FGF2, which then repress Sonic Hedgehog (SHH) in adjacent pre-pancreatic endoderm. The repression of SHH allows the expression of pancreas specific genes which control development of the pancreas (Hebrok et al., 1998).

In zebrafish *flh* mutant embryos, specification of the pancreas primordium is severely perturbed, but there is still some primordium indicating that other signalling centres (such as the floorplate) may contribute to its specification (Biemar et al., 2001). In addition, *ntl* mutant embryos show normal pancreas development. Therefore, the notochord mutants *no tail* (*ntl*) and *floating head* (*flh*) show that any signalling required for pancreas formation can be accomplished by the chordamesoderm and does not depend on a differentiated notochord.

Signals from the notochord are also essential for cell migration. In zebrafish embryos the dorsal aorta is positioned just ventral to the notochord, and the axial vein lies

between the endoderm and the dorsal aorta. Signals from the notochord are required to guide angioblasts to form the dorsal aorta. *ntl* and *flh* mutant embryos fail to form a dorsal aorta and are both cell autonomous mutations. Analysis of mosaic *flh* mutant embryos show that mutant cells expressing *flk-1*, a marker for angioblasts, assemble at the midline below wild-type notochord and form an aortic primordium (Fouquet et al., 1997), suggesting that the failure to form a dorsal aorta in these mutants is a consequence of a guidance deficiency resulting from defective signalling from the notochord, which may not necessarily be direct. Similarly, experiments in chick embryos, where notochord ablation and chick/quail paraxial mesoderm chimeras were created showed that the notochord functions as a barrier for endothelial cells (Klessinger and Christ, 1996). Although this was not proven to be a chemical barrier, it is most likely that this is the case since there is no hint of a mechanical barrier from histological sections and there are no evidences for a electrical field arising from the notochord.

The notochord also regulates neural crest migration. In chick embryos, the notochord seems to repel trunk neural crest cells along the ventral pathway. This leads to a neural crest free space of about 85 microns width surrounding the notochord (Pettway et al., 1990; Stern et al., 1991). The repulsion of neural crest cells by the notochord is age dependent and seems to be contact dependent (Stern et al., 1991). Chondroitin sulfate proteoglycans and collagen IX appear to be directly involved in the guidance role (Pettway et al., 1996; Ring et al., 1996).

The guidance role of the notochord affects not only cell migration, but also axon guidance of neurons such as the dorsal root ganglia (DRGs). The DRGs neurons are part of the sensory nervous system and develop from clusters of trunk neural crest cells that migrate ventrally into the somites and stay in the anterior half sclerotome. At the time of differentiation, the DRGs are adjacent to the neural tube, dorsolateral to the notochord

and between adjacent posterior half sclerotomes. DRGs are bipolar neurons and extend axons in a highly stereotyped manner. These axons are guided by neighbouring tissues, including the notochord. In *in vitro* experiments, the notochord, in concert with the dermomyotome and ectoderm, was found to chemorepel the DRG axons and in this way help to direct their sprouting (Keynes et al., 1997; Nakamoto and Shiga, 1998).

In zebrafish, it has also been found that the most anterior notochord regulates cardiac cell fate, by delimiting the posterior extent of the heart field (Goldstein and Fishman, 1998; Serbedzija et al., 1998). Ablation of the anterior notochord tip between the 4-somite and 12-somite stages leads to posterior expansion of expression of *Nkx2.5*, a molecular marker for myocardial precursors position. In addition, cells lateral to the anterior notochord tip that normally do not contribute to the heart are redirected to a heart cell fate. The analysis of zebrafish mutants has produced some evidence in support of this role of the notochord, since *ntl* mutant embryos show a posterior expansion of *Nkx2.5* (Goldstein and Fishman, 1998).

In conclusion, notochord signalling is required for several distinct developmental processes that range from specification of cardiac cell fate to guidance of DRG axons. In zebrafish, the large collection of mutants affecting embryogenesis provide us with animals models for studying, at a molecular level, these and many other processes. Characterisation of the mutations, in particular of the notochord mutations, will aid us in the discovery and refinement of notochord roles. An essential part of this characterisation is the cloning of the mutant loci.

1.3 Aspects of zebrafish genomics

1.3.1 Cloning of genes identified by mutation in zebrafish

In order to clone mutant loci two approaches are currently used successfully: candidate gene approach and positional cloning. Both have been successful in zebrafish, e.g., *no tail* (*ntl*) (Schulte-Merker et al., 1994) and *floating head* (*flh*) (Talbot et al., 1995) have been cloned by the candidate gene approach, while *one eyed-pinhead* (*oep*) (Zhang et al., 1998) and *sauternes* (*sau*) (Brownlie et al., 1998) have been cloned by positional cloning.

In the candidate gene approach, a set of cloned genes that have some properties expected of the mutated gene is compiled. Each one of these is then tested according to a number of criteria. The criteria for selection of candidate genes are the expression pattern and mutant phenotype in other species. Linkage analysis is also performed to test whether the candidate gene corresponds to the mutated locus. There are two limitations to this approach. First, in zebrafish, the number of isolated genes is not yet as big as in other species, such as mouse or human, and second, the selection criteria may be subjective.

For the majority of interesting zebrafish mutants, there are no obvious candidate genes. In these cases the positional cloning approach is the only solution. A typical positional cloning strategy consists of several consecutive steps. First, a mapped genetically linked marker has to be found to determine the chromosome/linkage group (LG) that contains the mutated locus, usually a centromere marker. Second, two flanking genetic markers closely linked to the mutated locus are identified. These are used to isolate large-insert DNA clones. In an iterative process known as "chromosome walking", markers from the ends of large insert-insert clones are used to identify new

large-insert clones, which are then mapped to determine proximity to the mutation. Eventually a contig of overlapping clones that span the mutation is found. This process is repeated until the size of the contig is small enough to be practical to take on several additional approaches such as: full sequencing of the contig; random sequencing of contig sub-sequences; identification by hybridisation of the genes within the interval; or to test whether known genes or ESTs are contained in that interval. Usually, the size of the desired genomic interval is about 100Kb.

Once a candidate gene is identified, it can be tested in several ways: by rescue of the mutant phenotype by injection of PAC/BAC DNA, cDNA or RNA; phenocopy of the mutant phenotypes using anti-sense morpholino oligonucleotides and direct sequencing of the mutant allele of the gene.

Both cloning approaches have been quite successful in zebrafish due to the existence and improvement of many genetic tools, such as: genetic and physical maps, knock out of genes by anti-sense morpholinos oligonucleotides, mutant rescue by DNA or RNA injection and manipulation of ploidy and parental origin.

1.3.2 Zebrafish genetic tools

1.3.2.1 Manipulation of ploidy and parental origin

The manipulation of ploidy and parental origin of the genome can be manipulated in zebrafish by a variety of *in vitro* techniques. These methods have been used both to accelerate the screening process and to generate genetic linkage maps, but are also useful for mapping mutant loci (Postlethwait and Talbot, 1997).

Fertilisation of eggs by UV-treated sperm generates gynogenetic haploid (GH) embryos that can develop through most embryonic stages. GH offspring of a heterozygous female resulting from a cross between two different strains is used to map

polymorphic DNA markers by following their segregation. Such fish can also be used to identify mutations. Heat shock treatment of GH embryos at the one-cell stage suppresses the embryo's first mitotic division, generating homozygous gynogenetic diploid embryos (HGD). These embryos are homozygous for maternal alleles at all loci and can be used to obtain clonal lines of fish. When eggs fertilised by UV-treated sperm are subjected to an early pressure treatment (EP) the second meiotic spindle is dissolved preventing the formation of a polar body. The result is gynogenetic half-tetrad diploid (GH-TDs) embryos, which can survive to adulthood.

It is also possible to generate embryos with chromosomes that have only paternal origin. Fertilisation of γ-ray irradiated eggs by normal sperm generates androgenic haploid (AH) embryos. These embryos are useful for comparison of recombination rates in male and female meiosis. Heat shock treatment of AH embryos at one-cell stage suppresses the embryo's first mitotic cleavage division, generating homozygous androgenetic diploid (HAD) embryos. These embryos are homozygous for paternal alleles at all loci. They can be used to study the role of genetic imprinting.

The advantage of GH-TD embryos arises from the fact that in zebrafish there is only one crossover per chromosome (double cross-overs are rare) (Streisinger et al., 1986), so GH-TD embryos chromosomes that have recombined are homozygous for loci centromere-proximal to the crossover. This is used to map loci to linkage groups and to estimate the genetic distance between a locus and its centromere. Mutant GH-TD embryos from hybrid females are homozygous for the centromere region linked to the mutation, while they are usually heterozygous for each of the other centromere regions. Thus, by analysis of the alleles of 25 centromeric markers (one for each linkage group) it is possible to identify the linkage group that carries the mutation. In addition, the frequency of mutant offspring gives an approximation to the genetic distance between a

locus and its centromere. These centromeric markers are just a small subset of a large collection of widely distributed genetic markers that are available in genetic and physical maps.

1.3.2.2 Genetic and physical maps

The existence of genetic and physical maps fulfills two major roles for cloning of genes identified by mutation. First, they are used to locate mutations within specific recombination intervals, e.g., centromere linkage analysis. Second, they can be used directly to identify large-insert genomic clones (i.e. Yeast Artificial Chromosome (YACs), P1-derived Artificial Chromosome (PACs) or Bacterial Artificial Chromosome (BACs)) when performing a chromosome walk.

A dense meiotic map is a powerful tool for genomic analysis in any species.

To generate such a map several technologies employed in other systems have been applied to zebrafish. The first systematic analysis was based on the characterisation of random amplified polymorphic DNA (RAPD) markers in GH offspring of a heterozygous female obtained from a cross between two strains of zebrafish (Postlethwait et al., 1994). A total of 134 decamers primers identified 401 loci, which fell into 29 linkage groups (4 more than the expected haploid complement of 25 chromosomes suggested by karyotype analysis (Daga et al., 1996; Schreeb et al., 1993)). Further characterisation of this cross using additional oligonucleotides increased the number of loci to 652 and consolidated the number of linkage groups to 25, with a estimated total genetic size of 2700 centimorgans (cM) (Johnson et al., 1996).

The RAPD map was useful as a framework for the localisation of PCR-based markers employing either simple sequence length polymorphisms (SSLPs) or single-strand conformational polymorphisms (SSCPs). However, the routine application of

RAPD analysis for genetic mapping has severe limitations. The efficiency of amplification of fragments using decamers is very sensitive to reaction conditions. This is particularly problematic when integrating mapping data from different crosses by comparison to common reference markers. In addition, many loci are not truly co-dominant, i.e., both alleles are not equally detectable in heterozygotes. Finally, even though amplified fragments can be cloned, sequenced and converted into sequence tagged sites (STSs) markers (Johnson et al., 1996), the primer binding site is the source of polymorphism, thus the sequence obtained between the primers is not necessarily polymorphic.

In mammals, the identification of a large collection of primers that amplify SSLPs at loci distributed across the genome has been one of the major tools for genetic mapping. In zebrafish, SSLPs were shown to exist (Goff et al., 1992) and at first 102 SSLPs were characterised (Knapik et al., 1996). They segregated into 25 linkage groups in an analysis of 520 intercross progeny (1040 meioses). The current meiotic map has about 3000 microsatellites and over 1000 genes and expressed sequence tags (ESTs) (Kelly et al., 2000).

An easy alternative to meiotic mapping of genes or genomic fragments is to localise them in a high-resolution physical map with respect to more easily scored PCR markers. Their genetic localisation is determined by statistical inference and comparison to meiotic maps. Two radiation hybrids (RH) panels have been developed, the "Goodfellow" (Kwok et al., 1998) and the "Ekker"(Hukriede et al., 1999) panels. RH mapping is very useful in chromosome walks to test linkage of large-insert clones and routinely map cDNAs and ESTs.

Another way of localising genes is to extrapolate their position with respect to other genes. For that, gene order is assumed to be conserved across species. This is a very

stringent requirement. Conservation of gene order between mouse and human has been described in sub chromosomal regions and their boundaries are well defined. Some of the linkage conservation may be functional, so it is quite likely that there are conserved regions between zebrafish and mouse and human. This is becoming more important because the information with respect to gene position in the zebrafish genetic map is rapidly increasing. Comparison between the zebrafish gene map and a selection of mammalian genomes has revealed significant synteny (Postlethwait et al., 1998). As an example of the utility of synteny in cloning of mutant loci, the gene *gli2* was identified, by synteny, as the gene mutated in *you-too* (*yot*) (Karlstrom et al., 1999).

Over the next couple of years, the zebrafish genome is going to be sequenced and will become an excellent tool for any work in zebrafish genomics and in particular, for positional cloning projects. With knowledge of the genome, chromosome walks will skip the identification of large-insert clones and instead will use genomic sequences to generate polymorphic markers. In addition, the identification of the mutated gene from a small contig will consist of testing the genes that will be known to be contained in that genomic interval.

1.3.2.3 Test of candidate genes

One of the ways to test a candidate gene is to use anti-sense morpholino-modified oligonucleotides (morpholinos) to knock products down. Morpholinos specifically inhibit translation in zebrafish, allowing conserved vertebrate mechanisms and diseases to be studied in a systematic way and *in vivo* (Ekker, 2000; Nasevicius and Ekker, 2000). In addition, the use of morpholinos, at the right concentrations, can extend the knowledge arising from characterisation of some mutant phenotypes, since it also allows the knock

out of maternal components, revealing early functions which are masked in mutant embryos.

Candidates can also be tested also by rescue of the mutant phenotype either by microinjection of DNA (PAC/BAC or cDNA) or mRNA. The ultimate proof comes from the direct sequencing of the mutant allele of the gene or of its regulatory elements to find the genetic lesion.

Using a positional cloning approach which involved random sequencing of contig sub-sequences, morpholino oligonucleotide and sequencing of cDNA alleles, the *sneezy* gene was identified as *copa,* a gene that encodes a protein known to be essential for transport in the early secretory pathway.

1.4 The early secretory pathway

1.4.1 From protein translation to ER processing

Translation of proteins is initiated on cytosolic ribosomes. For soluble and transmembrane proteins, the first protein sequence to be translated contains a short hydrophobic N-terminal signal sequence (Rapoport et al., 1996). The newly translated signal sequences are then recognised by a protein complex called signal recognition particle (SRP). The interaction leads to a delay in the translation of the mRNA, during which the complex consisting of the protein that is being translated, the SRP and the ribosome docks onto the ER membrane. After docking, the signal peptide is inserted into an aqueous channel, called the translocon. Translation proceeds and the remainder of the protein is inserted into the ER lumen through the translocon. Once in the ER lumen, the signal sequence can be cleaved off by peptidases, depending on the type of protein. The presence of the signal sequence in conjunction with the presence or absence of additional

hydrophobic transmembrane domains are crucial to define the status of a protein as soluble or as an integral membrane protein (Hegde and Lingappa, 1997). Soluble proteins and type I transmembrane proteins (which also contain a C-terminal transmembrane domain) have their signal cleaved, while maintenance of a signal peptide results in a cytosolic N-terminal type II topology.

In the ER, proteins are folded, assembled into a complex (if necessary), some are glycosylated and in general they all undergo a "quality control". Proteins that do not pass the "quality control", for example due to improper folding, are retrotranslocated into the cytosol, where they are ubiquinated and sent to the proteosomes for degradation.

Proteins that are correctly processed in the ER either stay in the ER if that is their "home" organelle or they are transported along the secretory pathway. This transport is highly dependent on membrane traffic (Rothman, 1996).

1.4.2 Traffic in the early secretory pathway

The membrane trafficking between the ER and the Golgi complex is bidirectional (Mellman and Simons, 1992; Rothman, 1996). Newly synthesised proteins and lipids are transported from the ER to the Golgi complex and escaped ER resident proteins and machinery proteins are recycled back to the ER. Transport from the ER to the Golgi and cis to trans within the Golgi cisternae is called anterograde transport. Transport in the opposite direction is called retrograde transport.

Proteins and lipids exit the ER from ribosome free transitional elements coated with COPII. COPII is a cytosolic complex consisting of a small GTPase Sar1p and the heterodimeric proteins complexes Sec23p-Sec24p and Sec13p-Sec31p (Barlowe et al., 1994).

After COPII vesicles' fission, they lose the COPII coat, fuse and form vesicular tubular clusters (VTCs) (Bannykh et al., 1998; Hauri et al., 2000). These clusters are then translocated to the Golgi complex along microtubules, where they fuse to the most cis cisternae (Presley et al., 1997; Scales et al., 1997). COPI vesicles are involved in retrograde transport from the Golgi stacks and VTCs back to the ER (Cosson et al., 1998; Cosson and Letourneur, 1997), but there is COPI-independent retrograde transport (Girod et al., 1999; White et al., 1999) and not all retrograde transport is vesicular, since there is some tubular transport associated with microtubule mediated translocation (Lippincott-Schwartz, 1998). COPI vesicles are also involved in anterograde transport (Orci et al., 1997), allowing a fast track transport as opposed to the slow track mediated by cisternae maturation/progression (Bonfanti et al., 1998; Volchuk et al., 2000). The secretory cargo is finally transported by clathrin coated vesicles from the trans Golgi network towards the cell membrane.

1.4.2.1 The role of tethering proteins in COPI transport within the Golgi complex

Within the Golgi stacks, vesicles are linked to the membranes by flexible protein tethers, that are molecularly distinct from one face of a cistern to next (Kooy et al., 1992). For example, studies have shown that a complex of at least three proteins; p115 (Bannykh et al., 1998; Nelson et al., 1998; Waters et al., 1992), giantin (Linstedt et al., 1995; Linstedt and Hauri, 1993; Seelig et al., 1994) and GM130 (Nakamura et al., 1995), tethers COPI vesicles to the Golgi membranes (Nakamura et al., 1997; Nelson et al., 1998; Sonnichsen et al., 1998). p115 binds giantin on the vesicles and GM130 on the membranes.

Tethering functions in several ways. It physically restricts the COPI vesicles to fuse close to where they pinch off, limiting transport to adjacent cisternae (Orci et al., 1998; Sonnichsen et al., 1998). At the same time, it optimises transport because vesicles cannot diffuse away. Finally, since tethers differ between faces of cisternae, they may mediate the directionality of COPI vesicles transport. Alternatively, the COPI vesicles may move in a stochastic way and the tethers function exclusively in limiting their movement between adjacent cisternae. Although the stochastic movement of vesicles would be less efficient than unidirectionally movement, simulations reveal that, on average, it would require only double the number of vesicles (Glick et al., 1997).

1.4.3 COPI vesicles: from assembly to fusion

COPI vesicles are functionally and structurally distinct from others vesicles such as COPII vesicles. The structure of the main component of their coat, the coatomer, has been investigated and many interactions between subunits were identified. Using the yeast two-hybrid system, several interacting pairs were found: β/δ, γ/ζ, α/ε, α/β', α/β, β/β', γ/β', γ/ε and β/ε (Eugster et al., 2000; Faulstich et al., 1996). In addition, *in vitro,* the coatomer can be disintegrated in high salt buffers into subcomplexes retaining partial functions. The subcomplexes obtained in this way are: α/β'/ε which interacts with KKXX motifs and α/β/γ/δ/ζ which is not stable and tends to disassemble into β/δ and γ/ζ (Cosson and Letourneur, 1994; Fiedler et al., 1996; Lowe and Kreis, 1995; Pavel et al., 1998). It is also known that once assembled, the coatomer is a stable complex with a half-life of approximately 28 hours in mammalian cells and no exchange of subunits occurs (Lowe and Kreis, 1996).

The first step in COPI vesicle assembly is the recruitment of the guanine nucleotide exchange factor for ARF1 (ARF-GEF), to the membrane (by an unknown mechanism).

Then ARF1 is recruited and binds to the membrane. The presence of both in the same membrane stimulates the GTP exchange onto ARF1, in a fungal metabolite Brefeldin A (BFA) sensitive way (Donaldson et al., 1992; Helms and Rothman, 1992). BFA acts as a competitive inhibitor that stabilises the ARF-GDP-ARG-GEF protein complex (Mansour et al., 1999; Peyroche et al., 1999). As a result a conformational change of ARF1 exposes its myristoylated N-terminus allowing it to be inserted in the membrane during early steps of the GTP exchange onto ARF1 (Beraud-Dufour et al., 1999; Kahn and Gilman, 1986; Nuoffer and Balch, 1994; Randazzo et al., 1993). ARF1-GTP is thought to bind to an unidentified receptor in the membrane, whose existence is deduced from *in vitro* studies that showed that binding to the membranes is saturable (Donaldson et al., 1992; Finazzi et al., 1994; Helms et al., 1993). The binding to the membrane is mediated by protein kinase C (PKC) and IgE receptors (De Matteis et al., 1993).

Once ARF1-GTP is bound to the membrane, it stimulates phospholipase D1 (PLD1) activation (Brown et al., 1993; Cockcroft et al., 1994), in a process modulated by phosphatidylinositol-4,5-bisphosphate (PIP_2) (Brown et al., 1993). The activated PLD1 then mediates the conversion of phosphatidylcholine (PC) present in the membrane into phosphatidic acid (PA) and choline. A consequence of this catalytic reaction is that there is an increase in the negative charge which may be co-responsible for inducing the curvature of the membrane (Scales et al., 2000). In parallel, the activation of PLD1 induces a rearrangement of the membrane lipid environment facilitating in this way the binding of COPI by making membrane proteins, like p24 family proteins (of coat receptors and potential cargo receptors), available for interaction with the coatomer (Nickel and Wieland, 1997). Support for this second role comes from the observations that the coatomer cannot bind Golgi membranes without ARF and GTP, even when proteins of the p24 family are present (Palmer et al., 1993), but coatomer can bind to the

cytoplasmatic tails of p24 proteins either in solution or on coupled sepharose beads (Reinhard et al., 1999; Sohn et al., 1996). It is thought that the rearrangement of the lipid environment induces the dissociation the p24 family hetero-oligomeric complexes, allowing them to form homo oligomeric complexes that have higher affinity for the coatomer (Reinhard et al., 1999).

The binding of the cytosolic coatomer complex to a membrane is mediated by several factors. Coatomer subunits and subcomplexes are know to bind in different ways to the membrane. As examples: the coatomer can bind directly to phosphatidic acid in the membrane (Manifava et al., 2000); the β-COP subunit can bind ARF-GTP (Zhao et al., 1997); the dimer formed by β-COP and δ-COP bind to the membrane in an ARF-GTP dependent way (Pavel et al., 1998) and the trimer formed by β'-, α- and ε-COP subunits and the γ-COP subunit can interact with double lysine motifs and double phenylalanine motifs on membrane proteins (like the p24 protein family) (Hudson and Draper, 1997). There are other membrane proteins that are likely to bind to the coatomer or coatomer-adaptors. This binding may function in a cooperative way leading to further binding of coatomer and consequent budding. An example of one such protein is the KDEL receptor (see below).

The recruitment of several molecules of coatomer and their consequent polymerisation is thought to be the principal phenomenon driving budding of the membrane. Polymerisation of coatomers occurs from interaction with p24 family protein cytoplasmatic tails (Reinhard et al., 1999). It is in the process of polymerisation of coatomer and budding that cargo proteins and targeting proteins are incorporated (Bremser et al., 1999; Letourneur et al., 1994; Nagahama et al., 1996). In coated buds, fatty acyl-coenzyme A (CoA) induces periplasmic fusion of the membrane allowing it to pinch off and form a vesicle (Ostermann et al., 1993; Pfanner et al., 1989). Studies have

shown that two distinct populations of COPI vesicles may exist. One containing cargo (like VSV protein) and other containing KDEL receptor (Orci et al., 1997). This indicates that from the same Golgi membrane, distinct COPI vesicles can be assembled.

The interactions between the KDEL receptor or proteins of the p24 family with COPI provides some evidences of how different populations of COPI vesicles may be formed. The KDEL receptor oligomerises and binds ARF-GAP through a non-catalytic domain required for its recruitment to the membranes (Aoe et al., 1997). This may result in decrease of ARF-GTP hydrolysis and consequent halt in coatomer detachment. Similarly, specific sequences in the tails of proteins of the p24 family have been shown to affect the coatomer dependent GTP hydrolysis of ARF1 (Goldberg, 2000; Goldberg, 1999), although the precise role of coatomer in ARF1 hydrolysis is still controversial (Szafer et al., 2000).

Prior to vesicle docking and fusion with the host membrane, the coatomer detaches from the vesicle by GTP hydrolysis of ARF, mediated by the ARF-GTPase activating protein (ARF-GAP) (Antonny et al., 1997; Tanigawa et al., 1993; Zhao et al., 1999). It is know that the coatomer accelerates the rate of hydrolysis which led to the suggestion of a tripartite complex formed by ARF1, coatomer and ARF-GAP in the membrane of COPI vesicles (Goldberg, 1999). The coatomer dissociation exposes its v-SNAREs allowing vesicle fusion with the host membrane.

It is likely that docking and fusion of a particular vesicle to a membrane is regulated by Rab, Rab interacting and SNARE proteins (Rothman, 1996). The Rabs are cytosolic proteins from the Ras superfamily of small GTPases. The SNAREs are integral membrane proteins, with protein-protein interaction domains in their cytosolic tails. While the Rab and Rab interacting proteins are thought to recruit and/or function as docking intermediates for vesicles (Pfeffer, 1999; Schimmoller et al., 1998), the SNAREs

are thought to be involved in vesicle fusion with the membrane (Pfeffer, 1999; Rothman, 1996; Scheller, 1995). Vesicle SNAREs (v-SNAREs) interact with membrane SNAREs (t-SNAREs). This interaction may be involved in providing some specificity to the system, but not for cargo-containing COPI vesicles. COPI containing cargo possess the v-SNARE GOS28 (undetectable in others) (Orci et al., 2000). This v-SNARE interacts with the t-SNARE Syntaxin5 (Sed5p in yeast) to form a SNARE complex. Both GOS28 and Syntaxin5 are evenly distributed through the stack (Hay et al., 1998; Orci et al., 2000) therefore they cannot be involved in specificity for COPI vesicles.

1.4.4 Membrane trafficking models

The role of COPI vesicles has been instrumental in the way transport in the early secretory pathway has been modelled. There are two major models for membrane trafficking within the Golgi and between the ER and the Golgi: the vesicular transport model and the cisternal maturation model. The vesicular transport model prevailed until the mid eighties. The idea of anterograde transport mediated by COPI vesicles was widely accepted. In experiments using VSV G protein, a viral cargo protein destined to the plasma membrane, it was found that approximately half of the COPI vesicles contained the protein (Orci et al., 1986). In 1994, results from yeast genetics showed that COPI vesicles mediate retrograde transport from the Golgi to the ER (Cosson and Letourneur, 1994; Letourneur et al., 1994). The problem that arose was to understand how the same vesicles could mediate both types of transports. This led to the resurrection of the cisternal maturation model.

Another emerging model incorporates aspects of both traditional models (Fig.1.2).

In the vesicular transport model the Golgi complex is thought to be a stable entity. Golgi cisternae are pre-existing structures. Anterograde transport of newly synthesised

proteins and lipids from one cisterna to the next is mediated by COPI vesicles. This is accomplished by successive rounds of vesicle budding and fusion. Retention and recycling of components are performed by COPI vesicle retrograde transport. Thus COPI vesicles function in both anterograde and retrograde transport within the Golgi.

In the cisternal maturation model the Golgi is a very dynamic structure. Cisternae are transient and change their relative position in a cis to trans direction and their contents, in terms of resident proteins, in a trans to cis direction as they mature. Anterograde transport of newly synthesised proteins and lipids is mediated by cisternae as they maturate, while COPI vesicles mediate retrograde transport of resident contents of cisternae, leading to the exchange of their resident contents.

While it is clear that COPI vesicles mediate retrograde transport, there is controversy about whether COPI vesicles function in anterograde transport. Furthermore, membrane trafficking models are intrinsically associated with different COPI vesicle transport models. The most compelling results, however, come from immunoelectron microscope studies of intact cells. These studies reveal two distinct populations of COPI vesicles, one containing the KDEL receptor and no detectable cargo, the other containing cargo, like the VSV G protein, proinsulin, and residual KDEL receptor (Orci et al., 1997). Another study uses tandem repeats of spontaneously dimerising mutants of the FK506 binding protein, which accumulate in the cis most cisternae at 15°C. When the temperature block is released they move across the Golgi in megavesicles on a fast track like COPI vesicles (Volchuk et al., 2000). Immunoelectron microscopy of intact cells and cell free budding experiments reveal that Golgi residents like glycosyltransferases are present in COPI vesicles at lower concentrations (Orci et al., 2000; Sonnichsen et al., 1996). A quantitative pulse-chase experiments in conjunction with electron microscopy, showed that collagen precursors transverse the Golgi cisternae in animal cells. The

relevance of this finding is that these aggregates are too large to fit into COPI vesicles. The rate of this transport is slower in comparison with cargo transport mediated by COPI vesicles, like VSV G protein (Bonfanti et al., 1998).

Taken together the existing evidence suggests a model in which cisternae progression and maturation occurs coordinately with COPI bidirectional transport between adjacent cisternae. Within the Golgi, cargo can be transported in the anterograde direction in a fast vesicular track and in a slow track inside cisternae. The COPI dependent retrograde transport may be either direct or indirect. Indirect, if COPI retrograde vesicles percolate between cisternae, direct if they exit the donor cisterna and move directly to the ER.

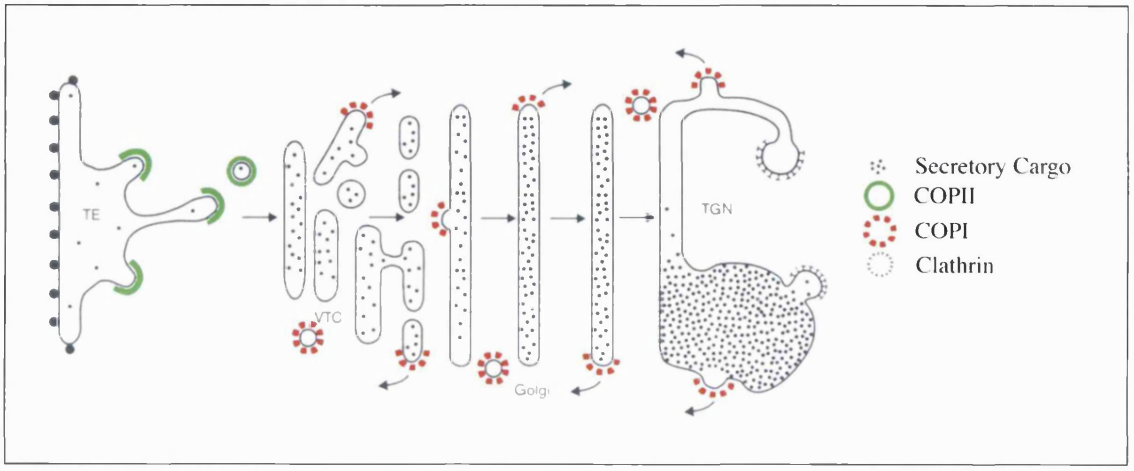

Figure 1.2. Transport in the early secretory pathway. Secreted cargo exit the ER from ribosome-free transitional elements (TE) into COPII vesicles. After pinching off, COPII vesicles lose their coat, fuse and form the membranes of vesicular tubular clusters (VTC). The maturation of VTCs gives rise to the cis-Golgi. In the Golgi complex, cisternae maturation and progression is responsible for a slow anterograde transport, while COPI vesicles are responsible for a fast anterograde transport within the Golgi complex and between VTCs and the Golgi. COPI vesicles are also involved in retrograde transport from the Golgi complex and VTCs back to the ER, allowing recycling and retention of proteins and lipids. Transport from the Golgi to the cell membrane and other organelles occurs from the trans-Golgi and is mediated by clathrin vesicles.

1.4.5 Other roles for COPI

1.4.5.1 The role of COPI in signal transduction

The coatomer complex is thought to function in mechanisms other than the vesicular transport within the Golgi complex and between the ER and the Golgi. Cdc42, a Rho family GTPase that is localised to the Golgi complex, interacts with γ–COP subunit of the coatomer, via a dilysine motif present in the carboxyl terminus of Cdc42 (Wu et al.,

2000). This result suggests that COPI may be involved in signal transduction pathways controlling the cytoskeleton, cell growth and transformation (Drubin and Nelson, 1996; Johnson, 1999) and reciprocally, that cdc42 may also be involved in transport in the early secretory pathway (Rothman, 1996; Schekman and Orci, 1996).

The currently accepted view is that the transformation potential of cdc42 is dependent on binding to γ-COP and the association of γ-COP with the other COPI subunits. The transformation potential of this association is distinct from the Ras induced transformation. Reciprocally, the cdc42-γ-COP complex mediates the secretion rates independently of its function in transformation (Wu et al., 2000). It is thought that the interaction with γ-COP enhances cdc42 signalling. The association brings cdc42 to the membrane whereby, via ARF function, PIP_2, a known stimulant of nucleotide exchange in the absence of GEF (Zheng et al., 1996), may enhance cdc42 GTP loading. Furthermore, the interaction does not block the cdc42 Ras effector loop or the Rho insert region which remain available for interaction with effector proteins, like IQGAP, an actin binding protein present in the Golgi which is known to associate with cdc42 (McCallum et al., 1998). In terms of secretion, it has been proposed that cdc42-induced hydrolysis would result in acceleration of secretion due to faster release of COPI from transport intermediates.

1.4.5.2 The role of COPI in the endocytic pathway

There is also evidence for a role of COPI in endocytosis. A form of coatomer containing ε-COP, but lacking δ-COP and β-COP has been found in endosomal membranes (Whitney et al., 1995). In addition, ε–COP^{ts}dlf cells are defective in endocytosis and microinjection of anti β-COP antibodies blocks the entry of viruses *in vivo* (Aniento et al., 1996; Whitney et al., 1995). Furthermore, the formation of

endocytic carrier vesicles from early endosomes *in vitro* is inhibited by coatomer immunodepletion or by use of ε–COP^{ts}dlf mutant cytosol (Aniento et al., 1996; Gu et al., 1997). Finally, it is also thought that COPI in the endosomes mediates the sorting and transport events that occur during receptor-mediated endocytosis (Daro et al., 1997).

1.5 Summary

During vertebrate development, notochord-derived signals pattern adjacent tissues such as the spinal cord and somites. The zebrafish notochord is furthermore an ideal system to study organogenesis, for several reasons. Specifically, the notochord is a simple structure that undergoes all of the key developmental processes underlying organogenesis and there is a wealth of mutations that provide access to the genes controlling notochord formation. I have studied one of these mutations, *sneezy*, and found that it encodes the zebrafish coatomer α protein, a protein essential for transport in the early secretory pathway. In the following chapters I will describe in detail the steps I took to identify the *sneezy* gene and understand its role in notochord development..

Chapter 2 Experimental Procedures

Table 2.1. Abbreviations

BCIP	X-phosphate/5-Bromo-4-chloro-3-indolyl-phosphate
BSA	Bovine serum albumin
DAB	Diaminobenzidine
DEPC	Diethylpyrocarbonate
DIG	Digoxygenin
DTT	Dithioerithritol
EDTA	Ethylene-diamine-tetra-acetate
HEPES	N-2-hydroxyethylpiperazine-N'-2-ethanesulfonic acid
HRP	Horseradish peroxidase
IPTG	Isopropylthio-β-D-galactosidase
NBT	4-Nitro blue tetrazolium chloride
OD	Optical density
PEG	Polyethylene glycol
SDS	Sodium dodecyl sulphate
X-Gal	5-bromo-4-chloro-3-indolyl-β-D-galactosidase
ATP	Adenosine 5'-triphosphate
CTP	Cytidine 5'-triphosphate
UTP	Uridine 5'-triphosphate
GTP	Guanidine 5'-triphosphate
TTP	Thymidine 5'-triphosphate

2.1 Embryo manipulations

2.1.1 Embryo collection

Zebrafish (*Danio rerio*) embryos were raised at 28°C in embryo water (red sea salt 0.03 g/l, methylene blue 2 mg/l) or in 0.3X Danieau solution (full strength (1X) Danieau solution is 58 mM NaCl, 0.7 mM KCl, 0.4 mM $MgSO_4$, 0.6 mM $Ca(NO_3)_2$, 5 mM HEPES, pH 7.6). Approximate stages are given in hours-post-fertilisation (hpf) at 28°C according to the morphological criteria provided in (Kimmel et al., 1995).

2.1.2 Embryo labelling for transplantation

Donor embryo chorions were removed by 4 minutes incubation in 0.5 mg/ml pronase (Sigma) in 0.3X Danieau solution followed by several washes in 0.3X Danieau solution. Donor embryos were then transferred into ramps made of 2% agarose in 0.3X Danieau solution covered with 0.3X Danieau solution. Donor embryos were labelled at the 1-4 cell stage by micro-injection into the yolk cell with 5% lysine-fixable fluorescein or lysine-fixable rhodamine dextran (Molecular Probes) and 5% lysine-fixable biotin dextran (Molecular Probes) in 0.2 M KCl.

2.1.3 Embryo microsurgery

Transplantation experiments were performed essentially as described by Saúde (Saude et al., 2000).

2.1.4 Whole-mount *in situ* hybridisation

Whole-mount *in situ* hybridisations were performed essentially as described by Thisse (Thisse et al., 1993).

2.1.5 Whole-mount antibody staining

The embryos were fixed in 4% paraformaldehyde, rehydrated in a series of methanol dilutions and then digested with proteinase K as described in 2.1.3. The endogenous alkaline phosphatase was inactivated by placing the embryos at 65°C for 30 minutes. The embryos were blocked in 2 mg/ml BSA, 2% goat serum in PBT for several hours. The embryos were incubated with the primary antibody diluted in 2 mg/ml BSA, 2% goat serum in PBT at 4°C overnight, with agitation. After washing at least 8 times for 15 minutes with PBT, the embryos were blocked again and incubated at 4°C overnight with the secondary antibody. The secondary antibody was washed at least 8 times 15 minutes. Detection was performed using the avidin-HRP (Vector Labs) as described in 2.3.6.

Immunolocalization of primary neurons and their ventral root axonal projections was carried out using the znp1 monoclonal antibody (Trevarrow 1990). The secondary antibody was HRP-conjugated goat anti-mouse IgG (BioRad, 1:100).

2.1.6 Immunolocalisation of the lineage tracers

The fate of transplanted embryonic tissues labelled with rhodamine dextran and biotin dextran was recorded by direct fluorescence observation or by staining with avidin-HRP (Vector Labs). Embryos were fixed in paraformaldehyde, dehydrated in a series of methanol dilutions and treated with proteinase K as described in section 2.1.3. For staining, embryos were incubated for 1 hour at room temperature with avidin-HRP complex in PBT, then washed 5X with PBT and incubated in 0.4 mg/ml DAB in PBT for 1 hour at room temperature. The staining reaction was initiated by the addition of a fresh solution of 0.4 mg/ml DAB/PBT containing 0.003% H_2O_2. After stopping the reaction with several washes of PBT, embryos were re-fixed in 4% paraformaldehyde/PBS.

Embryos were cleared with 20% glycerol/80% PBS, 50% glycerol/50% PBS and stored at 4°C in 80% glycerol/20% PBS.

2.1.7 Whole-mount apoptosis detection

Apoptotic cell death was detected using the Terminal Deoxynucleotidyl Tranferase System (ApopTag In situ Apoptosis Detection Kit-Peroxidase®, Oncor Inc.). The Embryos were manually dechorionated and fixed in 4% paraformaldehyde/PBS for 1 hour at room temperature or at 4°C overnight. After three 5 minute washes with PBS, they were transferred to methanol and stored at -20°C. Embryos were rehydrated by successive washes in 75% methanol/PBT; 50% methanol/PBT; 25% methanol/PBT for 5 minutes each and finally 4 times 5 minutes in 100% PBT. They were then digested with Proteinase K (10μg/ml) at room temperature for 10 minutes and washed twice in PBT for a few seconds. The postfixation involved two steps followed by five and three 5 minutes washes in PBT, respectively. After postfixation of the embryos in 4% paraformaldehyde/PBS for 20 minutes at room temperature, they were washed five times in PBT for five minutes each time. This was followed by a second postfixation step consisting of incubation with prechilled (-20°C) ethanol:glacial acetic acid (2:1) for 10 minutes at -20°C. After the second postfixation, the embryos were washed three times in PBT, for five minutes each time. The embryos were then incubated for 1 hour at room temperature in 75 μl (1 drop) of equilibration buffer and after its removal, they were incubated overnight at 37°C, in a small volume of working strength TdT enzyme (at least 17μl). For preparation of working strength TdT enzyme, the reaction buffer (S7105) was mixed with the TdT enzyme (S7107) (2:1) and TritonX 100 added to a final concentration of 0.3%. All the reagents were provided in the Apoptag In situ Apoptosis Detection Kit-Peroxidase; Oncor Inc.. The reaction was stopped by washing the embryos

in working strength stop/wash buffer for 3 hours at 37°C. For preparation of working strength stop/wash buffer, the stop/wash buffer (S7100-4) was mixed with distilled water (1:17). After blocking with 2mg/ml BSA, 5% goat serum in PBT for a minimum of 1 hour at room temperature, the embryos were incubated overnight at 4°C, in a 1/2000 dilution of preabsorbed sheep anti-digoxygenin-alkaline phosphatase conjugated Fab fragments. This was followed by washes with 2mg/ml BSA in PBT with at least 4 changes of blocking buffer for some hours. The embryos were then equilibrated three times for 5 minutes in NTMT reaction buffer. The color reaction was performed using X-phosphate/NBT (225 µl of 50 mg/ml NBT in 70% dimethylformamide and 87.5 µl of 100 mg/ml X-phosphate in 70% of dimethylformamide added to 50 ml of NTMT) in the dark. The reaction was stopped with washes in 100% PBS. The embryos were fixed in 4% paraformaldehyde/PBS for 30 minutes at room temperature. After three 5 minute washes with PBT, the embryos were cleared with 20% glycerol/80% PBS, 50% glycerol/50% PBS and stored at 4°C in 80% glycerol/20%PBS.

2.1.8 Electron microscopy

Whole zebrafish embryos were dechorionated manually and fixed overnight, with fixative solution (2% glutaraldehyde, 2% paraformaldehyde in 0.1M sodium cacodylate buffer (SCB) pH 7.2). On the next day, they were washed for 10 minutes in SCB and postfixed for 1 hour, in postfixation solution (1% osmium tetroxide, 0.1 M SCB). This was followed by another wash with SCB for 10 minutes and staining "en bloc" with 1% aqueous uranyl acetate for 1 hour. The samples were then dehydrated through a graded ethanol series, 50%, 75% and 90% for 10 minutes each and 3 changes of 100% for a total of 30 minutes, followed by 2 changes of propylene oxide over 20 minutes. Next , they were placed in Epon resin (Agar Scientific) (10 ml Agar 100 resin, 8 ml DDSA

(Dodecenyl Succinic Anhydride0, 4 ml MNA (Methyl Nadic Anhydride), 0.65 ml BDMA (Benzyldimethylamine)) for 24 hours. During these 24 hours the agar was changed several times. The blocks containing the samples were then polymerised at 70°C overnight. After polymerisation, 50nm ultra thin sections were cut on an Ultracut E microtome and mounted on pioloform coated slot grids. Prior to viewing of the sections, they were stained with 1% aqueous uranyl acetate for 15 minutes and Reynold's lead citrate (1.33 gm lead nitrate, 1.76 gm tri sodium citrate, 8ml 1N carbonate free NaOH, water up to 50 ml) for 7 minutes. Between the stainings the sections were washed with distilled water and dried on filter paper. The sections were visualised in a Jeol 1200 EX electron microscope.

2.1.9 Gynogenetic diploid half-tetrad embryos generation

Female heterozygous carriers were set up with wild-type males. The fish were separated before the females laid any eggs. Sperm from 10 males (± 10 µl) was collected from the wild-type males and placed in 100 µl I buffer pH7.2 (116 mM NaCl, 23 mM KCl, 6 mM $CaCl_2$, 2 mM $MgSO_4.7H_2O$, 29 mM $NaHCO_3$ and 5% fructose) on ice.

The sperm in I buffer was placed in a watch glass on ice and irradiated for 30 seconds using a stratalinker. To check that the sperm was not destroyed, a few drops of water were added to a small portion of the treated sperm (to see if the sperm was activated by the water) and visualised using a Zeiss Axiophot microscope.

Eggs were squeezed from the heterozygous carrier females onto a dry petri dish. Sperm was added to the eggs and after 2 minutes the dish was flooded with egg water. Immediately after the addition of egg water, the samples were placed into a scintilation vial that was placed into a French pressure cell. Within 84 seconds of adding the egg water, the eggs were subjected to 8000psi pressure for 6 minutes. The pressure was then

released over a 30 second period and the embryos were recovered from the vials and incubated at 28^{0}C.

2.1.10 Anti-sense morpholino oligonucleotide micro-injections

The cDNA sequences used to design morpholino oligonucleotides were obtained from GenBank. Morpholino oligonucleotides were obtained from Gene Tools, LLC. Morpholinos work through an RNase-H independent process that blocks translational initiation. Consequently, all morpholinos were arbitrarily designed to bind to the 5' UTR or sequences flanking and including the initiating AUG. The selected sequences were based on design parameters according to the manufacturer's recommendations, namely 21–25mer antisense oligonucleotides of 50% G/C and A/T content with no predicted internal hairpins. Four consecutive G or C nucleotides were also avoided. In addition, each design sequence was tested for representation elsewhere in the genome.

Each morpholino oligonucleotide was resuspended in 63 µl of deionised water to obtain a final concentration of ± 4.7 ηMoles/µl. Prior to microinjection, the morpholinos were diluted 8 to 32 fold using injection buffer (5 mM Hepes pH7.2, 0.2 M KCl and 2.5 mg/ml phenol red).

Each embryos was microinjected 1.3 nl (0.2 to 0.8 ρMoles) of diluted morpholino at 1-2 cell stage.

2.1.11 Photomicrography

Nomarski and live fluorescence images were obtained using a Leica compound microscope fitted with a Princeton Instruments, MicroMax cooled-CCD camera. MetaMorph image processing software was used to acquire images and overlay

fluorescence and Nomarski images. Whole-mount *in situ* hybridisation images were obtained using a Zeiss Axiophot microscope fitted with a Kodak DCS420 digital camera. Life embryos images were obtained using a dissection scope fitted with a Leica wild DMS52 film camera.

2.2 Molecular Biology Techniques

2.2.1 TOPO®Cloning

The cloning of PCR products was performed using the TOPO TA Cloning®kit (Invitrogen). The cloning reaction was performed according to the following conditions: 2 µl fresh PCR product and 0.5 µl pCR®-TOPO® vector. The two were mixed gently and incubated for 5 minutes at room temperature. After 5 minutes the ligation was transformed using electrocompetent TOP10 cells from the kit.

2.2.2 Plasmid transformation of competent bacteria

2.2.2.1 Transformation of chemically competent bacteria

Up to 100 ng of DNA was added to 100 µl of cells thawed on ice. The bacterial cells were kept on ice for 5 to 30 minutes and then heat shocked at 42°C for 30 seconds followed by cooling on ice for a few minutes. After this period, 250 µl of SOC medium was added and the mixture was incubated at 37°C for 1 hour with agitation. An aliquot of 10 to 200 µl from each transformation was spread onto a selective agar plate (100 mg/ml of ampicillin) and incubated overnight at 37°C. To select recombinants, 40 µl of X-Gal (20 mg/ml in dimethylformimide) and 40 µl of IPTG (200 mg/ml) were used per plate.

2.2.2.2 Transformation of electrocompetent bacteria

Up to 100 ng of DNA was added to 20 μl of cells thawed on ice and immediately transferred to a pre-cooled 0.1 cm electroporation chamber. Cells were electroshocked under 1.8 kV, 25 μF and 200 Ω. 1 ml of SOC medium was immediately added, the mixture was transferred to a plastic tube and incubated with shaking at 37 °C for 1 hour. Each transformation was platted as described in section 2.2.2.1.

2.2.3 Preparation of plasmid DNA

2.2.3.1 Small scale preparation of DNA

From a 3.5 ml overnight culture of bacteria in selective LB medium, 1.5 ml was transferred to a 1.5 ml microcentrifuge tube and spun for 20 seconds. The supernatant was removed completely and the pellet resuspended in 300 μl of Resuspension Buffer (Qiagen; 10 mM EDTA, 50 mM Tris.HCl pH 8.0, 100μg/ml RNase). 300 μl of Lysis Buffer (Qiagen; 0.2 M NaOH, 1% SDS) was added, mixed and left for 2 minutes at room temperature to allow alkaline lysis of the cells. Lysis solution was then neutralised by adding 300 μl of ice-cold Neutralisation Buffer (Qiagen; 3 M KOAc pH 5.5) and mixed carefully by inverting the tube a few times, followed by 10 minutes incubation on ice. The tube was spun for 15 minutes at room temperature. 700 μl of the supernatant was transfered into a fresh microcentrifuge tube and phenol/chloroform extraction was performed (see section 2.2.5.). DNA was precipitated from the aqueous upper layer by adding 650 μl of isopropanol, leaving 15 minutes and then spinning for 15 minutes at maximum speed, all at room temperature. After centrifugation the pellet was washed in 70% ethanol, air dried and resuspended in distilled water with 0.1 mg/ml RNase A (Sigma).

2.2.4 DNA quantification and manipulation

DNA and RNA were quantified by spectrophotometry at 260 nm (an OD of 1 equates to 50 μg/ml double stranded DNA, 35 μg/ml single stranded DNA and 40 μg/ml RNA). The ratio between the readings at 260 nm and 280 nm provided an estimate of the purity of the nucleic acid preparation (pure preparations of DNA and RNA should have OD_{260}/OD_{280} values of 1.8 and 2.0, respectively).

2.2.5 Phenol/Chloroform extraction

To remove proteins from nucleic acid solutions, a mixture of phenol:chloroform:isoamyl-alcohol (25:24:1 volume ration) was added in a 1:1 volume ratio to the DNA solution and vortexed for 1 minute. After a 3 minutes centrifugation, the upper (aqueous) layer was transferred into a new microcentrifuge tube and extracted with an equal volume of chloroform.

2.2.6 Ethanol Precipitation

Ethanol precipitation was carried out by adding 3 M NaOAc pH 5.5 (to a final concentration of 0.3 M) and 2.5 volumes of 100% ethanol to the DNA solution that was then left on dry ice for approximately 20 minutes. 1 μl of 10 mg/ml glycogen was often used as a carrier if the DNA amount to be purified was too small to be visualised as a pellet at the bottom of the tube. Centrifugation at 20 000 x g for 5 to 20 minutes was performed and the DNA pellet was then washed in 70% ethanol, dried and resuspended in TE or distilled water.

2.2.7 Restriction digestions

Restriction enzyme digests were performed at the recommended temperature for approximately 1 hour using commercially supplied restriction enzymes and buffers (Boehringer Mannheim, Promega, New England Biolabs). The enzyme component of the reaction never comprised more than 10% of the reaction volume. For enzyme digests using more than one restriction enzyme, the buffer suggested by the manufacturer was used.

2.2.8 Agarose gel electrophoresis of DNA and RNA

DNA separation and size estimation were performed by agarose gel electrophoresis. Gels were prepared by dissolving agarose in 0.5X TAE to a final concentration of 0.8% to 2% depending on the expected size of the DNA fragment. To visualise the DNA, 0.5 mg/ml ethidium bromide was added to the gel. DNA samples were mixed with 6X gel loading buffer and electrophoresis was performed at 5 to 20 V/cm of gel length, until the appropriate resolution was achieved. The resolved DNA was visualised using ultraviolet light at 302 nm, and the size was estimated by comparison with known size markers such as the 1 kb size marker (Gibco BRL).

2.2.9 RNA for *in situ* hybridisation

The RNA probes were prepared in a 20 μl reaction mixture containing: 1 μg of linearized template DNA (Table 2.2), 1x transcription buffer, 1x DIG-RNA labelling mix (Boehringer Mannheim), 20 units of RNase inhibitor (Promega), 40 units of the appropriate T7 (Promega), T3 (Boehringer Mannheim) or SP6 (Boehringer Mannheim) RNA polymerase. The reaction mixture was incubated for 2 hours at 37°C. To remove the plasmid DNA, the reaction mixture was incubated for 30 minutes at 37°C with 2 units

of RNase-free DNase I (Promega). The mixture was then subjected to size exclusion chromatography using Chroma Spin-30+DEPC-H2O columns (Clontech) to remove free nucleotides.

Table 2.2. Templates for antisense RNA probes used in this thesis.

Gene	Linearization site	RNA polymerase	Reference
col2α1	EcoRI	T7	(Yan et al., 1995)
ntl	XhoI	T7	(Schulte-Merker et al., 1994)
shh	HindIII	T7	(Krauss et al., 1993)
flh	EcoRI	T7	(Talbot et al., 1995)
gsc	EcoRI	T7	(Schulte-Merker et al., 1994)
pax2.1	BamHI	T7	(Krauss et al., 1991)
copa	EcoRI	T7	This thesis
admp	EcoRI	SP6	This thesis

2.2.10 Isolation of genomic DNA from adults

Genomic DNA from adult fish was obtained from very thin transverse sections of frozen fish. The sections were digested in a 1.5 ml microcentrifuge tube with 100 µl of lysis buffer for 5 hours at 55°C. The lysis buffer composition was 0.5% SDS, 0.1 M EDTA pH8, 10 mM Tris pH8 and 100 µg/ml Proteinase K.

2.2.11 Isolation of genomic DNA from embryos

The embryos were washed twice for a few seconds with Low TE (10 mM Tris pH.8, 0.1 mM EDTA). After that, they were placed in thermowell 96 well plates (Costar), one per well. Any droplets present in the wells were removed by pipetting. The embryos were lysed using 100 µl of lysis buffer per embryo (well), for 5 hours at 55°C.

2.2.12 Purification of genomic DNA from adult fish

After lysis, the samples were extracted with 100 µl phenol:chloroform:isoamyl alcohol (25:24:1) and ethanol precipitated with 250 µl 100% ethanol and 10 µl 3 M NaOAc pH 5.5. After centrifugation for 5 minutes at 13000 rotations per minute (rpm), the supernatant was decanted and the pellet air dried. The pellet was resuspended in 100 µl deionised water and stored at -20^{0}C.

2.2.13 Purification of genomic DNA from embryos

Sterile Multiscreen^{TM} 96-well filtration plates (MILLIPORE), with membranes with pore size of 0.22 µm and low protein and nucleic acid binding properties, were used to purify genomic DNA. The plates were fixed with sticky tape on top of sterile polystyrene 96-well cell culture cluster plates, with flat bottom (Costar) and then each well of the Multiscreen plate was filled in with Sephacryl S-400-HR (Sigma). The plates were then centrifuged in a SORVAL RT6000B centrifuge (DuPont) at 2500 rpm, for 5 minutes at 4^{0}C. The flow through was discarded and each well was loaded with 100 µl of Low TE. The plates were then centrifuged as before and the flow through discarded. These last two steps were repeated twice to wash the sephacryl matrix. Prior to DNA filtration, the side walls of clear polycarbonate thermowell 96 well plates (Costar) were cut and one of these plates was fitted in between each multiscreen plate and the culture cell plate. After

the low TE washes, the DNAs were loaded into the Multiscreen plates and each plate was centrifuged as before. The purified DNA/ flow throughs were collected in the thermowell plates. The plate with the purified DNA sit over the culture plate and was closed using the Multiscreen plate lid.

The plates with the purified DNAs were stored at -80^{0}C.

2.2.14 SSLP analysis of genomic DNA from embryos

2.2.14.1 Oligonucleotide labelling with [γ^{32}P]ATP

Oligonucleotides were labelled with [γ^{32}P]ATP by T4 polynucleotide kinase (PNK). The reaction conditions per oligonucleotide pair (and for 24 distinct DNA samples) were as following: 0.25 µl PNK buffer, 0.05 µl PNK (10 U/µl), 0.75 µl [γ^{32}P]ATP (6000Ci/mmole) and 1.45 µl 10 µM oligonucleotide. The mixture was incubated at 37°C for 30 minutes, in a PTC-100 Programmable Thermal Controller (PCR machine), with heated lid.

2.2.14.2 Polymerase chain reaction (PCR) with genomic DNA templates

The purified genomic DNA from each mutant embryo or from adult fish was diluted 10 fold with deionised water to be used as DNA templates for PCR reactions. The general conditions for setting up PCR reactions using genomic DNA were as follows: 7.25 µl reaction mix, 0.075 µl labelled oligonucleotide (for each one), 0.1 µl Taq polymerase (5U/µl) and 2.5 µl genomic template. The reactions were overlayed with mineral oil prior to incubation. The PCR program consisted of a first denaturing step at 94^{0}C for 3 minutes followed by 35 cycles of 92°C for 1minute, then 58°C-60 °C for 1

minute and finally 72°C for 1minute and 30 seconds. The last step was an extension step at 72°C for 7 minutes.

The reaction mix was made of 122 µl 10X Taq buffer, 9.8 µl 25 mM dNTPs and 740.8 µl deionised water.

2.2.14.3 Electrophoretic analysis of PCR results

2.2.14.3.1 Electrophoresis gel composition

The electrophoresis gels used were 43 cm in length, 6% denaturing polyacrylamide gels.

A 60 ml gel was made up of 14.4 ml of SequaGel concentrate (Natural Diagnostics), 39.6 ml SequaGel diluent (Natural Diagnostics) and 6 ml of gel buffer. The composition of the gel buffer was the following: 50% urea (m/v), 0.108% Tris base (m/v), 0.053% boric acid (m/v), 2 mM EDTA pH 8 and 10 ml N, N, N', N'-tetramethyl-ethylenediamine (TEMED) for each litre. The gel polymerisation was catalysed by addition of 600 µl 10% ammonium persulfate (APS) per gel prior to pouring of the gel.

2.2.14.3.2 Gel loading

To each 10 µl of PCR product, 10 µl of loading buffer were added, mixed and denatured at 95°C for 5 minutes. The composition of the loading buffer was: 98% formamide (v/v), 0.025% bromophemol blue (v/v), 0.025%xylene cyanol (v/v), 10 mM EDTA pH 8. The loading was performed using a 8-channel needle pipette and approximately 4 µl of denatured product was loaded per well.

2.2.14.3.3 Electrophoresis conditions

The gels were pre run at a constant power of 85Wper gel for 1 hour, and they run at the same constant power for 1-2 hours (depending on the PCR product size and length polymorphism). The electrophoresis buffer was 1X TBE.

2.2.14.3.4 Processing the gels

The gels were lifted from the bottom plates with a 35 x 43 cm interleaving paper sheet and involved in Saran film. They were then placed with X–ray films inside cassettes with intensifier screens. The films were exposed overnight at -80°C.

2.2.14.3.5 Processing the films

The films were developed in a film processing machine and analysed manually.

2.2.15 RFLP analysis of genomic DNA from embryos

The procedure applied to analyse SSCP markers was identical to the one described for SSLPs. The only differences were that only one of the oligonucleotides used in the PCR reaction was labelled with [γ^{32}P]ATP (to make marker analysis easier), the PCR reaction volume was doubled and the PCR products underwent restriction digestion prior to loading. The three RFLP markers used in this thesis were 75G10-1, O12224sp6 and L16134sp6 and the labelled primers were 75G10-1 reverse, O12224sp6 reverse and L16134sp6 forward, respectively.

The restriction digest reaction conditions for 75G10-1 were 8 µl of PCR product plus 2 µl of the following: 0.2 µl buffer M, 0.068 µl $MgCl_2$, 0.2 µl Tru 9I and 1.532 µl deionised water. The reaction was incubated at 65°C for 1 hour.

The restriction digest conditions for O12224sp6 were 8 µl of PCR product plus 2 µl of the following: 0.2 µl buffer A, 0.2 µl RSA I, 1.6 µl deionised water. The reaction was incubated at 37°C for 1 hour.

The restriction digest reaction conditions for L16134 were 4 µl of PCR product plus 6 µl of the following: 1 µl 10X NE buffer 3 (Biolabs), 0.1 µl 100X BSA, 0.1 µl Hinc II and 4.8 µl deionised water. The reaction was incubated at 37°C for 1 hour.

2.2.16 Large insert genomic libraries screen

The YAC (Research Genetics) and PAC (library706, RZPD) libraries were screened by PCR. The PCR reactions were set up using the following conditions: 5 µl of DNA template, 2.5 µl Taq buffer, 0.2 µl 25 mM dNTPs, 0.2 µl Taq, 15.1 µl deionised water, 1 µl of 10 µM oligonucleotide (from each one). The PAC DNA templates used were 10 fold dilution of the stocks. The PCR program used for these reactions was: a first denaturing step at 94^{0}C for 3 minutes, followed by 35 cycles of 92^{0}C for 1 minute, 72^{0}C for 1 minute and 72^{0}C for 1 minute and 30 seconds. The PCR reaction was terminated with a final extension step of 72^{0}C for 7 minutes. The results were analysed in a 1% agarose gel.

2.2.16.1 YAC end rescue

2.2.16.1.1 Isolation of yeast genomic DNA

The yeast clones were streaked on YPD agar plates and incubated for 2 days at 30^{0}C. From the plates, single clones were picked with a sterile loop and used to inoculate 30 ml YPD medium cultures. The yeast cultures were left to grow until saturation at 30^{0}C, when they were collected by centrifugation for 2 minutes. After that, the supernatant was discarted and the pellet was resuspended in 0.5 ml of distilled water. The suspension was

transferred to a 1.5 ml centrifuge tube for collection of cells by centrifugation for 5 seconds. The resulting supernatant was decanted and the cells were resuspended in the residual liquid by vortexing. The cells lysis was performed by addition of 0.2 ml of 2% Triton X-100, 1% SDS, 100 mM NaCl, 10 mM Tris-HCl pH8 and 1mM Na_2EDTA. To this mixture, 0.2 ml of phenol:chloroform:isoamyl alcohol (25:24:1) and 0.3 g of acid-washed glass beads (0.45-0.5 mm beads (Sigma]) soaked in nitric acid and washed in distilled water) were added. After vortexing for 4 minutes, 0.2 ml of TE, pH8 was added. The lysate was then centrifuged for 5 minutes after which the aqueous layer was transferred to a fresh tube. 1 ml of 100% ethanol was added. The sample was mixed by inversion, centrifuged for 2 minutes and after decanting the supernatant, the pellet was resuspended in 0.4 ml of TE plus 3 µl of a 10 mg/ml solution of RNAse A (in 50 mM potassium acetate pH 5.5, boiled for 10 minutes). After incubation for 5 minutes at 37°C, the DNA was precipitated with 10 µl of 4M ammonium acetate plus 1 ml of 100% ethanol. The DNA samples were centrifuged for 2 minutes and the DNA pellet (± 20 µg DNA) was resuspended in 50 of Low TE.

2.2.16.1.2 Recovery of the YAC ends

5 µl of yeast DNA (± 2 µg) was digested with BamH1 (or Spe1), for 5 hours at 37°C. The restriction digests were set up according to the following conditions: 2 µl BamH1 (Spe1), 10 µl buffer B (H), 5 µl yeast DNA and 83 µl deionised water. The digestion products were extracted with phenol:chloroform:isoamyl alcohol (25:24:1) and ethanol precipitated. The samples were then centrifuged for 15 minutes at 12000 x g at 4°C. The resulting supernatants were decanted and the pellets were resuspended in 25 µl Low TE. The YAC ends formed plasmids by self ligation. The ligation reaction was set according to the following conditions: 25 µl restriction products, 10 µl ligase buffer, 5 µl ligase

(400 units/µl New England Biolabs) and 60 µl deionised water. The mixture was incubated overnight at 16^{0}C. On the next day, the ligation product was ethanol precipitated and centrifuged at 12000 x g for 15 minutes at 4^{0}C. The pellet was resuspended in deionised water and electroporated into electrocompetent *E.coli.*

2.2.16.2 Preparation of YAC end DNA

This was performed as described in section 2.2.6

2.2.16.3 Preparation of PAC DNA

The PAC preparation procedure was adapted from the Quiagen Maxi-prep kit and made use of the buffer available in the kit.

The bacterial clones were streaked on selective LB agar plates (10µg/ml kanamycin) and incubated overnight at 37^{0}C. From the plates, single clones were picked up with a sterile loop and used to inoculate 10 ml selective LB medium cultures (25µg/ml kanamycin). These 10 ml cultures were then used to inoculate 250 ml selective LB medium cultures (25µg/ml kanamycin), which were left to grow overnight at 37^{0}C. The final cultures were split into two tubes and centrifuged at 3500 x g for 30 minutes. After decanting the resulting supernatant, the pellets were resuspended in10 ml buffer 1 with RNase. To accomplish this the tubes were shaken for 30 minutes at 37^{0}C. To lyse the cells, 10 ml of buffer 2 was added to each tube. The mixture was then mixed gently and incubated for 5 minutes at room temperature. Neutralisation was done by addition of 10 ml of buffer 3. The samples were mixed gently again and placed overnight at 4^{0}C. Next morning, the samples were centrifuged at 21000 x g for 30 minutes. While the samples were being centrifuged, the elution buffer QF was heated to 65^{0}C and the Quiagen Tip 500 were equilibrated with 10 ml of buffer QBT. At this step, the supernatants were recombined, poured into a cartridge filter and strained through the filter into the column.

Each supernatant passed throught the column twice, before the column was washed with 30 ml of buffer QC, 4 times. After the washes, the PAC DNA was eluted using 2 times 10 ml of heated elution buffer QF. This was followed by isopropanol precipitation. The samples were split again and 0.7 ml isopropanol was added to each one. After mixing gently, they were placed at -20^{0}C for at least 4 hours and centrifuged at 15000 x g for 30 minutes. The supernatants were discarded and the pellets washed with cold 70% ethanol, by centrifugation for 2 minutes. The ethanol was decanted and the pellets left to air dry for 20 minutes. The pellets were resuspended in 200 µl of deionised water, overnight.

2.2.17 RH mapping

The physical mapping of genomic fragments and ESTs was performed using the Ekker RH panel. The DNA templates used (5 µl per reaction) were 5 fold dilution of the stocks. The conditions for setting up the reactions and for PCR were as described in 2.2.16. The analysis of the result was done using the RHMAPPER available from htpp://zfin.org/ZFIN/.

2.2.18 Total RNA extraction

The RNA extraction was performed using TRIzol®Reagent (Life Technologies). Approximately 100 embryos were homogenised in 1 ml of TRIzol reagent using a seringe and a needle. The homogenised sample was then incubated for 5 minutes at room temperature to allow the complete dissociation of nucleoprotein complexes. To complete phase separation, 0.2 ml chloroform was added to the sample, which was then shaken for 5 minutes and centrifuged at 12000 rpm for 20 minutes at 4^{0}C. Next the RNA (aqueous phase) was transferred to a fresh tube and precipitated with 0.5 ml isopropanol alcohol. The samples were incubated at room temperature for 10 minutes and centrifuged at

12000 rpm for 15 minutes at 4^{0}C. The supernatant was discarded and the pellet washed with 75% ethanol. After a brief centrifugation, the ethanol was decanted and the pellet left to air dry. The RNA was resuspended in RNAse-free water and stored at -20^{0}C.

2.2.19 Reverse transcriptase-polymerase chain reaction (RT-PCR)

The reverse transcriptase-polymerase chain reaction (RT-PCR) was performed according to the following conditions: 2 µl 5mM dNTPs, 1 µl deionised water, 3 µl N6CAS oligonucleotide (0.166 µg/µl), 4 µl 5X first strand buffer, 5 µl M-MLV reverse transcriptase (200 U/µl), 2 µl DTT (0.1 M) and 3 µl total RNA (± 5 µg). The mixture was overlayed with 2 drops of mineral oil and incubated at 42^{0}C for 1 hour.

2.2.20 Automatic DNA sequencing

The DNA sequencing was done using an ABI PRISM®377 DNA sequencer, with the sequencing dyes BigDye™Terminator Chemistry (Applied Biosystems). The sequencing gels were made using standard length 36 cm WTR sequencing gel plates, 0.2 mm spacers and 36-, 48- lane combs.

2.2.20.1 DNA sequencing reactions

2.2.20.1.1 Plasmid DNA sequencing reactions

The plasmid DNA sequencing reactions were set up according to the following conditions: 5 µl DNA template (0.5-1 µg), 2 µl BigDye terminator dyes, 3 µl 5X CSA buffer, 2 µl 1.6 pmol/µl oligonucleotide and 8 µl deionised water. The final reaction solution was overlayed with 2 drops of mineral oil prior to the beginning of the reaction.

The PCR program conditions were the following: 25 cycles of 96^{0}C for 30 seconds, 50^{0}C for 15 seconds and 60^{0}C for 4 minutes.

2.2.20.1.2 PAC sequencing reactions

The PAC end sequencing reactions were set up according to the following conditions: 10 µl DNA template (2-4 µg), 8 µl BigDye terminator dyes and 2 µl 1.6 pmol/µl oligonucleotide. The final reaction solution was overlayed with 2 drops of mineral oil prior to the beginning of the reaction. The PCR program conditions were the following: 35 cycles of 96^{0}C for 30 seconds, 50^{0}C for 15 seconds and 60^{0}C for 4 minutes.

2.2.20.2 Preparation of loading samples

The preparation of the sequencing loading samples consisted of two steps, a purification step and a resuspension step.

Sterile Multiscreen^{TM} 96-well filtration plates (MILLIPORE), with membranes of pore size 0.22 µm and low protein and nucleic acid binding properties, were used to purify the sequencing reaction products. The plates were fixed with sticky tape on top of sterile polystyrene 96-well cell culture cluster plates, with flat bottom (Costar) and then each well of the Multiscreen plate was filled in with Sephacryl S-200-HR (SIGMA). The plates were then centrifuged in a SORVAL RT6000B centrifuge (DuPont) at 2500 rpm, for 5 minutes at 4^{0}C. The flow through was discarded and each well was loaded with 100 µl of low TE (10 mM Tris pH.8, 0.1 mM EDTA). The plates were then centrifuged as before and the flow through discarded. These two last steps were repeated twice to wash the sephacryl matrix. Prior to products filtration, the side walls of clear polycarbonate thermowell 96 well plate (Costar) were cut and one of these plates was fitted in between each multiscreen plate and culture cell plate. After the low TE washes,

the products were loaded into the Multiscreen plates and each plate was centrifuged as before. The purified sequencing reaction products were collected in the thermowell plates and transferred to 1.5 ml tubes. The samples were then dried in a speedvac.

The sample pellets were resuspended in 4 µl loading buffer (for each 5 parts of formamide, 1 part of 25 mM EDTA pH8 and blue dextran (50 mg/ml)).

2.2.20.3 Sequencing gel preparation

A 50 ml gel was made by mixing 18 g of urea in 26 ml of deionised water. The urea was stirred until it was completely dissolved. Then it was mixed with 5 ml of 10X TBE, 5 ml Long Ranger®gel solution and 35 µl N, N, N', N'-tetramethyl-ethylenediamine (TEMED). Prior to pouring of the gel, the gel was filtered using a 0.22 µm bottle filter and 250 µl of 10% APS was added to allow faster polymerisation. The gel were left to polymerise for 1 hour.

2.2.21 Sequencing of cDNA

The sequencing of cDNA was performed by sequencing overlapping cDNA fragments that had been amplified by PCR from partial cDNAs and cloned using the TOPO TA Cloning®kit (Invitrogen) (see section 2.2.1). The sequencing conditions have been described in section 2.1.19.1.1.

The PCR conditions used to amplify cDNA fragments were the ones described in section 2.1.14.2, with 2 µl of RT-PCR product used as a template for the reaction.

2.2.22 DNA and protein analysis.

Nucleotide sequence alignments and contig assembly were performed using SEQUENCHER (Gene Codes Coporation). The nucleotide contigs were used to screen GenBank databases at the National Center for Biotechnology Information (NCBI) web

page (http//:www.ncbi.nih.gov/BLAST/). The tools used were blastx to compare the six-frame translation products of the nucleotide queries against the protein database and blastn to compare the nucleotide queries against the nucleotide database. Translation of cDNAs was also performed using SEQUENCHER. The identification of protein domains was done using Simple Modular Arquitecture Research Tool (S.M.A.R.T.), at http//:smart.embl-heidelberg.de/. The phylogenetic trees and similarity tables were generated using MEGALIGN part of the DNA-star package (Lasergene).

Table 2.3. Formulation of frequently used solutions.

1X PBS	137 mM NaCl, 2.7 mM KCl, 4.3 mM $Na_2HPO_4.7H_2O$, 1.4 mM KH_2PO_4
1X PBT	1X PBS, 0.1% Tween 20
1X TAE	40 mM Tris.Acetate, 2 mM $Na_2EDTA.2H_2O$ (pH 8.5)
1X TE	1 mM EDTA, 10 mM Tris.HCl pH 8.0
20X SSC	3 M NaCl, 0.3 M $Na_3citrate.2H_2O$, adjust pH to 7.0 with 1 M HCl
Sequencing loading buffer	for each 5 parts of formamide, 1 part of 25 mM EDTA pH8 and blue dextran (50 mg/ml)
Gel electrohporesis loading buffer	98% formamide, 0.025% bromophemol blue, 0.025%xylene cyanol, 10 mM EDTA pH 8
6X gel loading buffer	6X TAE, 50% v/v glycerol, 0.25% w/v bromophenol blue

Table 2.5. Formulation of frequently used growth media.

YPD	1% yeast extract, 2% peptone, 2% glucose pH6.5
LB (L-Broth)	1% w/v bacto-tryptone, 0.5% w/v bacto-yeast extract, 1% w/v NaCl
SOC	2% Tryptone, 0.5% Yeast Extract, 10 mM NaCl, 2.5 mM KCl, 10 mM $MgCl_2$, 10 mM $MgSO_4$, 20 mM glucose

Table 2.6. Oligonucleotides for CA repeat markers.

Name	Sequence
M13 Forward (-20)	5'-GTAAACGACGGCCAG-3'
M13 Reverse	5'-CAGGAAACAGCTATGAC-3'
Z11023 Forward	5'-CAGTGCTGCTTCGTGGTAAA-3'
Z11023 Reverse	5'-TGCAGTGCTGTAATTGAGGG-3'
Z7632 Forward	5'-CTCTCTTAATGGAAGAGCAGCC-3'
Z7632 Reverse	5'-CAAGCCAGTCTGATGGAACA-3'
Z10838 Forward	5'-TGGGCATTTGGATGTAACAA-3'
Z10838 Reverse	5'-CCCCTAAATTGGCACTTATGA-3'
Z8448 Forward	5'-ATGTGGGTAAGACTGGCAGG-3'
Z8448 Reverse	5'-AACCCATGCATCTGAAGAGG-3'
Z4300 Forward	5'-GCACAAATGAAGGCCTTTGT-3'
Z4300 Reverse	5'-GTGTCATTTTGGAAATGGGG-3'
Z3412 Forward	5'-AGGCAAACAGAAGCATTTGGC-3'
Z3412 Reverse	5'-GGAAAGTCCAAGTACCTTGCGC-3'

Table 2.7. Oligonucleotides for YAC/PAC ends.

Name	Sequence
T3	5'-AATTAACCCTCACTAAAGGG-3'
T7	5'-GTAATACGACTCACTATAGGGC-3'
PACsp6	5'-GGCCGTCGACATTTAGGTGACAC-3'
PACT7	5'-CCGCTAATACGACTCACTATAGGG-3'

Table 2.8. Oligonucletides for YAC/PAC end polymorphic markers.

Name	Sequence
75G10-1 Forward	5'-TGCCCTAAAATAGCCACAGC -3'
75G10-1 Reverse	5'- CAGCACAGCAATTCTTCTGG -3'
L16134sp6 Forward	5'-GCCATACACGCATATGAACG-3'
L16134sp6 Reverse	5'-TTTTACCAAACCCCCATCCT-3'
O12224sp6 Forward	5'-GGTTGCAATCAGAATATGCAC-3'
O12224sp6 Reverse	5'-ACTATTCTGCCTCGGGTCAA-3'
M4238T7 Forward	5'-AAATGGCACAATTTGGATCG-3'
M4238T7 Reverse	5'-GGACCACGAGAGTGAAACCA-3'
19G3T3 Forward	5'-CCAGCATGTCCAAAGTTCCT-3'
19G3T3 Reverse	5'-TGAATGTCCTGTGCCACAAT-3'

Table 2.9. Oligonucleotides for *copa*.

Name	Sequence
*copa*1 Forward	5'-CATTATCAGTGGAGATGTTGACC-3'
*copa*1 Reverse	5'-CATGGTGGAAGAATGTGGTG-3'
*copa*2 Forward	5'-AAGCTGCGTCGATGTCTTTT-3'
*copa*2 Reverse	5'-CACCTCAGTGTCCACAGCAC-3'
*copa*3 Forward	5'-GATCAGACTGTGCCCGTGT-3'
*copa*3 Reverse	5'-ATCTCTGCGAAAGGTCTGGA-3'
*copa*4 Forward	5'-ACCTCAACCTGTTTGCTGCT-3'
*copa*4 Reverse	5'-AAGTGCAGCCTCACCAAGAC-3'
*copa*5 Forward	5'-CAGTTTGGCACTGGAGTGTG-3'
*copa*5 Reverse	5'-TTCAGCTTCCTCATCCATCC-3'
*copa*6 Forward	5'-TCAAGAACTGTGGGCAGAAG-3'
*copa*6 Reverse	5'-CTCCGTCGTCTTTCCCAAT-3'
*copa*7 Forward	5'-AACTGGCCTTTGCTCACAGT-3'
*copa*7 Reverse	5'-TCTCAAAAGAGCCAGCCAGT-3'
*copa*8 Forward	5'-GATCTGGATCTCCCACCAGA-3'
*copa*8 Reverse	5'-GCTCTGAAGCGTTCCACG-3'
*copa*9 Forward	5'-CCTGAGGAACTGGAAGGACA-3'
*copa*9 Reverse	5'-TGCGCAGTTTGAAGAAAAGA-3'
*copa*10 Forward	5'-CGGAGAGGAAGAAACTCCCTA-3'
*copa*10 Reverse	5'-ACCCTGCAGACCTCTCCTTT-3'
*copa*11 Forward	5'-GGGCGACCTGTAGAGAAATG-3'
*copa*11 Reverse	5'-TTTGCACTGAGTGACAGATGC-3'

Table2.10. Morpholino oligonucleotides.

Name	Sequence
axin1-MO	5'-CCTTCTCGTTTACACTCATGCTCAT-3'
copa-MO	5'-ATTTGGTCAACATCTCCACTGATAA-3'
pxf-MO	5'-CCTGGTGCTCTGATGCTGACGCCAT-3'
copβ-MO	5'- TGTCATGATGTCAGCTCTTCTTCCC-3'
copβ'-MO	5'-TTTGCGCTTGATGTCCAGCCTCAG-3'

Table 2.11. Other oligonucleotides.

Name	Sequence
N6CAS	5'-GATGCGGCCGCCTCGAGCTCANNNNNN-3'

Chapter 3 Molecular Characterisation of *sneezy*

3.1 Introduction

As mentioned in Chapter 1, the notochord cells of *sneezy* mutant embryos fail to differentiate at 24 hpf. The notochord cells do not acquire large vacuoles and there is maintenance of expression of early notochord molecular markers (Fig.3.1). In addition, *sneezy* mutant embryos have a severe reduction in pigmentation and generalised degeneration prior to death, which occurs during the third day of life.

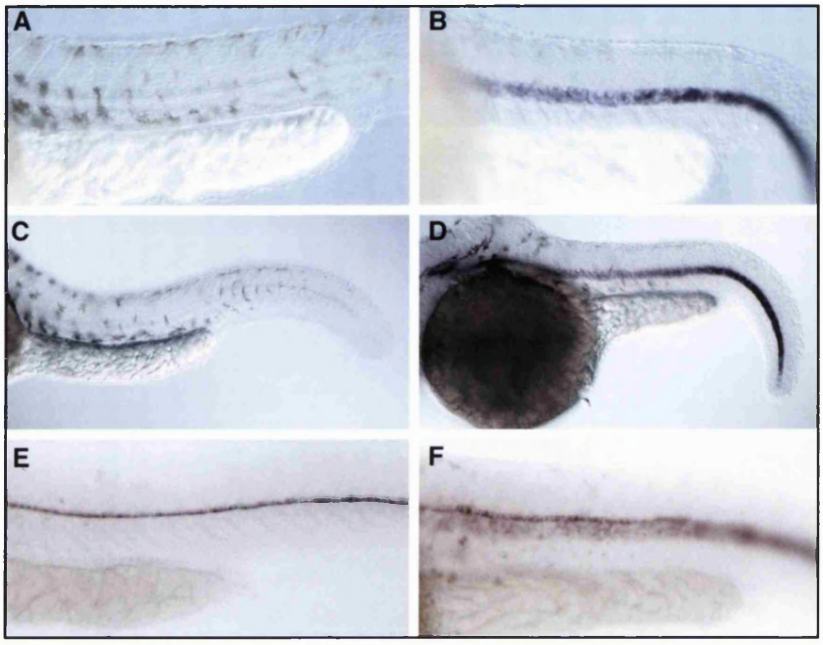

Figure 3.1 Maintenance of expression of early notochord molecular markers in *sneezy* embryos. Wild-type embryos (A, C and E) and *sneezy* mutant embryos (B, D and F) stained for the expression of *ntl* (A, B), *col2α1* (C, D) and *shh* (E, F) at 32 hpf. While in wild-type siblings the expression of early notochord markers has ceased, in the mutants expression persists.

3.2 Identification of the protein encoded by *sneezy*

Since no obvious candidate genes for *sneezy* existed, it was necessary to undertake a positional cloning project. However, data concerning the cell-autonomy of the gene would be helpful for screening potential candidate genes. Therefore, I decided to test first the cell-autonomy directly using transplantation methods.

3.2.1 *sneezy* is shield derivatives autonomous

The zebrafish dorsal organiser, the embryonic shield, gives rise to the hatching gland, prechordal plate, notochord and floorplate (Saude et al., 2000). When a shield is

transplanted to the ventral side of another embryo, it gives rise to a new complete secondary axis, in which the donnor tissue produces the normal shield derivatives. (Saude et al., 2000). In addition, under the correct conditions, the donor embryo lacking a shield will regenerate shield derivatives and develop normally (Saude et al., 2000).

Using this technique, chimeras were generated to test whether the *sneezy* gene is autonomous to the shield-derived tissue, or not. Mutant shields were transplanted into the ventral side of wild-type embryos and vice-versa. When *sneezy* mutant shields were transplanted into wild-type host embryos, the notochords in the secondary axes fail to form vacuoles normally, i.e., they were mutant (Fig.3.2 G and H). Similarly, wild-type shields transplanted into *sneezy* mutant host embryos produce wild-type notochords (Fig.3.2 D and E).

The findings described above indicate that the *sneezy* gene has to expressed either in the shield or in shield-derivative tissue. Therefore, any candidate gene identified by positional cloning has to satisfy this condition.

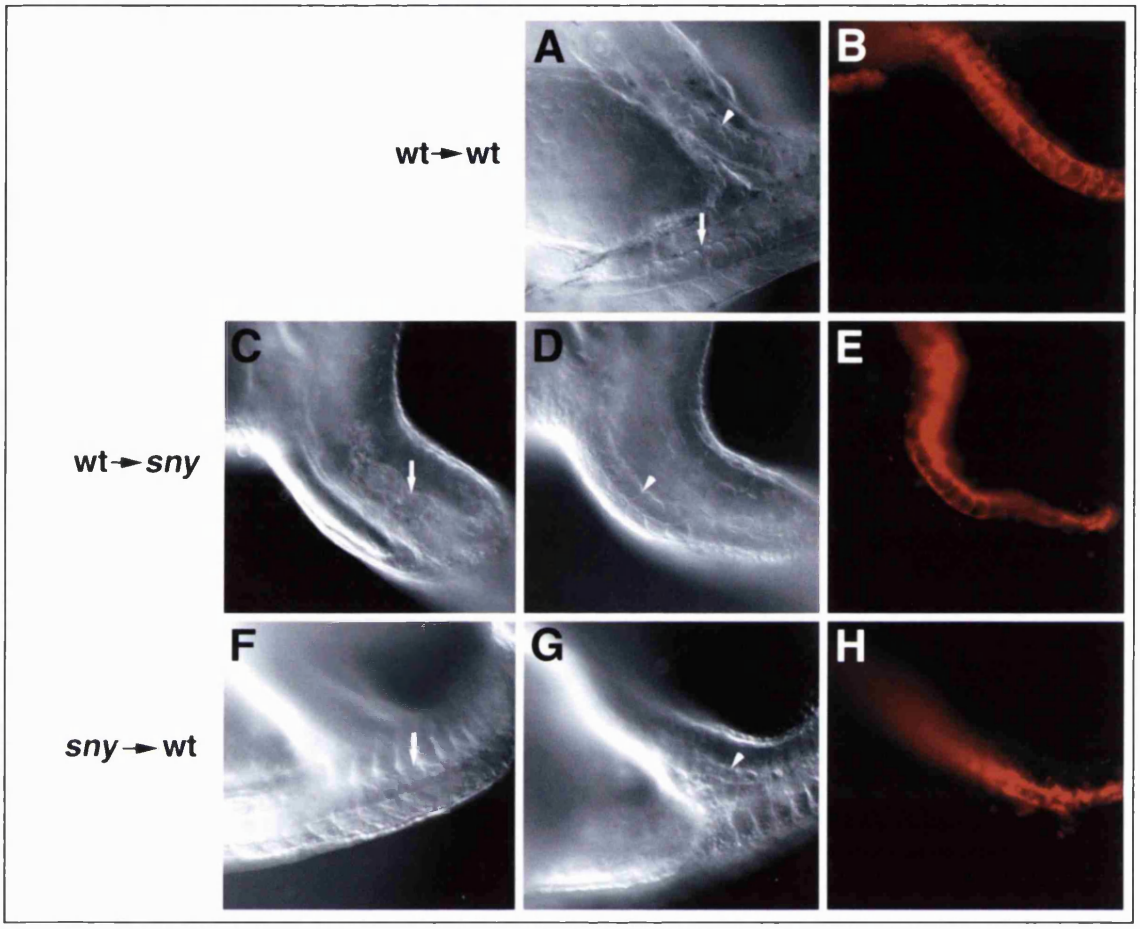

Figure 3.2. *sneezy* functions autonomously within the shield derivatives. Wild-type shields taken from Rhodamine-dextran labelled embryos transplanted into the ventral margin of wild-type (A, B) or *sneezy* host embryos (C-E) give rise to secondary axes with wild-type notochords (white arrowhead in (D)), as seen by Nomarski (D) and fluorescence (E). Reciprocally, labelled *sneezy* shields transplanted into the ventral margin of wild-type embryos (F-H) give rise to secondary axes with mutant notochords (white arrowhead in (G)), as seen by Nomarski (G) and fluorescence (H). In (C) and (F) the white arrows point to the notochords of the primary axes.

3.2.2 Positional cloning of *sneezy*

To identify the gene underlying the *sneezy* mutation I used the *sneezy*^{m456} allele from the Boston screen (Stemple et al., 1996) in an AB stock background. Heterozygous *sneezy*^{m456} carriers were crossed with wild-type fish of the WIK strain (Fig.3.3). The WIK strain was chosen because AB and WIK are polymorphic with respect to the majority of the genomic markers available.

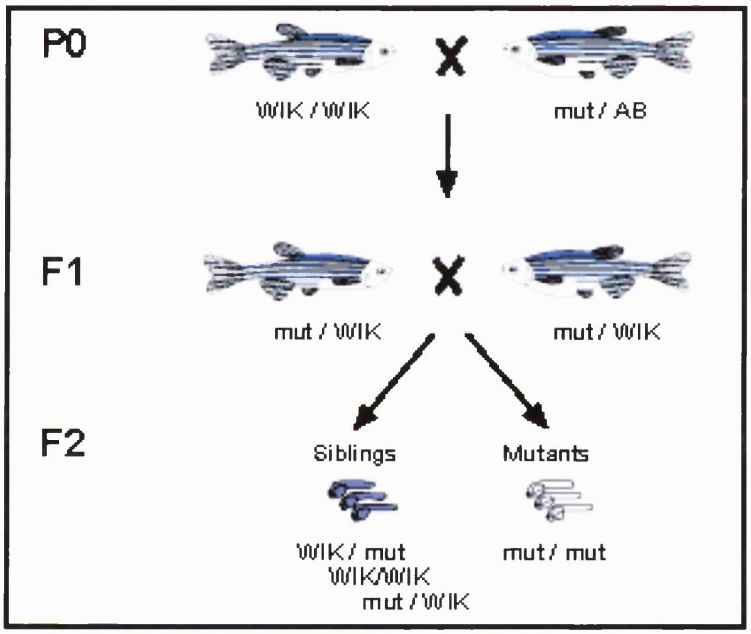

Figure 3.3. Generation of heterozygous *sneezy* carriers. Wild-type WIK fish were crossed with AB *sneezy* carriers (P0) to generate heterozygous *sneezy* carriers (F1). The genomic DNA of the mutant progeny of (F1) fish is AB around the mutant locus. Figure adapted from www.eb.tuebingen.mpg.de

Gynogenetic half-tetrad diploid embryos (EP) were generated from hybrid female carriers and used in conjunction with centromeric SSLP markers to define the linkage group that contains the *sneezy* locus. After testing centromeric markers, I found sneezy

to be linked to z4300, on linkage group 2 (Fig.3.4). In addition, the frequency of gynogenetic half-tetrad diploid mutants suggested that the *sneezy* locus is at 34.5cM ± 8.6cM from the centromere (Streisinger et al., 1986) (Table 3.2).

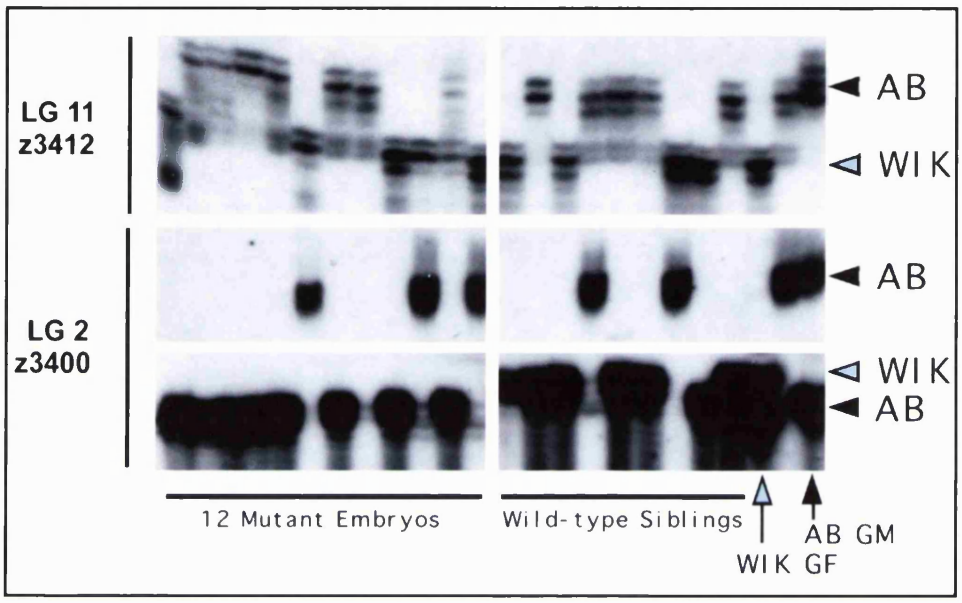

Figure 3.1. The *sneezy* locus is in linkage group 2 (LG2). Centromeric linkage analysis of gynogenetic half-tetrad diploid embryos shows that the *sneezy* locus is linked to z4300 (a centromeric SSLP for LG2) (C-F), since all mutant EP embryos display the z4300 AB alleles (C and E), while wild-type EP siblings have both the AB and WIK alleles (D and F). (A and B) are an example of a centromeric SSLP that is not linked to the *sneezy* locus. Both mutant (A) and wild-type (B) EP embryos have the Z3412 AB and WIK alleles.

Table 3.1. Distance from the *sneezy* locus to the centromere of LG2.

	Number of wild-type GH-TDs embryos	Number of *sneezy* GH-TDs embryos	Average distance from the *sneezy* locus to the centromere	Standard deviation
Experiment 1	*40*	*9*		
Experiment 2	*19*	*5*		
Experiment 3	*87*	*9*		
Experiment 4	*119*	*10*		
			34.5 cM	8.6 cM

The distance between a recessive mutation and the centromere is calculated from the frequency of half-tetrad mutants. The frequencies of non-recombinant half tetrads and mutant half-tetrads is the same, therefore the frequency of recombinant half-tetrads is 1-2f, where f represents the frequency of mutant half-tetrads. In a meiosis with a single cross-over between the mutation and the centromere, only one of the two chromatids in each half-tetrad is a recombinant chromatid, thus the frequency of recombinant chromatids is half the frequency of recombinant half-tetrads, i.e., (1-2f)/2. Using this formula and the results of four independent experiments, the average distance from the *sneezy* locus to the centromere and the standard deviation of these distances were calculated.

Knowing that the *sneezy* locus is on LG2, I subsequently used the available CA repeat markers to find the smallest interval containing the mutant locus. Previous work in the lab had localised another mutation, *sleepy*, to linkage group 2. Hence I had z10838, z8448 and z21490, three CA repeat markers I knew to be polymorphic between AB and WIK strains. By linkage analysis using z10838 and 48 *sneezy* mutant embryos, from hybrid parents, I found *sneezy* to be linked to z10838 (Table 3.3) at 5.2cM. Furthermore, using z10838, z8448, z21490 and z11023 and the fact that in zebrafish multiple cross-overs are extremely rare, I was able to conclude that the *sneezy* locus is centromeric relatively to these markers (Table 3.3). Hence, among the markers tested the smallest interval containing the *sneezy* locus was defined by the flanking CA repeat markers, z11023 and z7632 (Table 3.3)

Table 3.2. The *sneezy* locus is flanked by the CA repeat markers z11023 and z7632.

L44.12	1...12	13...24	25...36	37...48
Z10838	2112100101122	11111111211	010011111111	111111211110
Z8448	2111100101122	011111111210	011111101111	111111211110
Z21490	111010010111	011111111211	011111111111	011111211110
Z11023	111100010111	011111011211	111111111101	111111111110
sneezy	111111111111	111111111111	111111111111	111111111111
Z7632	111110010111	011121111111	011111111111	011111112100

Each column represents a mutant embryo. The numbers in the columns represent the z-marker alleles that a specific embryo has. The (**0**) alleles represent a reaction that did not work, the (**1**) alleles represent homozygous AB and the (**2**) represent heterozygous AB and WIK.

To increase the mapping resolution, I screened approximately 1500 mutant embryos and found the interval defined by these two marker to be approximately 3.3cM. Between *sneezy* and z7632, I initially found 68 recombinations and between *sneezy* and z11023, I found 23 recombinations. Assuming that the crossing-over rates are not sex-dependent, these recombination numbers place z11023 and z7632 at 0.8cM and 2.47cM away from the *sneezy* locus, respectively (Fig.3.5).

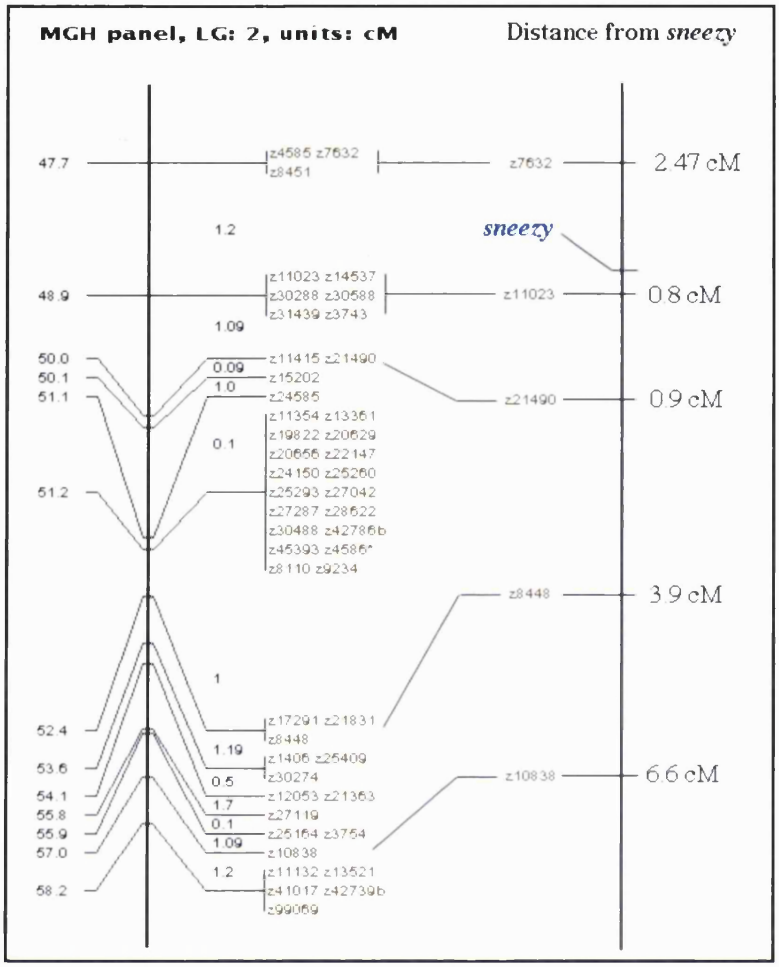

Figure 3.5. The *sneezy* CA repeat markers map. Linkage analysis using CA repeat markers from meiotic maps like the MGH panel, identified z11023 and z7632 as the closest CA repeat markers flanking the *sneezy* locus.

3.2.2.1 A chromosome walk narrows the search down to a YAC clone

In the interval that contains the *sneezy* locus there were three identified markers: the two CA repeat markers defining the interval and a gene, *elav related A* (*elrA*). Using oligonucleotides for all three markers, a YAC library was screened by PCR and a few positive YACs for each marker were obtained. The next step was to rescue the ends from

each YAC, sequence them, design oligonucleotides to amplify corresponding genomic intervals, sequence the corresponding AB and WIK alleles of those and look for polymorphisms.

In one YAC, 75G10, which was positive for *elrA*, one of the ends, 75G10-T3, was polymorphic, allowing the development of restriction fragment length polymorphism (RFLP). A test of the recombinant mutant embryos, identified only 2 recombinations between that marker and the *sneezy* locus, placing it at 0.069cM away from the *sneezy* locus. Analysis of the mutants that had the recombinations revealed that 75G10-T3 is in the same side of *sneezy* as z11023. From the other end of the insert of 75G10, 75G10-T7, which was not polymorphic, another YAC, 19G3, was identified by screening the YAC library.

The sequence of the insert end 19G3-T3, revealed a new SSLP marker. Using this SSLP, I found that between 19G3-T3 and the *sneezy* locus there was only one recombination out of 2746 meioses and that 19G3-T3 and 75G10-T3 flanked the mutant locus. 19G3-T3 was approximately 0.036 cM away from the *sneezy* locus. At this point, I had determined a YAC containing the *sneezy* locus, 75G10 and had a 0.1 cM interval containing the locus (Fig.3.7).

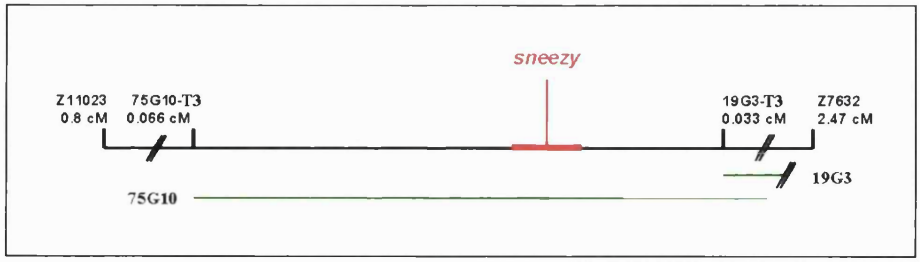

Figure 3.6. The *sneezy* YAC walk diagram. The YAC inserts are represented by green lines. The genomic region containing *sneezy* is represented in red. Polymorphic markers are represented by their names on top of the black line that represents a larger genomic interval containing *sneezy*.

3.2.2.2 *sneezy* does not encode the zebrafish elav related A

The product of the *elrA* gene belongs to a large family of proteins that are thought to bind RNA and function in post transcriptional regulation. In zebrafish, *elrA* is expressed in all adult tissues and at all developmental stages (Good, 1995), with higher levels of expression in the anterior nervous system at 24 hpf (Fig.3.7).

Figure 3.7. Expression pattern of *elrA* in wild-type embryos, at 24 hpf. The staining for *elrA* is ubiquitous, but not uniform. There is a much higher level of staining in the anterior nervous system.

Between 75G10-T3 and 19G3-T3 only one gene was mapped, *elrA*. To find if *elrA* was the gene mutated in *sneezy*, I tried to develop SSLP markers for *elrA* from its mRNA sequence, without any success, so I had to sequence the mutant and wild-type AB alleles of *elrA* and compare them. No aminoacid differences were found between the two alleles, therefore ruling out *elrA* as a good candidate.

3.2.2.3 A contig of three PACs covers the *sneezy* locus

The strategy for the PAC walk was the same as the one applied for the YAC walk. The only differences were technical, i.e., for PACs, the insert ends do not have to be rescued, since it is possible to sequence directly from PAC DNA. The flanking polymorphic markers, 75G10-T3, 19G3-T3 and the gene *elrA* were used to screen the PAC library by PCR. From one of the positive PAC identified using the 75G10-T3 marker, 224O12, a new RFLP was developed, 224O12sp6. The only recombinations for this RFLP were those that had already been identified for 75G10-T3, placing it at the same genetic distance from *sneezy* as 75G10-T3. Oligonucleotides for 224O12sp6 amplified from 75G10 DNA, suggested that it was physically closer to *sneezy* than 75G10-T3.

Among the PACs identified from the PAC library screen with the two other markers, there was a common PAC, 134L16. Using this PAC another RFLP was developed, 134L16sp6. There was no recombination found between 134L16sp6 and the mutant locus in the recombinant mutant embryos, placing it extremely close to the mutation. At the same time, another SSLP, 238M4T7 was developed from one of the ends of 238M4 (a PAC identified using 224O12sp6 primers). Although all recombinant mutant embryos plus another 600 mutant embryos (corresponding to 2100 mutant embryos in total) were tested for recombination events using this marker, no recombination was found placing

this marker extremely close to the mutation, as well. Screening the PAC library with 238M4T7 led to the identification of a PAC, 143A1, that had also been identified for *elrA*. In conclusion, the three PACs, 238M4, 143A1 and 134L16, form a contig covering the *sneezy* locus and there are two polymorphic markers in the middle PAC, 238M4T7 and 134L16sp6, for which no recombination between them and the *sneezy* locus was found (Fig.3.8). I then sought to determine all genes on the central PAC by shotgun sequencing.

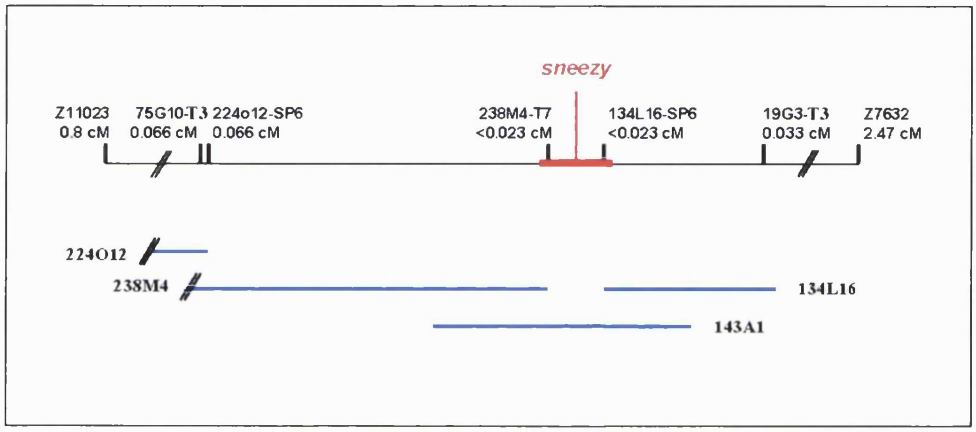

Figure 3.8. The *sneezy* PAC diagram. The PAC inserts are represented by blue lines. The genomic region containing *sneezy* is represented in red. Polymorphic markers are represented by their names on top of the black line that represents a larger genomic interval containing *sneezy*.

3.2.2.4 Shotgun sequencing of a PAC identifies genes closely linked to *sneezy*

238M4T7 and 134L16sp6 were very close to the mutation and neither end of the insert of the middle PAC, 143A1, was polymorphic; they were however genetically linked by RH mapping, therefore I decided to sequence 143A1. A shotgun library from 143A1 was generated for sequencing. PAC DNA was sheared by pressure, the fragment

ends were then filled in to generate blunt ended fragments. These fragments were cloned and the plasmids electroporated into competent *E.coli.* Insert containing clones were selected at random and sequenced using an ABI 377 automatic sequencer. The strategy to identify the mutated gene was to sequence only as much of the PAC as necessary. As an internal control for the percentage of the PAC insert sequenced, I estimated the amount of the sequenced PAC (Fig.3.9). Sequencing to 50% completion corresponded to ~ 60Kb of PAC insert sequenced. At this level of coverage I identified three distinct genes: *coatomer subunit a* (*copa*); *translocation protein 1* (*tloc1*) and *apolipoprotein D* (*apoD*). In addition, the PAC end 134L16sp6 contained an exon for *peroxisomal farnesylated protein* (*pxf*).

The peroxisomal farnesylated protein functions in peroxisome membrane synthesis (Sacksteder et al., 2000). The coatomer subunit α, translocation protein 1 and apolipoprotein D are all proteins involved in intracellular transport. α-COP protein is involved in transport in the early secretory pathway, within the Golgi complex and between the endoplasmic reticulum and the Golgi complex. The apoD protein is thought to be a multi-ligand, multi-functional transporter. It is able to bind molecules *in vitro* like cholesterol, progesterone, pregnenolone, bilirubin and arachidonic acid. The apoD accumulates at sites of regenerating peripheral nerves and in the cerebrospinal fluid of patients with neurodegenerative conditions, such as Alzheimer's disease. Therefore, it is thought to be involved in maintenance and repair within the central and peripheral nervous systems (Rassart et al., 2000). The last gene encodes tloc1, which is the vertebrate homologue of SEC62p, a protein that constitutes an essential component of the Sec-complex. In *Saccharomyces cerevisiae* SEC62p is responsible for post translational protein translocation across the membrane of the endoplasmic reticulum (Wittke et al., 2000).

Using a new method to disrupt gene function, I tested some of theses genes to determine which corresponds to *sneezy*.

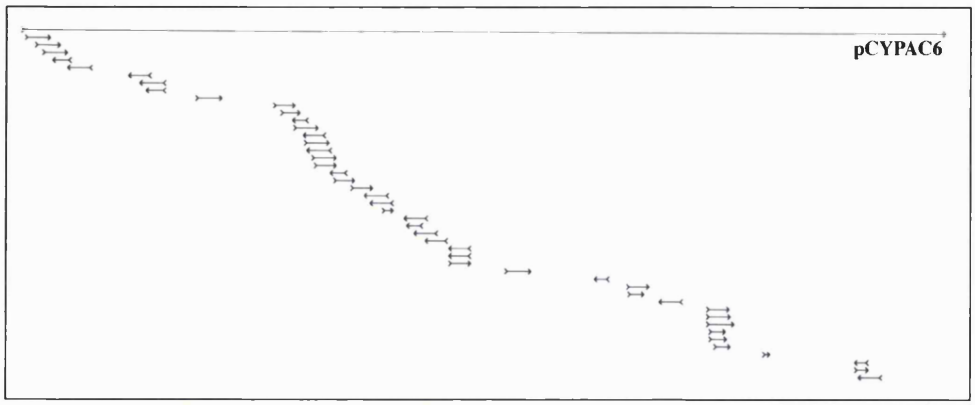

Figure 3.9. pCYPAC vector as a control. The percentage of PAC vector sequenced is a good estimate of the percentage of the PAC insert that has been sequenced. In addition, the distribution of the fragments sequenced in pCYPAC indicates the quality of the shotgun library.

3.2.2.5 Antisense morpholino oligonucleotide injection identifies *copa* as the *sneezy* gene

Anti-sense morpholino oligonucleotide (MOs) provide a simple means to disrupt gene function in early zebrafish embryos. To test the candidate genes identified by sequencing I initially generated MOs against the start of translation of the *pxf* and *copa* genes.

Embryos microinjected with *pxf* morpholino showed some defects. The defects were different, however, from those that characterise *sneezy* mutant embryos, for example the notochords of *pxf*-MO injected embryos were wild-type. By contrast, injection of *copa* morpholino (*copa*-MO) completely phenocopied *sneezy* mutant embryos (Fig.3.10-12).

The notochords of *copa*-MO injected embryos do not differentiate properly as assessed by the absence of large vacuoles (Fig.3.10-12) and maintenance of expression of early chordamesoderm genes like *copa* (Fig.3.20). In addition, they show severe reduction in pigmentation, absence of developing fins and prior to death they undergo generalised degeneration (Fig.3.12).

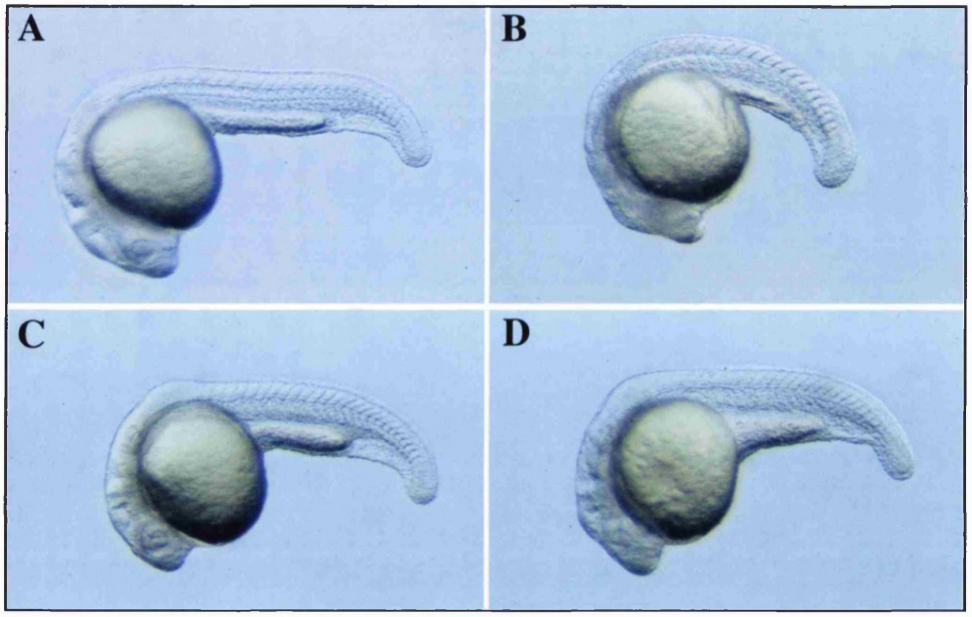

Figure 3.10. *copa*-MO injected embryos phenocopy the *sneezy* mutation at 24 hpf. At 24 hpf, the notochord of wild-type embryos (A) has differentiated, while in *pxf*-MO (B), *copa*-MO (C) and *sneezy* embryos (D) it has not. *copa*-MO (C) and *sneezy* mutant (D) embryos have the same body shape.

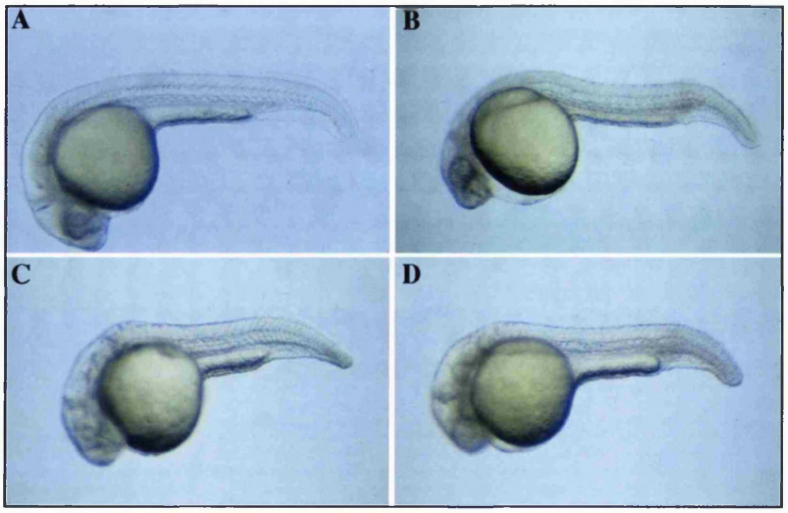

Figure 3.11. *copa*-MO injected embryos phenocopy the *sneezy* mutation at 32 hpf. At 32 hpf, the notochord of *pxf*-MO (B) has differentiated, while in *copa*-MO (C) and *sneezy* embryos (D) it has not. *copa*-MO (C) and *sneezy* mutant (D) embryos have the same body shape. Wild-type (A) and *pxf*-MO (B) embryos develop fins, while *copa*-MO (C) and *sneezy* mutant (D) embryos do not.

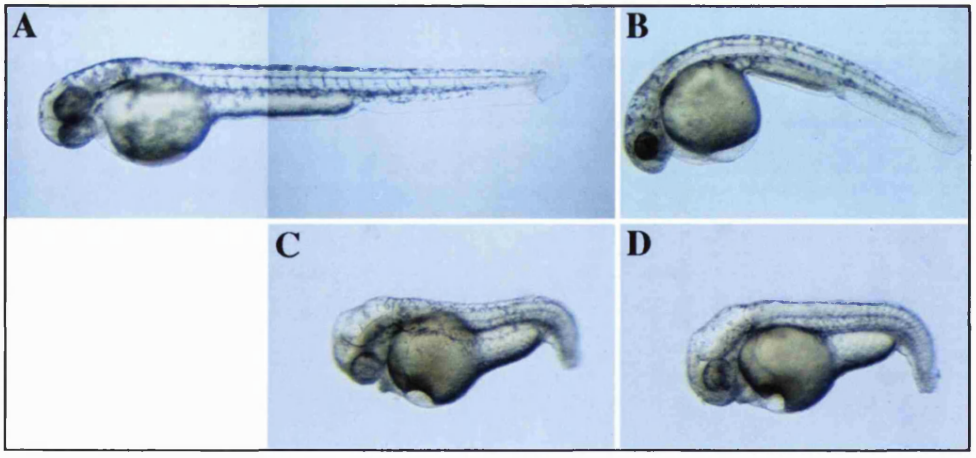

Figure 3.12. *copa*-MO injected embryos phenocopy the *sneezy* mutation at 48 hpf. At 48 hpf, *pxf*-MO (B) embryos have normal pigmentation, while *copa*-MO (C) and *sneezy* embryos (D) have a severe reduction. *copa*-MO (C) and *sneezy* mutant (D) embryos have the same body shape. *copa*-MO (C) and *sneezy* mutant (D) embryos have not developed fins, in contrast to wild-type (A) and *pxf*-MO (B) embryos.

3.2.2.6 The *copa* gene is mutated in *sneezy*

The *copa* gene is very closed linked to the *sneezy* locus. In addition, MOs designed against the *copa* start of translation phenocopy the *sneezy* mutation. Subsequently, I decided to directly sequence *copa* cDNA from mutant and wild-type sibling embryos to see if any mutation in the coding region could be found.

Using the human and the bovine *copa* cDNA sequence, GenBank was searched for zebrafish ESTs of *copa*. Among the ESTs, there was no indication of the existence of more than one *copa* paralogue in zebrafish. In addition, from contigs generated using the EST sequences, the 5' untranslated (5'UTR) and 3' untranslated (3' UTR) ends were identified, as well as the majority of the coding sequence for the gene. To fill in the gaps, reverse transcriptase polymerase chain reaction (RT-PCR) was used to amplify the missing intervals. These were then cloned into appropriate vectors, processed and sequenced (Fig.3.13).

The zebrafish *copa* gene (Fig.3.14) encodes a protein with seven WD40 domains at the N-terminus and is highly conserved with other vertebrate α-COP proteins (Fig.3.15-16). The WD40 domains are protein-protein interaction domains that generate a toroid like structure when the protein is assembled (Fig.3.17). This domain has been shown to be required for α-COP function in KKXX traficking in the early secretory pathway (Eugster et al., 2000).

GAATCAAACACGCAAAGTCCCTTCCTACCGGGGGATGATTTTAGGCTTCTAATTCGCATAAACGGATCAATATCTTCACACATAACAC
ATTCCTGTTAATTTTACATTATCAGTGGAGATGTTGACCAAATTTGAGACAAAGTCGGCCCGAGTGAAAGGGCTGAGTTTCCATCCAA
AGCGGCCCTGGATACTCGCTAGTTTGCACAATGGTGTCATCAGCTGTGGGATTATCGCATGTGCACTCTAATCGACAAGTTTGATGAA
CACGATGGTCCAGTCAGAGGTATTGACTTTCATAAGCAGCAGCCTCTGTTTGTGTCTGGAGGAGATGACTACAAGATCAAGGTTTGGA
ACTACAAGCTGCGTCGATGTCTTTTCACTCTTCTTGGACATCTTGACTACATTCGCACCACATTCTTCCACCATGAGTACCCCTGGAT
CTTGAGTGCTTCAGATGATCAGACTATTCGTATTTGGAACTGGCAGTCCAGGACGTGTGTCTGTGTGCTGACGGGACATAATCATTAT
GTGATGTGCGCACAGTTCCATCCCTCTGAGGACCTGGTGGTGTCGGCAAGCTTGGATCAGACTGTGCGCGTGTGGGATATTTCCGGTC
TGAGAAAGAAGAACTTATCTCCGGGTGCTGTGGACACTGAGGTGCGCGGCATCTCTGGTGTCGACCTGTTTGGAGCCTCTGATGCAGT
AGTCAAACATGTTCTGGAGCAGGGTCATGATCGAGGCGTAAACTGGGCAGCTTTCCATCCTAGCATGCCTCTTATTGTGTCAGGAGCC
GATGACCGGCAGGTGAAGATTTGGAGGATGAATGAGTCTAAAGCATGGGAGTTGGACACCTGTCGAGGACACTACAACAATGTGTCCT
GTGCGGTGTTTCACCCCCGTCAGGAGCTCATTCTGTCCAACTCTGAGGACAAGAGCATCCGTGTGTGGGATATGTCCAAGAGAACAGG
CGTCCAGACCTTTCGCAGAGATCACGACCGCTTCTGGGTTCTGGGTGCTCACCCCAACCTCAACCTGTTTGCTGCTGGCCATGACAGT
GGAATGCTGGTGTTTAAACTGGAAAGGGAACGTCCAGCTTATGCAGTGTATGGCAACATGCTTTACTATGTAAAGGATCGTTTCCTGC
GTCAGCTCGACTTTAACAGCAGTAAAGATACAGCTGTGATGCAGCTACGCAGTGGATCCAAATTCCCAGTGTTCAGCATGTCCTACAA
CCCAGCGGAAAATGCTGTGCTGTTGTGCACTAGAGCTACTAATTTGGAAAACAGCACCTATGATCTGTACTCCATTCCCAGAGAGAGT
GACTCCCAGAATCCTGATGCTCCTGAGGGAAAACGCTCCTCTGGTCTGACTGCAGTTTGGGTGGCCAGGAACCGATTTGCTGTACTTG
ACCGCATGCACTCTCTCTTGATAAAGAACCTGAAGAATGAGATTGTGAAGAAGGTCCAGGTCCCGAGCTGTGAGGAGATTTTCTATGC
TGGAACTGGCTCACTCCTGCTGCGGGATGCTGAAGGAGTCACTCTATTTGATGTCCAGCAGAAGCGCTCTCTGGCCACGGTCAAAATA
GCCAAAGTCAAATATGTGGTGTGGAGCTCCGACGCCAACCACGTGGCCCTGCTGGCCAAACATGCCATCATGATCTGCAACAAGAAGT
TAGAGAGTCTCTGCAACATCCATGAGAACATCCGGGTGAAGAGTGGAGCCTGGGCTGAGAATGAAGTCTTCATCTACACCACCTCCAA
CCATATCAAATATGCTCTGACTTCTGGCGATCATGGTATAATCCGTACATTGGATCTGCCCATCTATGTGACAAGAGTGAGGGGTAAC
AGTGTTTATTGCCTGGATCGGGAGTGCAGACCACGTGTGCTTAACATTGACCCCACCGAGTACCGCTTTAAACTGGCTCTGGTCAACC
GCAAATATGAAGAGGTTCTTCACATGGTGCGTAATGCTAAGCTAGTAGGCCAGTCCATCATTGCCTACCTACAAAAGAAGGGCTACCC
AGAGGTCGCGCTGCATTTCGTCAAAGATGAGAAGACYCGTTTCAGTTTGGCACTGGAGTGTGGAAACATTGAGGTGGCGCTGGAGGCT
GCAAAAGCCCTAGATGAGCGAAGCTGTTGGGAGCGTCTTGGTGAGGCTGCACTTCTGCAGGGCCATCACCAGGTGGTGGAGATGTGCT
ACCAGAGAACCAAGAACTTTGACAAGCTCACATTTCTGTACCTCATCACTGGCAACCTGACAAAGCTCAGGAAGATGATGAAARATCGC
TGAGATAAGAAAGGACATGAGTGGACACTATCAGGGCGCTCTGTACCTGGGTGACGTCAGTGAGCGAGTGCGGATCCTCAAGAACTGT
GGGCAGAAGTCTCTAGCTTACCTGACCGCTGCCACTCACGGGATGGATGAGGAAGCTGAAGCCCTGAAGGAGACCTTTGACCTTGAAA
AAGAAATGGTGCCAGAGGTGGACCCCAACGCTCAACTGCTGCAGCCTCCACCTCCCATCAACCCTCTGGACACAAACTGGCCTTTGCT
CACAGTCTCCAAGGGCTTCTTTGAGGGAGCTATCGCTGCCAAAGGACGAGCAGGGCAGATGGTTGCTGATCTGGACATGGATGCTCCA
GGAGGAGAAGGGTGGGGAGAAGATGCAGAACTTCATTTGGATGAAGACGGCTTCATGGATGCTCAGGAGGGACTGGGTGATGAGGGAG
CCATTGGGAAAGACGACGGAGGAGGCTGGGATGTTGAAGAAGATCTGGATCTCCCACCAGAGCTGGACGTACCTTCTGTTGGTGGAGG
TGGCGCAGAGGGTGAAGGCTTCTTTGTGCCACCCACTAAGGGCACAAGCCCAACCCAGATGTGGTGCAACAACTCTCAGCTGTCAGTG
GATCACATACTGGCTGGCTCTTTTGAGACTGCTATGAGGTTACTACATGACCAGGTTGGCGTTGTTCAGTTTGGGCCATATAAGCAGC
TCTTCATGCAGACTTTGTCCCGCGGCCGCACCTGTTACCTGGGCCTGCCATCTTTGCCCTGCCTGCACAGTTTTCCCCTGAGGAACTG
GAAGGACAGCGGGCCTAAAGGAGGTCTGCCAGCAGTGGGTCTGCGTCTCGCTGACCTCATCTCTCGCCTGCAGCAGTGCTATCAGCTG
ACCACCTCAGGCCGATTCGAAGATGCCGTGGAACGCTTCAGAGCCATTCTCCTCTCCGTGCCTCTGCTCGTGGTCGACAACAAACAAG
AGATTGCAGAGGCCCAGCAGCTGATCACTATTTGTAAGGAGTATATTATTGGCCTCACGATGGAGACGGAGAGGAAGAAACTCCCTAA
AGACAGTCTTGATGAGCAGAAGAGAATTTGTGAGATGGCGGCGTATTTCACACACTGCAGTCTTCAGCCTGTCCACATGGTGTTGGTT
TTGAGAACGGCACTCAATCTTTTCTTCAAACTGCGCAACTTTAAAACTGCAGCAGGTTTTGCTCGCCGTCTGCTTGAGCTAGGCCCCA
AACCTGAAGTGGCACAGCAGACACGTAAAATTCTCGCTGCCTGTGAGAAGAGTCTGACAGATGCTCACCAGCTCAACTATGATCCCCA
CAATCCCTTCGACATCTGCGCAGCCTCTTACACTCCTCTGTACCGCGGGCGACCTGTAGAGAAATGTCCCTTGTCTGGAGCCTGCTAC
TGCCCCAAATACAAAGGAGAGGTCTGCAGGGTCACACAGGTAACTGAGATTGGGAAAGATGTGATCGGGTTGCGTGTCAGTCCACTGC
AGTTCCGCTGAACATATAAACGTGGATGAAAATAAACATGCTTCTCCACACATATGCTTTTCCTTTATAAGATGAAGTAATGAGATCT
TTTAAGATCAGAACGTGATTAAAAATATCTTGTTATGTGACTAAATACTCTGTGACTATCCTTTCTGTTACTACAGTATATCTGAGAG
CTCTACTGTCTGTATGCTTGCATTCATATGAATATCATAATAATAATAATTGTGCATCTGTCACTCAGTGCAAAACAAGTTTCTTTTT
TTTGTGAACTCTCTAAATATTAAAATAAAATTCTGGTAAACAAAATGTTTGGCTACTTAATTGTCATCAATTTATTGCCAGTAACTTA
AAATAAAACCCTAAATTGCTTAAAAAAAAAAAAAAAAAAACGATAAG

Figure 3.13. The zebrafish *copa* cDNA sequence. The start codon is in blue and the stop in red.

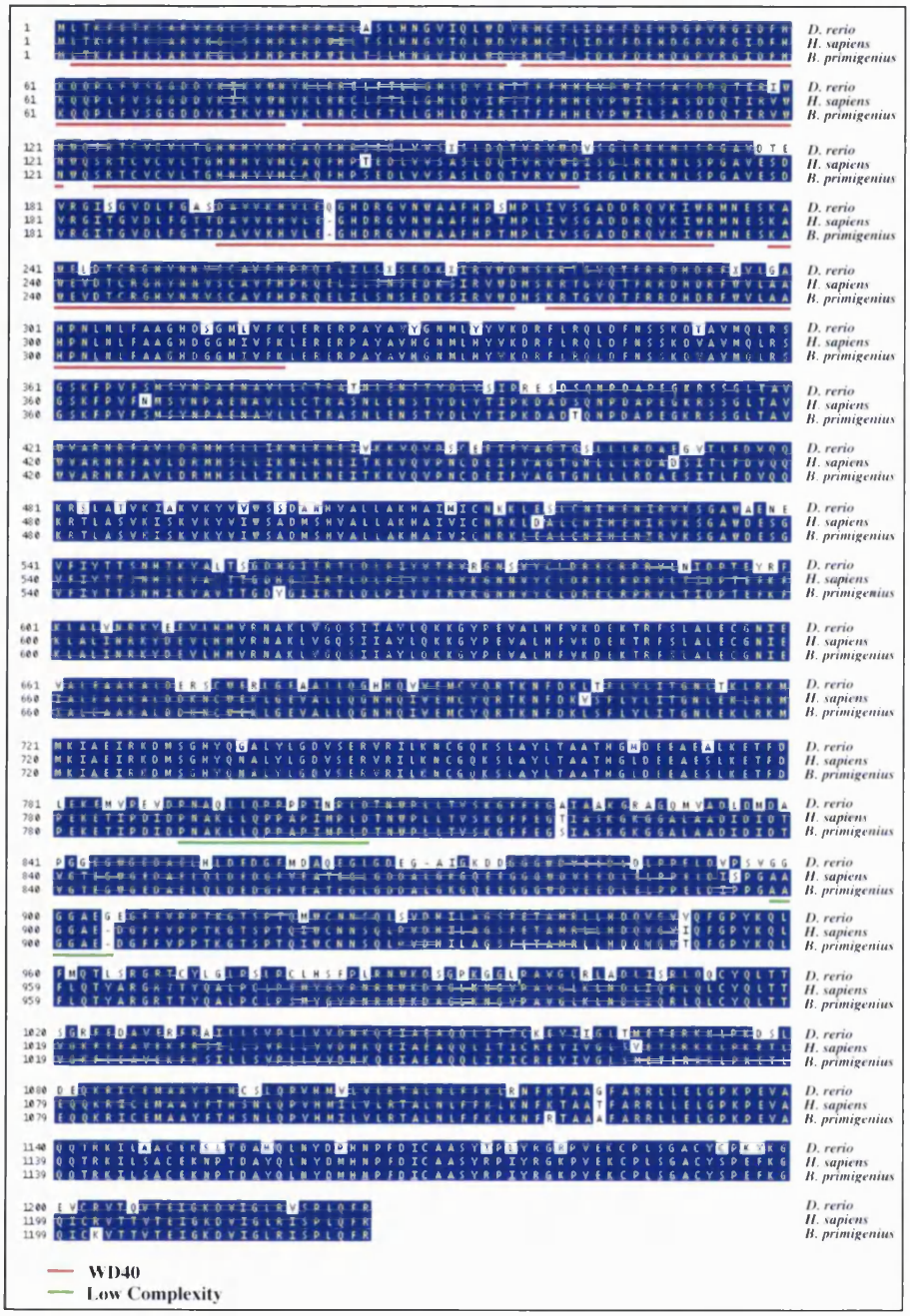

Figure 3.14. Protein comparison of zebrafish α-COP and other vertebrate α-COP proteins. The WD40 domains are underlined in red, while the low complexity regions are underlined in green.

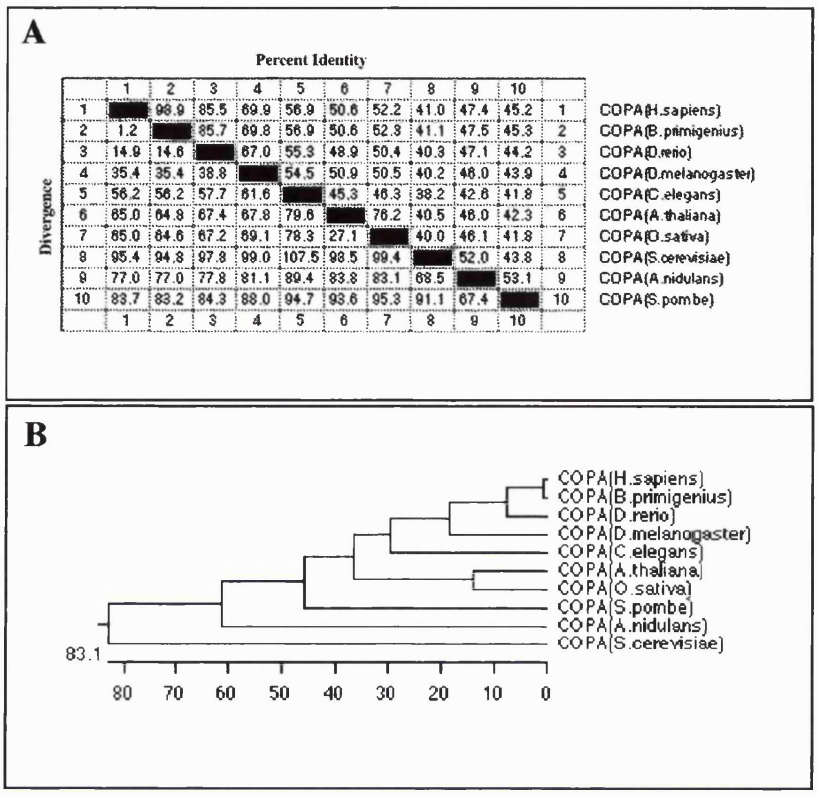

Figure 3.15. Comparison between the zebrafish α-COP and all the other known α-COP proteins. The α-COP proteins are quite well conserved across all species (A), particularly among vertebrates, as seen from a α-COP proteins phylogenetic tree (B).

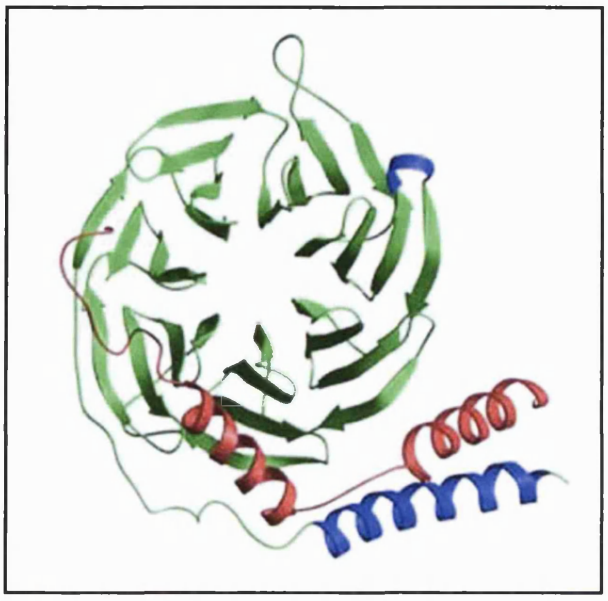

Figure 3.16. The seven WD40 domains in the N-terminus of α-COP form a toroid-like structure. Each set of three (different sizes and orientations) green arrows represents a WD40 domain. Adapted from www.cellsignal.com.

Sequencing of the *sneezy* and wild-type sibling *copa* cDNAs confirmed that the *sny*^{m456} allele contains a mutation. The sequence of two independent *sneezy copa* partial cDNA clones showed deletion of the same five nucleotides, GTGAG (Fig.3.17). This deletion results in a frameshift which leads to a premature stop codon and a shorter α-COP protein with 1117 aminoacids, instead of the 1225 found in the wild-type protein (Fig.3.18).

From mutation analysis in yeast, this mutation would be predicted to be functionally null: the C-terminus of α-COP is required for cell survival, as seen in *sneezy* mutants and in the yeast deletion mutant *ret1Δ1034-1201*. In addition, study of *ret1Δ1034-1201* also revealed that an approximately 170 residue C-terminal region of α-COP is required for interactions with coatomer subunit β' (β'-COP) and with coatomer subunit ε (ε–COP).

This region is necessary for incorporation of coatomer subunit α into the coatomer complex, contributing to the integrity of the α, β', and ε – COP sub-complex and of the coatomer as a whole (Eugster et al., 2000).

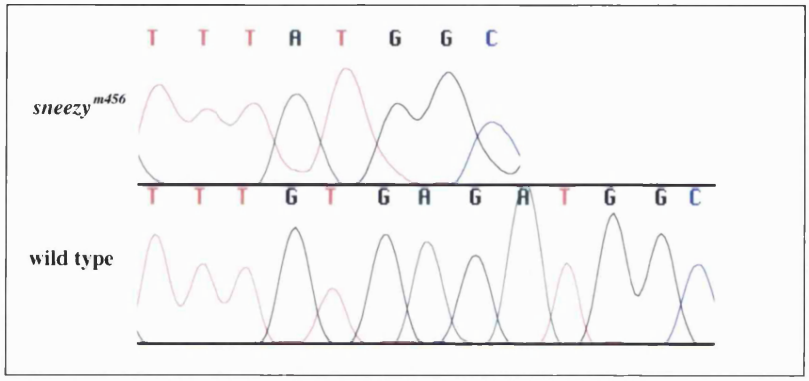

Figure 3.17. The *sneezy*^{m456} allele of *copa* has a five nucleotide deletion. The nucleotides GTGAG at position 1244-8 in the coding region of *copa* are deleted in *sneezy*^{m456}.

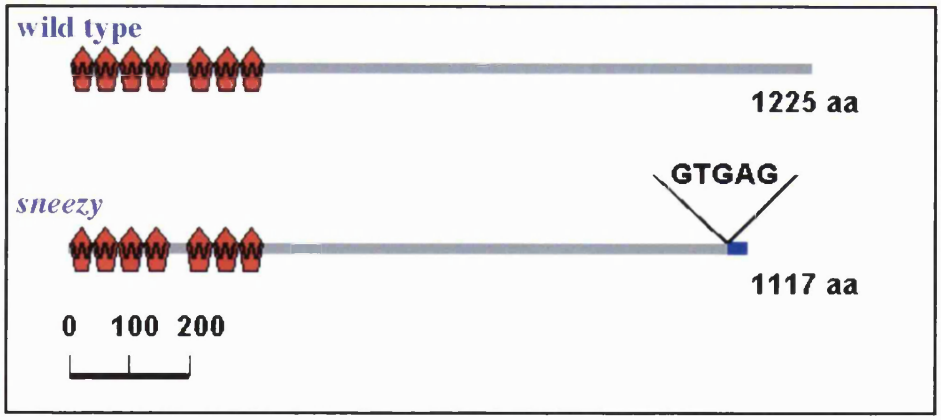

Figure 3.18. Comparison diagram of wild-type α-COP protein and *sneezy*^{m456} α-COP protein. The *sneezy*^{m456} α-COP has a small deletion that induces a frame shift that results in premature truncation of the protein.

3.3 *copa* expression during embryogenesis

The GenBank database contains several *copa* ESTs including fb13c12, corresponding to the RZPD clone WUSMp623F232. This plasmid was used to generate a 3' probe for whole-mount *in situ* hybridisation. *copa* was detected in all cells and at several distinct stages during the first 24 hpf (Fig.3.19). The detection prior to mid blastula transition (Fig.3.19.A), reveals that *copa* mRNA is maternally expressed. *copa* expression levels are uniform in all cells, later on, expression levels in the notochord are much higher than in the rest of the embryo, until 24 hpf, when the notochord differentiates. This high level of expression correlates with the role of the notochord as an active secretory tissue. As the notochord cells differentiate, the expression of *copa* is either down-regulated to indistinguishable levels from the levels in surrounding tissues, or ceases. Since it is ubiquitous, it is impossible in whole-mount *in situ* hybridisation to distinguish between these two possibilities.

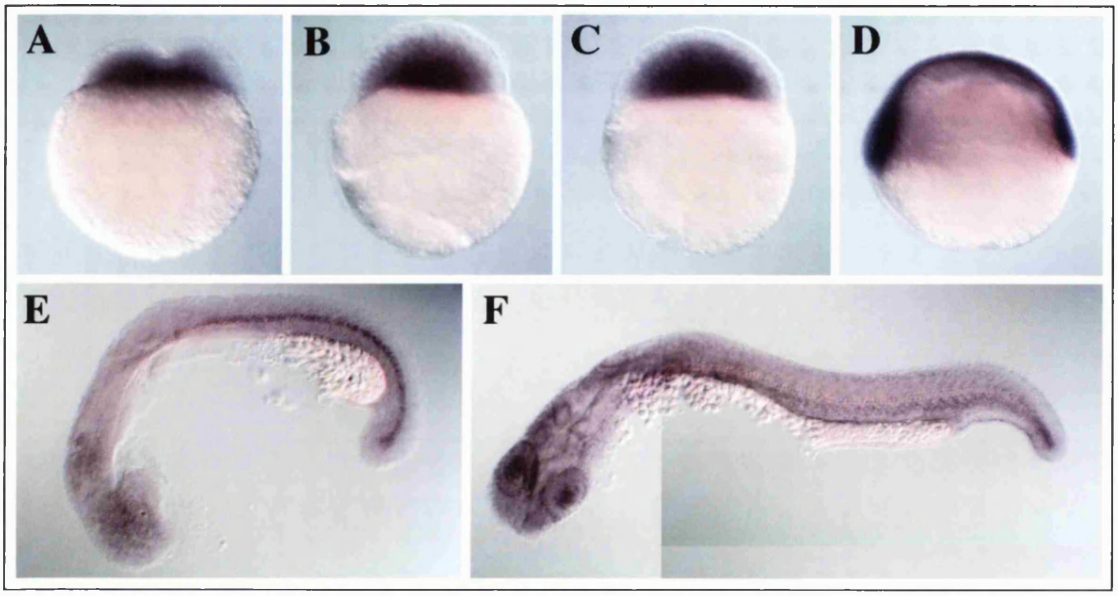

Figure 3.19. *copa* expression pattern in early zebrafish development. 4-cell stage embryos stained for *copa* expression (A) reveal that it is deposited in the egg by the mother. While the expression is ubiquitous at high (B), sphere (C) and shield (D) stages, at somitogenesis stages, like 20-somites (E), prior to notochord differentiation, it is highly expressed in the chordamesoderm (the notochord precursor). At 24 hpf (F), as the notochord differentiates, the levels of expression in the notochord become indistinguishable from these in the surrounding tissues.

The expression pattern of *copa* in *sneezy* mutant embryos revealed one difference from the expression pattern in wild-type siblings. In wild-type siblings notochord *copa* expression is down-regulated (Fig.3.20.A). By contrast, in *sneezy* mutant embryos levels of *copa* expression are maintained (Fig.3.20.B) reinforcing the notion that *sneezy* notochord does not differentiate properly.

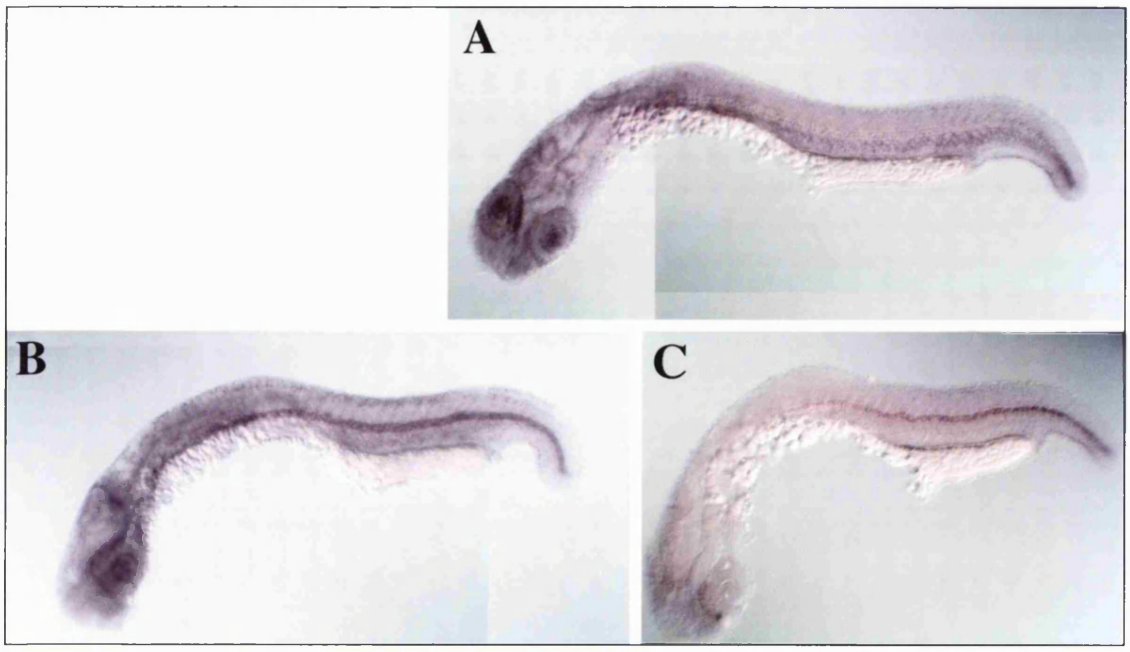

Figure 3.20. Comparison of the *copa* expression pattern between wild-type, *sneezy* mutant and *copa*-MO injected embryos, at 24 hpf. While in wild-type embryos, as the notochord differentiates, the expression of *copa* in the notochord is down regulated (A), in *sneezy* mutants (C) and in *copa*-MO injected (B) embryos, the expression in the notochord is maintained.

In conclusion, by positional cloning I have found that *sneezy* encodes the zebrafish α-COP. In addition, I have found that *copa* expression pattern correlates with a role for α-COP in the differentiation of the notochord. Based on this findings, I decided to investigate a correlation between α-COP function and the defects in *sneezy* mutant embryos.

Chapter 4 Cellular Characterisation of *sneezy*

4.1 Introduction

The protein encoded by *sneezy*, coatomer subunit α (α-COP), plays an important role in notochord differentiation, in formation of pigmented cells and in prevention of generalised degeneration, as seen in *sneezy* mutant embryos. In addition, coatomer subunit α is known to be required for vesicle transport in the early secretory pathway. An interesting question was how to correlate the defects found in *sneezy* mutants with α-COP function.

4.2 *sneezy* disrupts the early secretory pathway

α-COP is necessary for transport in the early secretory pathway. By analogy to studies in yeast, the *sneezy* α-COP protein should not be functional and therefore should lead to a block in the early secretory pathway when the levels of wild-type maternal protein become too low for normal function. This led me to investigate potential defects in the Golgi complex and endoplasmic reticulum (ER) using electron microscopy.

I found that cells of *sneezy* mutant embryo have severe defects in the morphology of the Golgi complex and endoplasmic reticulum (Fig.4.1-2). The endoplasmic reticulum (ER) is swollen while the Golgi complex is fragmented into large, round vesicles. The ER defect is found not only in notochord cells, but also in other cell types such as, for example, epidermal cells (Fig.4.3) and notochord cells adjacent to the notochord (Fig.4.4).

The intracellular defects found in the Golgi complex, endoplasmic reticulum and nuclear membrane seem to be a direct consequence of α-COP loss of function in *sneezy* mutant embryos. To prove this I decided to investigate notochord cell morphology in *sleepy* mutant embryos. The ER of *sleepy* mutant embryos is much thinner that wild-type siblings (Fig.4.2), further evidence that the defects found in *sneezy*, in the Golgi and ER, are not a consequence of the notochord's failure to differentiate. In addition, from the appearance of the ER, it seems that, in *sleepy* notochord cells, the levels of secretion are significantly lower than that of wild-types notochord cells.

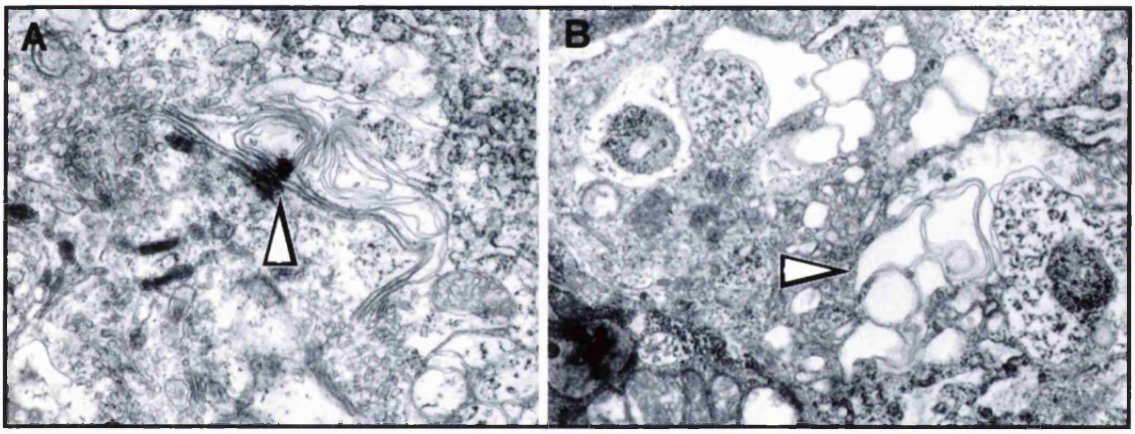

Figure 4.1. The Golgi complex is defective in *sneezy* mutant notochord cells at 32 hpf. In wild-type notochord cells (A), the Golgi complex has several cisternae and small vesicles are present near the extremities of the most trans Golgi cistern. In contrast, in *sneezy* notochord cells (B), the cisternae are completely replaced by these large vesicles. The white arrowheads point to Golgi complexes.

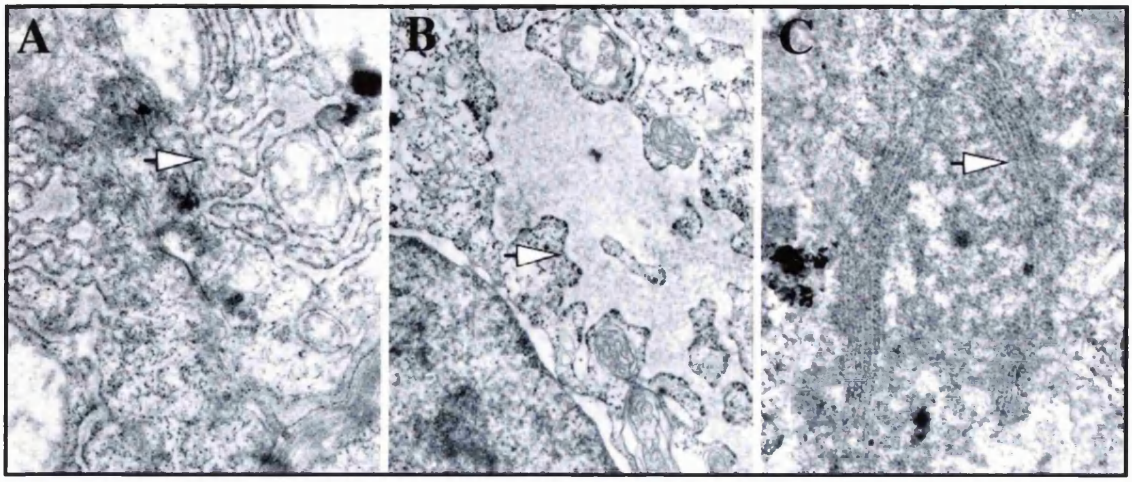

Figure 4.2. The endoplasmic reticulum in *sneezy* and *sleepy* mutant notochord cells at 32 hpf. While the ER of notochord cells in wild-type embryos is slightly enlarged (A), revealing high levels of secretion, in *sneezy* embryos, it is very swollen (B), revealing secretion problems. The ER of notochord cells in *sleepy* embryos is as shrunk (C) as it would be expected in wild-type cells with low levels of secretion. The white arrows point to the ER.

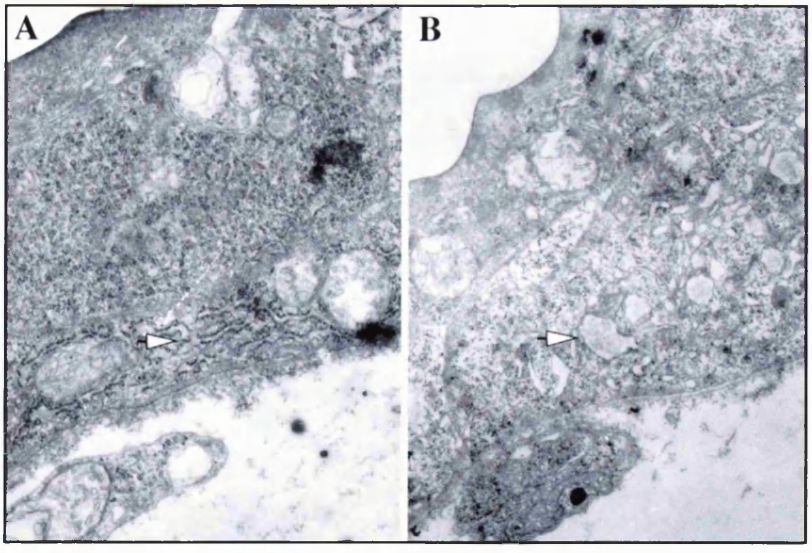

Figure 4.3. The endoplasmic reticulum is defective in *sneezy* dorsal epidermis cells at 32 hpf. Cells in the dorsal epidermis of *sneezy* mutant embryos have swollen ER (B) in comparison to wild-type ER (A) in the same cells. The white arrows point to the ER.

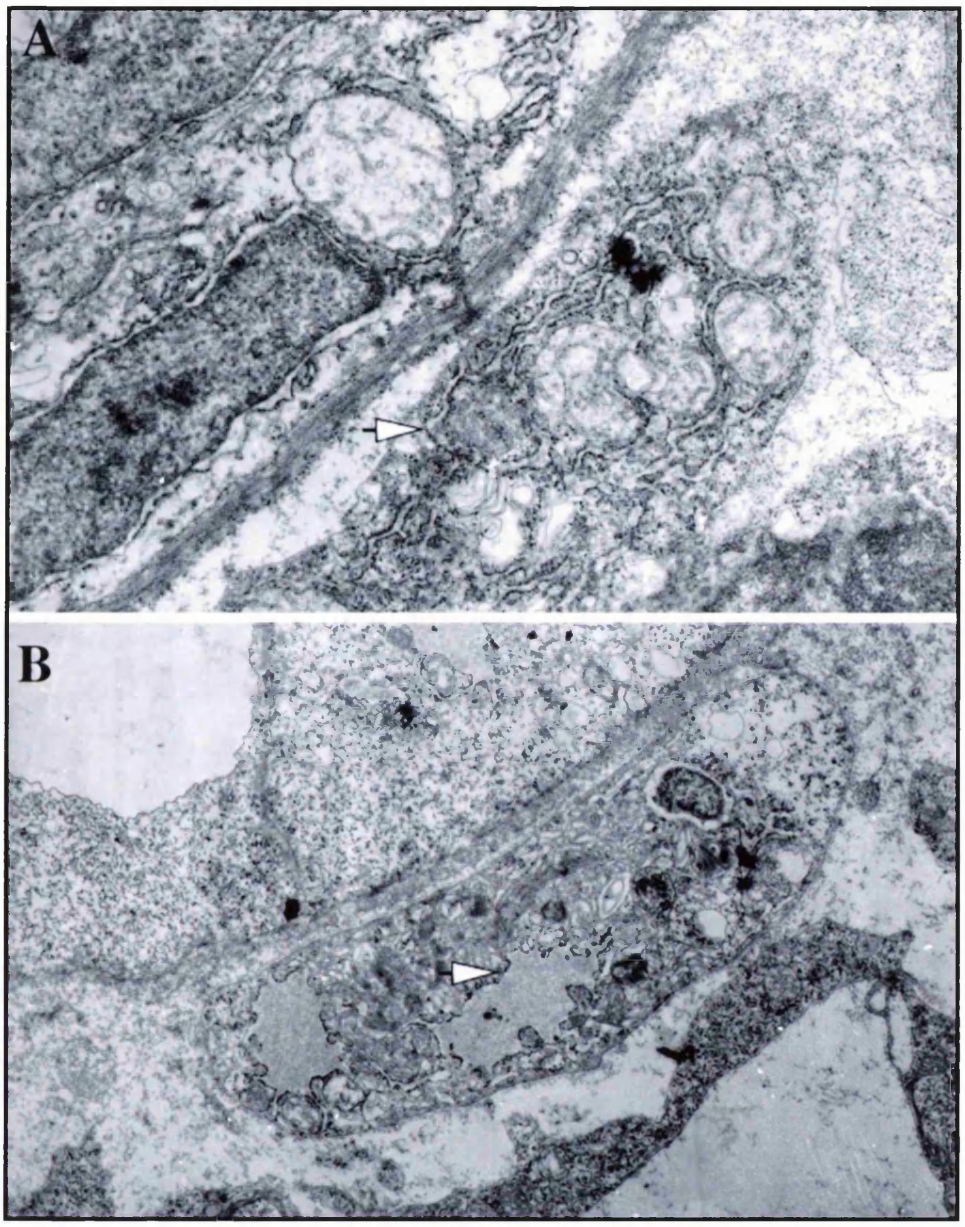

Figure 4.4. The endoplasmic reticulum is defective in *sneezy* notochord neighbour cells at 32 hpf. Cells adjacent to the notochord of *sneezy* mutant embryos have swollen ER (B) in comparison to wild-type ER (A) in the same cells. The white arrows point to the ER.

4.3 The perinotochordal basal lamina is defective in *sneezy* and *sleepy* embryos

The notochord differentiation mutations *sleepy, grumpy and bashful,* have genetic lesions in genes that encode laminin-1 chains (Appendix 1 and Mike Parsons, Steve Pollard and Derek Stemple; in preparation). Laminin-1 is the major component of the perinotochordal basal lamina. This led me to investigate, by electron microscopy, the status of the perinotochordal basal lamina in *sneezy* and *sleepy* embryos.

At 32 hpf, in wild-type embryos, the notochord is surrounded by a thick basal lamina showing at least two levels of organisation (Fig.4.5 A). While the inner sheath is made of ECM fibre bundles oriented perpendicular to the A-P axis, the external sheath seems to be made of fibre bundles oriented in parallel to the notochord.

In *sleepy* mutant embryos, at the same stage, there is no basal lamina sheath (Fig.4.5 C). Although it is possible to find small fragments resembling the inner sheath and other fragments of the ECM external sheath, the distribution of these fragments is not uniform around the perimeter of the notochord. In addition, it is possible to identify abnormal fibre bundles inside the notochord (Fig.4.6). It is not possible to tell whether these bundles are between or within the notochord cells.

At the same developmental stage, *sneezy* mutant embryos possess some perinotochordal basal lamina (Fig.4.5 B). The sheath is quite thin compared to wild-type and although there is some basal lamina, it resembles the external sheath and never the inner one. The basal lamina is uniformly distributed around the notochord perimeter. The absence of an inner sheath may reflect a loss of organisation or a temporal selective defect in the secretion of a necessary component for the formation of the inner layer of the perinotochordal sheath. Although the perinotochordal defect in *sneezy* mutant

embryos is not as severe as in *sleepy* mutant embryos, it may be one of the factors responsible for the notochord's failure to differentiate.

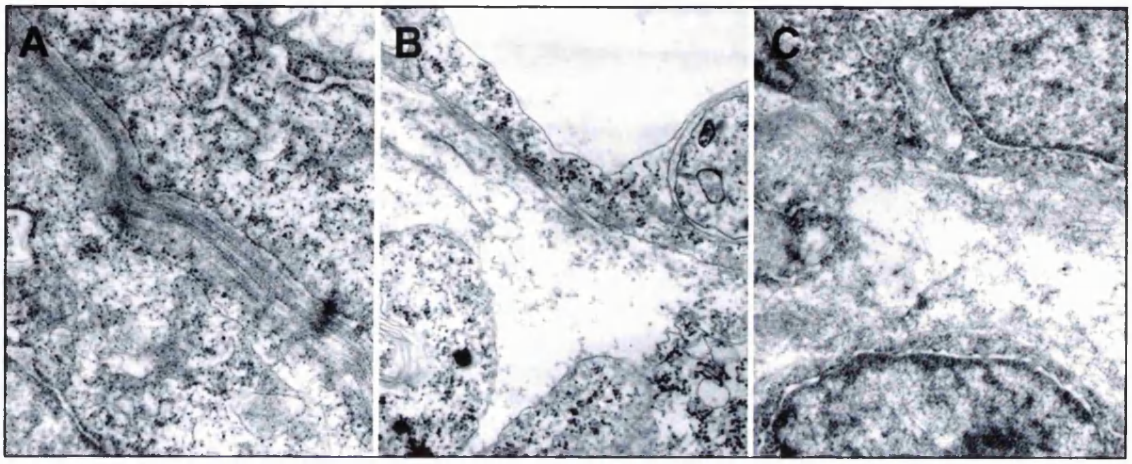

Figure 4.5. *sleepy* and *sneezy* mutant embryos have defects in the perinotochordal basal lamina at 32 hpf. In wild-type embryos (A), the perinotochordal sheath is composed of two thick and well organised layers. In *sneezy* mutant embryos (B), the perinotochordal sheath is much thinner and less organised than in wild-type embryos. The outer layer does not form and some of its components seem to be loose in the surroundings of the notochord. The inner layer is thinner that in wild-type embryos, but retains some organisation. In *sleepy* mutant embryos (C), neither layer is organised, instead there are loose fibre bundles around the notochord cells, that look like the inner layer fibres. In addition, there are also loose particles that resemble outer layer components.

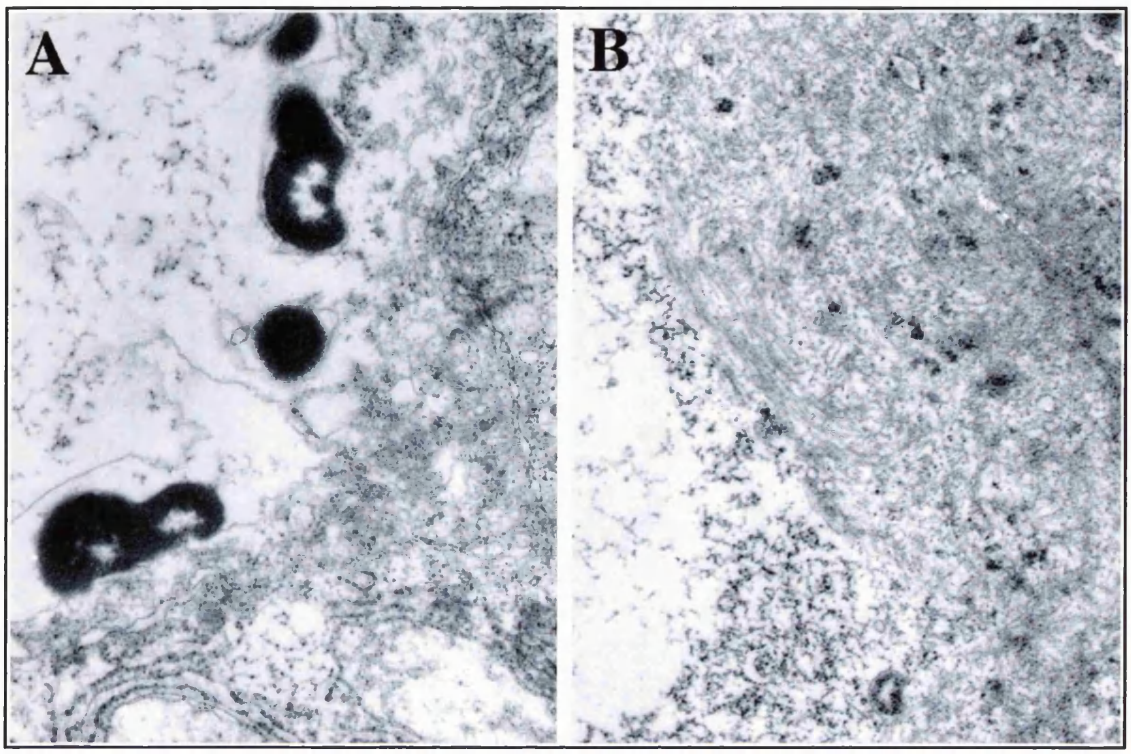

Figure 4.6. Fibre bundles are found within the notochord of *sleepy* mutant embryos at 32 hpf. In *sneezy* mutant notochords, fibre bundles similar to the ones found in the inner layer of the perinotochordal sheath are found within the notochord, either inside the vacuoles or in between cells (B). In wild-type notochords, these fibres are always found in the basal lamina and never in the vacuoles (A).

4.4 Apoptosis in *sneezy*

4.4.1 Introduction to apoptosis in development

In 1972, Kerr and colleagues described a clear distinction between the cell death that occurs in animal development and the pathological cell death that occurs at the centre of acute lesions such as trauma and ischemia (Kerr et al., 1972). The latter type of cell death, apoptosis, was also found to be associated with tissue homeostasis and some pathological states. Apoptotic cells shrink and condense. The organelles and plasma membrane retain their integrity and cells are quickly phagocytosed by neighbouring cells and macrophages, before there is any leakage from the interior of the cells. This phenomenon prevents inflammation. In the second case, known as necrosis, cells and their organelles tend to swell and rupture and the leakage of the cellular contents induces an inflammatory response.

Apoptosis plays an essential role in development. It functions to sculpt parts of the body, e.g. in the formation of digits of some higher vertebrates (Jacobsen et al., 1996; Milligan et al., 1995), in hollowing out solid structures to create luminae (e.g. the preamniotic cavity in early mouse embryos is formed by the death of ectodermal cells in the core of it) (Coucouvanis and Martin, 1995), formation of tubes or vesicles from epithelial sheets (e.g., formation of the vertebrate neural tube) and fusion of epithelial sheets (e.g., formation of mammalian palate) (Glucksman, 1951), deletion of unwanted structures (e.g., the tail during metamorphosis in amphibia tadpoles) and adjustment of cellular population, e.g., neurons and oligodentrocytes (Barde, 1989; Oppenheim, 1991).

Since apoptosis is potentially so destructive, it requires tight control. This is achieved by activation and survival signals. In the metamorphosis of amphibian tadpoles, for example, increased thyroid hormone induces apoptosis in the tail (Kerr et al., 1974). Developing sympathetic neurons, as another example, depend on nerve growth factor (NGF) for survival and without it undergo apoptosis (Levi-Montalcini, 1987).

4.4.2 Apoptosis in *sneezy* correlates with defects

The generalised degeneration in *sneezy* mutant embryos from 2 dpf onward, led me to investigate the levels of apoptosis in the mutant embryos. Using an *in situ* apoptosis detection assay (TUNEL), I found abnormally high levels of apoptosis in the notochord, floor plate, neural tube and tail bud of *sneezy* mutant embryos (Fig.4.7). The abnormal levels of apoptosis in the notochord and floorplate were detected as early as 24 hpf and persisted in all subsequent developmental stages investigated. The anterior notochord always showed much higher levels of apoptosis than the posterior notochord. At a slightly later stage, 26 hpf, abnormal cell death was detected in the posterior dorsal neural tube. In time this pattern extended anteriorly and also ventrally and at 44 hpf most of the dorsal and medial spinal cord showed abnormally high levels of apoptosis. The high levels of apoptosis in the tail bud appeared at 28 hpf and reached a maximum at around 32 hpf, when all the axial and a few paraxial cells in the tail bud were apoptotic. At 44 hpf, the levels of apoptosis were almost uniform across the tail bud. There were still some remaining apoptotic axial cells and the majority of the paraxial cells had undergone apoptosis. The abnormally high levels in the notochord and dorsal neural tube correlate with the notochord's failure to differentiate and reduction of pigmentation.

Embryos injected with *copa*-MO also show abnormally high levels of apoptosis in the notochord, floor plate, neural tube and tail bud (Fig.4.8).

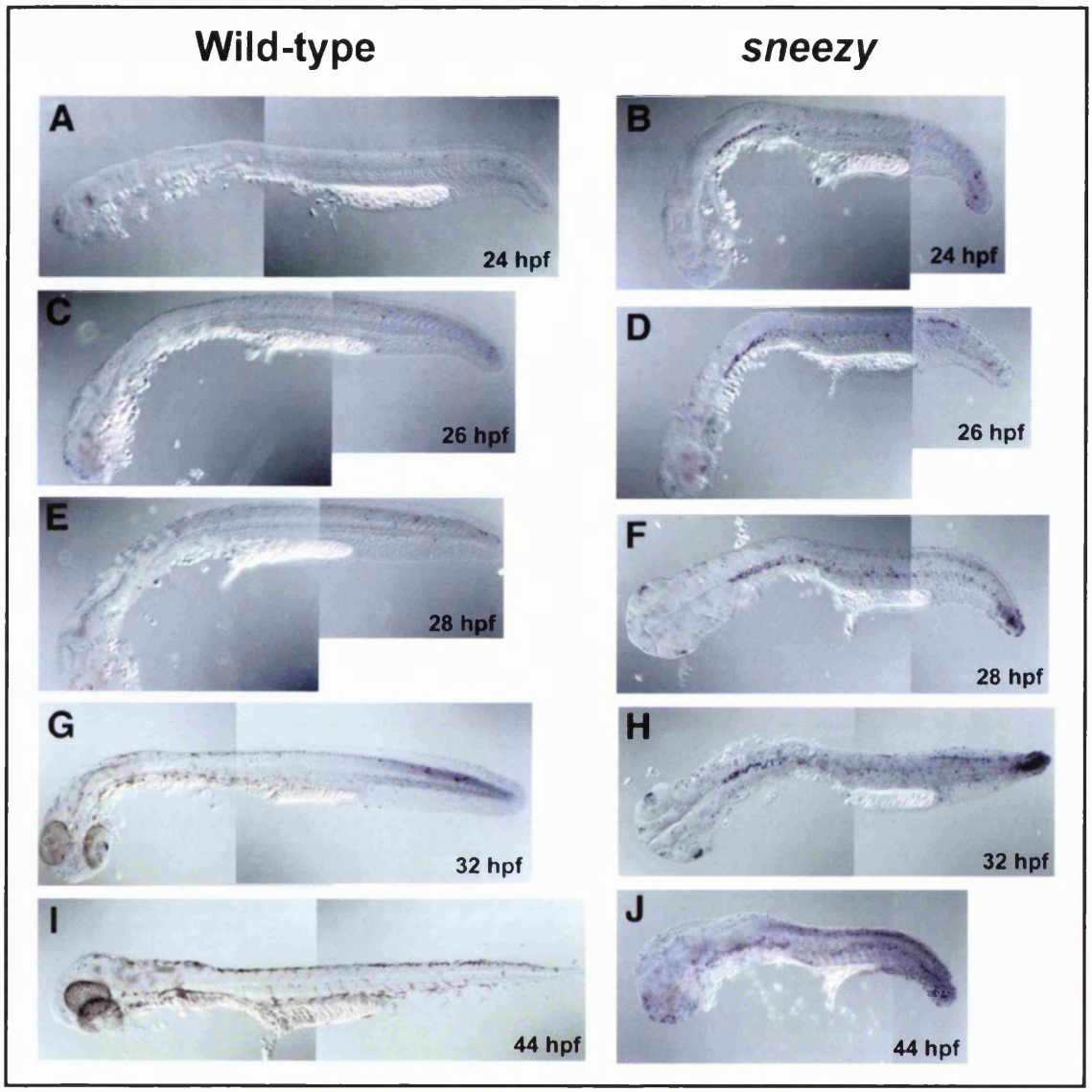

Figure 4.7. *sneezy* mutant embryos have abnormally high levels of apoptosis in the notochord, floor plate and neural tube. A TUNEL assay reveals that from 24 hpf onward, abnormally high levels of apoptosis are found in the notochord and floorplate of *sneezy* mutant embryos (B, D, F, H and J). In comparison, in wild-type siblings, no apoptosis is found in these structures (A, C, E, G and I). Between, 26 hpf and 32 hpf, abnormally high levels of apoptosis appear in the posterior dorsal neural tube and tail bud of *sneezy* mutant embryos (D, F and H). At later stages, the abnormal levels of apoptosis in the neural tube of *sneezy* mutant embryos extend anterior and ventrally (J).

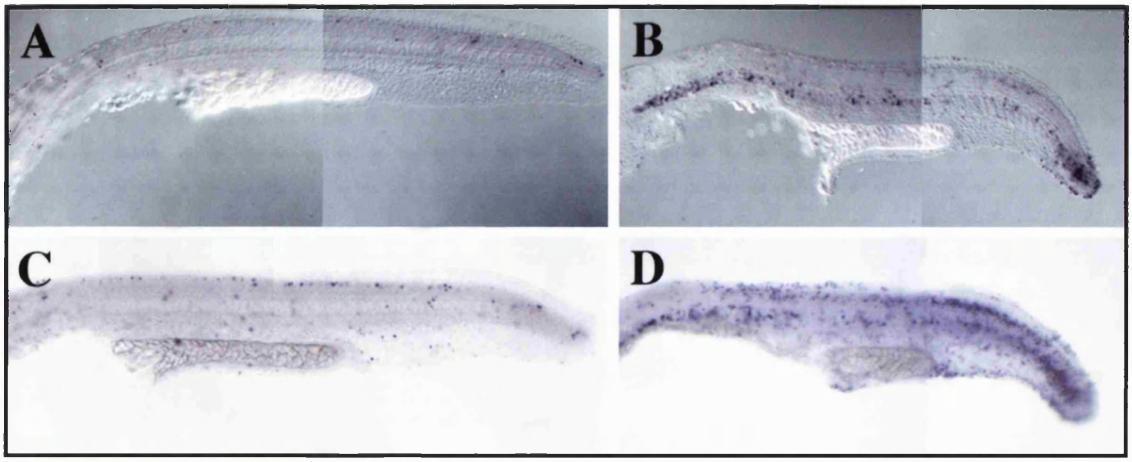

Figure 4.8. Embryos injected with *copa*-MO show abnormally high levels of apoptosis. At 28 hpf, the pattern of apoptosis in *sneezy* mutant embryos (B) and *copa*-MO injected embryos (D) is equivalent. Wild-type siblings have very few TUNEL positive cells and they are mainly in the epidermis (A,C)

4.5 The *sneezy* melanocyte pigmentation defect

In *sneezy* mutant embryos, there is a severe reduction in pigmentation, in particular in the number of pigmented melanophores. At 32 hpf, while in wild-type sibling embryos it is possible to see pigmented migrating melanophores, in mutant embryos theses are visible only in the head.

4.5.1 Introduction to pigmentation development in zebrafish

The larval zebrafish pigment pattern results from the spatial arrangement and coloration of three types of neural crest derived pigmented cells (Kelsh et al., 1996; Lister et al., 1999; Odenthal et al., 1996): the melanophores (black), the xanthopores (yellow) and the iridophores (reflective).

The melanophores have melanosomes which contain melanin pigments. The melanophores form four longitudinal stripes: the dorsal stripe that runs from the head to

the tail, the ventral stripe that also runs from the head to the tail, the yolk sac stripe that runs from under the heart to the anus and the lateral stripe that runs in the horizontal myoseptum of somites 6 to 26 out of 30-34 normal somites.

The iridophores contain reflecting platelets composed of purines and are associated with three of the melanophore stripes with unique spatial patterns in each stripe. They form a medial array in the dorsal stripe, a series of bilateral pairs and a pair of lateral patches in the ventral stripe and a dense band in the yolk sac stripe.

The xanthopores have pterinosomes, which contain pteridine pigments. Individual xanthopores are not distinguishable, but together they give a yellow look to the larval body, specially to the dorsal side. More ventrally this is quite weak and they are not visible ventral to the melanophore ventral stripe.

The pterinosomes and melanosomes derive from the Golgi complex (Obika and Fukuzawa, 1993).

The larval pigmentation becomes visible during the second day of development. First, melanin appears in melanophores in the retinal epithelium (at 24 hpf) and a few hours later in migrating melanophores. Both xanthophores and iridophores become visible much later by the end of the second day of development, at around 42 hpf. The embryonic pattern develops over the next four days and by day 6 of development the final early pattern is established. This pattern remains unchanged until around day 14 of development.

In the Boston and first Tübingen ENU large-scale systematic screens, for recessive-zygotic mutations affecting embryogenesis, a large number of mutations affecting larval pigmentation was identified (Kelsh et al., 1996; Odenthal et al., 1996). This set of mutations could be further partitioned into subsets of mutations according to the process of pigmentation development they seem to affect. The developmental processes were

pigment cell specification and proliferation, pattern formation, differentiation and survival. Some of the genes mutated in some of the pigmentation mutations have been identified, allowing a better understanding of the development of pigmented cells (Table 4.1).

Table 4.1. Cloned pigmentation mutations.

Locus name	Pigmentation phenotype	Gene mutated
nacre [1]	Melanophores absent throughout development. Increase in the number of iridophores.	*microphthalmia--associated transcription factor (mitf)*
Sparse [2]	Reduction in the number of melanophores at 60 hpf. A big proportion of the melanophores is found close to their sites of origin. Almost complete absence of melanophores by 11 dpf.	*c-kit* orthologue
Panther [3]	A big proportion of the xantophores is found close to their sites of origin. Severe reduction in xantophore numbers at 3 dpf. Poorly formed stripes anteriorly and absence of stripes posteriorly in adults.	*c-fms* orthologue
Rose [4]	Fewer melanophores between day 21 and day 28 of development. In adults, the number of melanophores is reduced to approximately half of the number present in wild-type. In adults, the melanophore reduction is more severe ventrally than dorsally. In adults, there is a severe deficit of iridophores.	*endothelin receptor b1 (ednrb1)*
Colourless [5]	Severe reduction of all three types of chromatophores	*Sox10*

[1] (Lister et al., 1999), [2] (Parichy et al., 1999), [3] (Parichy et al., 2000), [4] (Parichy et al., 2000) and [5] (personal communication).

There are, at the moment, several models for the function of each one of the genes identified from Table 4.1 in melanophore development.

The *colourless* gene, which encodes *sox10,* is thought to be necessary for the development of all non-ectomesenchymal neural crest derivatives (Kelsh et al., 2000), including melanophores. The *mitf* gene product is thought to be involved in the activation of the melanophore differentiation program (Lister et al., 1999) while *c-kit* is required for normal migration and for survival of embryonic melanophores. The *c-kit* gene product may also be involved in proliferation and maintenance of melanophore precursors (Parichy et al., 1999). For xanthophore development, *fms* plays a role similar to that of *c-kit* in melanophore development (Parichy et al., 2000). In addition, *fms* promotes differentiation of a sub population of adult melanophores, the *rose* dependent melanophore precursors, probably by promoting the proliferation of their precursors. The *fms* gene also functions indirectly in melanophore development, since the xantophore defects in *panther* result in an increase in melanophore death and melanophore migration defects (Parichy et al., 2000). Finally, *ednrb1* is thought to promote the development of only one of the populations of pigment cell precursors, in this case the one that gives rise to the melanophores that appear between 21 and 28 days (Parichy et al., 2000).

4.5.2 The *sneezy* melanocyte defect is CNS autonomous

The notochord is a major signalling centre during development and since *sneezy* encodes for α-COP, a protein essential for secretion, there was the possibility that the melanocyte defect could be a consequence of defective secretion by the notochord of a factor required for melanophore development. Since *copa* morpholinos phenocopy completely the *sneezy* phenotype I decided to use *copa*-MO injected embryos, in order to

get as many defective embryos as necessary to optimise experiments where transplantation of tissue was required.

To address the problem of the autonomy of the melanocyte defect, chimeric embryos were generated where part of the CNS was wild-type and the rest of the embryo was a *copa*-MO injected embryo. This leads to a dramatic rescue of the melanophores (Fig.4.9, B and D). Melanophores had a wild-type appearance and migrated in a wild-type fashion.

On its own, this experiment was not conclusive, because it could be that in the chimeras some of the floor plate cells were wild-type and could be responsible for the rescue. To rule out this possibility, another type of chimera had to be generated. Chimeric embryos were generated where almost all cells in shield derived tissues were wild-type and the rest of the cells were from a *copa*-MO injected embryo. These chimeras looked like wild-type with one exception: they had the same pigmentation defect as *sneezy* or *copa*-MO injected embryos (Fig.4.9, B and D). This experiment on its own does not rule out a potential role for the mutant epidermis or somites in the melanophore defect in *sneezy*. Taken together these two chimera experiments show that the *sneezy* melanophore defect is autonomous to cells emanating from the neuroectoderm.

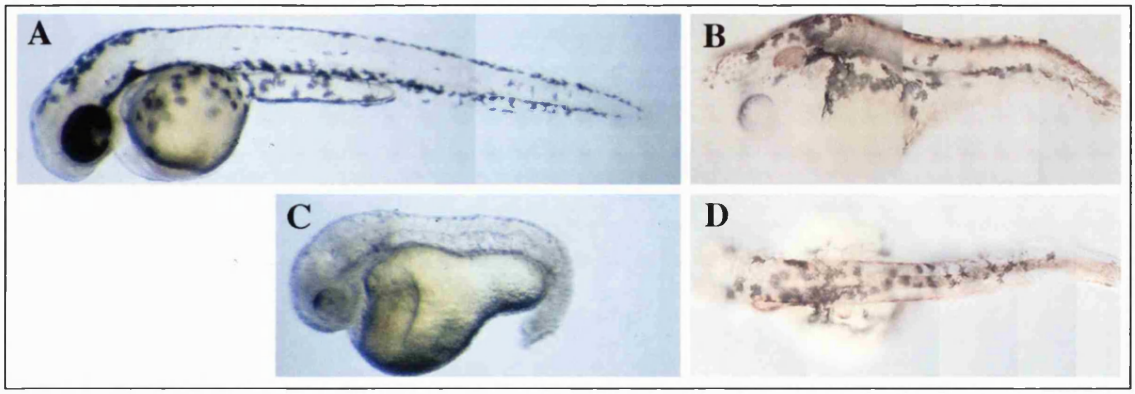

Figure 4.9. Wild-type neural tube is able to rescue the pigmentation defect in *copa*-MO injected embryos. At 48 hpf, *copa*-MO embryos (B) have severe reduction in pigmentation in comparison to wild-type siblings (A). Very few melanophores are visible (C). At shield stage, cells that were fated to give rise to the neural tube of *copa*-MO injected embryos were replaced by labelled equivalent wild-type cells. Lateral (B) and dorsal views (D) of chimeric embryos show rescue of the pigmentation defect. In the chimeras, wild-type melanophores are visible and have migrated (B and D)

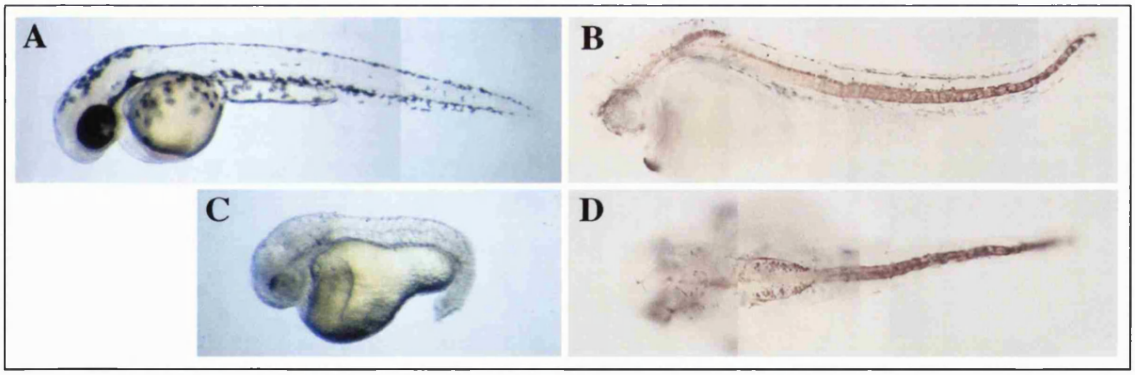

Figure 4.10. Wild-type shield derivatives are not able to rescue the pigmentation defect in *copa*-MO injected embryos. At 48 hpf, *copa*-MO embryos (B) have severe reduction in pigmentation in comparison to wild-type siblings (A). Very few melanophores are visible. Shields of *copa*-MO injected embryos were replaced with labelled wild-type shields. Lateral (B) and dorsal views (D) of chimeric embryos do not show any rescue of the pigmentation defect.

In conclusion, the morphological defects in the Golgi complex and ER of *sneezy* cells show that *sneezy* blocks the early secretory pathway. This blockage leads to the defects found in the perinotochordal basal lamina of *sneezy* mutant embryos. Since the perinotochordal basal lamina is known to be required for notochord differentiation, the defects found in *sneezy* notochords suggest that the chordamesoderm's failure to differentiate may be partially due to disruption of the formation or maintenance of the perinotochordal sheath. Furthermore, the chordamesoderm cells in *sneezy* undergo apoptosis at the time when wild-type sibling chordamesoderm cells differentiate.

There are abnormally high levels of apoptosis in other tissues. The abnormally high levels in the posterior dorsal neural tube correlate with the absence of pigmentation in the posterior trunk of *sneezy* mutant embryos. Later on, apoptosis spreads to all cells and correlates with the previously described generalised degeneration.

I have also found that the melanophore defect is autonomous to cells emanating from the neural tube.

The three mutations *sneezy*, *dopey* and *happy* lead to similar defects. Knowing that *sneezy* encodes *copa* suggests that the other two mutations may encode genes essential for transport in the early secretory pathway. In the next chapter, I report the initial data that I have obtained concerning this possibility.

Chapter 5 Other Notochord Mutations

5.1 Characterisation of *dopey*

5.1.1 Molecular characterisation of *dopey*

Members of the notochord/degeneration mutant class bear a striking resemblance to one another. For example, *dopey* mutant embryos are indistinguishable from *sneezy* mutant embryos. The phenotypic description of *sneezy* mutant embryos in Chapter 3 is an exact match of the description of *dopey* mutant embryos. As an example, *dopey* mutant embryos also display maintenance of expression of early notochord specific molecular markers (Fig.5.1). In particular, they also show maintenance of high levels of *copa* expression in the notochord (Fig.5.2).

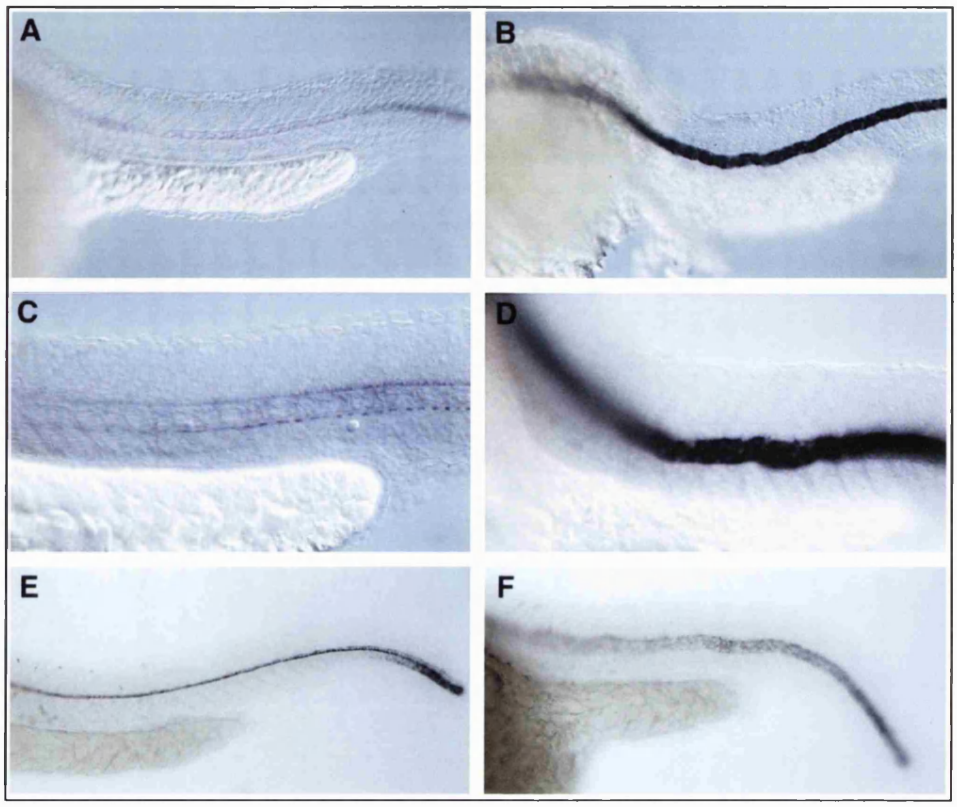

Figure 5.1. Maintenance of expression of early notochord molecular markers in *dopey* embryos. Wild-type embryos (A, C and E) and *dopey* mutant embryos (B, D and F) stained for the expression of *ntl* (A and B), *col2α1* (C and D) and *shh* (E and F) at 24 hpf. While in wild-type siblings the expression of early notochord markers has ceased, in *dopey* mutant embryos expression persists.

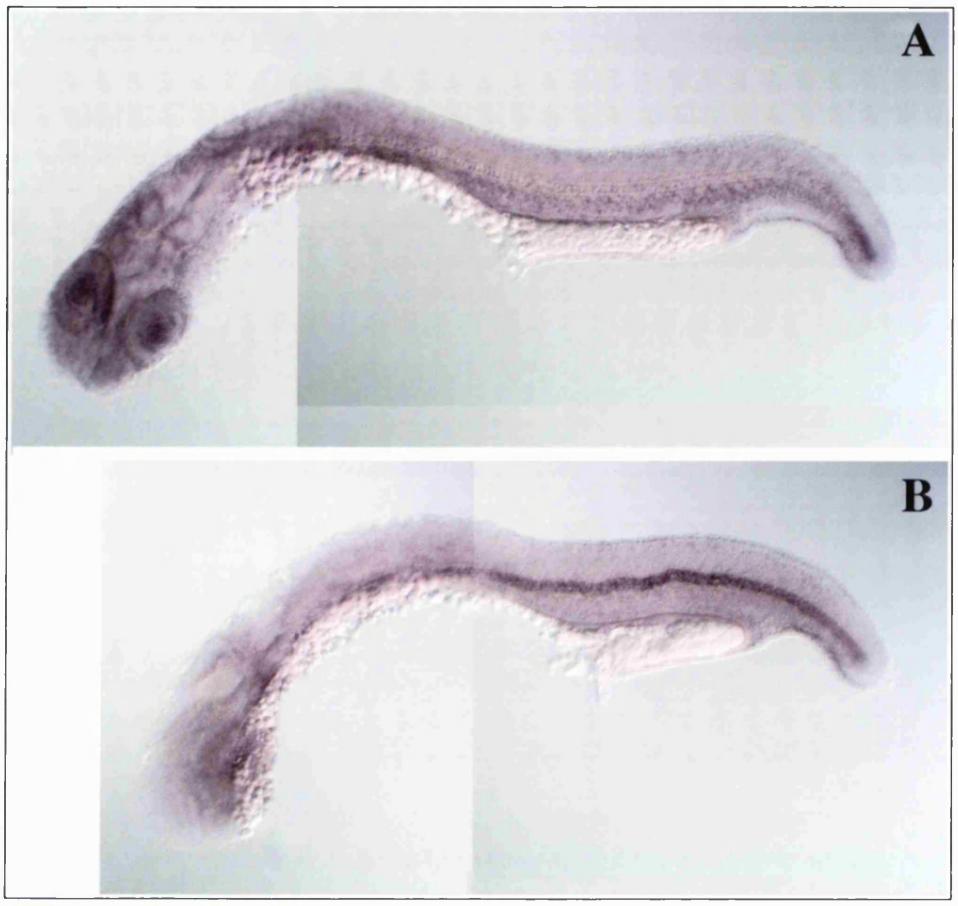

Figure 5.2. High levels of *copa* expression in the notochord are maintained in *dopey* mutant embryos at 24 hpf. At 24 hpf, while in wild-type embryos (A), as the notochord differentiates, the levels of expression of *copa* in the notochord become indistinguishable from the levels in surrounding tissues, in *dopey* mutant embryos (B), *copa* expression levels in the notochord are maintained.

5.1.2 A candidate gene for *dopey*

Although the dopey locus has not yet been mapped, the phenotypic similarities between *dopey* and *sneezy* mutants led me to consider several genes involved in the early secretory pathway as good candidate genes. In particular, genes encoding for other

coatomer subunits. During the Boston and first Tübingen screens, five *dopey* alleles were identified, therefore I would predict a gene encoding a protein of around one thousand aminoacids, by analogy to the relationship between the size of α-COP and the number of alleles of *sneezy*. This assumption, restricts the candidate coatomer subunits to just three: β, β' and γ (Table 5.1). Since *happy* must encode for the zebrafish coatomer subunit β (see section 5.2), it leaves coatomer β' and γ as the remaining good candidates.

Analysis of zebrafish ESTs for genes encoding COPI components did not indicate the existence of more than one *copβ'* or *copγ* genes (Table 5.2), but showed that for some of the other COPI genes there are two homologues in zebrafish: *copζ*, *copδ* and *arf1* have at least two homologues in zebrafish.

Table 5.1. COPI proteins sizes and notochord/degeneration mutations.

Mammals	Yeast	Size	Mutation	Number of alleles
α-COP	Ret1p	~140 kDa/ 1224 aa	*sneezy*	7
β-COP	Sec26p	~107 kDa/ 953 aa	*happy*	6
β'-COP	Sec27p	~102 kDa/ 906 aa	*dopey*	5
γ-COP	Sec21p	~97 kDa/ 905 aa		
δ-COP	Ret2p	~57 kDa/ 518 aa		
ε-COP	Sec28p	~35 kDa/ 293 aa		
ζ-COP	Ret3p	~20 kDa/ 177 aa		
ARF1	yARF1,2,3	~20 kDa/ 181 aa		

Table 5.2. Identified zebrafish COPI proteins.

Mammals	Zebrafish
α-COP	α-COP
β-COP	β-COP
β'-COP	β'-COP
γ-COP	γ2-COP
δ-COP	δ1,δ2COP
ε-COP	ε-COP
ζ-COP	ζ1,ζ2-COP
ARF1	zARF1.1,1.2

5.1.3 Antisense morpholino oligos phenocopy the *dopey* mutation

An anti-sense morpholino oligonucleotide against coatomer β' is able to phenocopy the *dopey* phenotype (Fig.5.3). This result underscores the idea that one of these coatomer subunits may encode for the gene mutated in *dopey*.

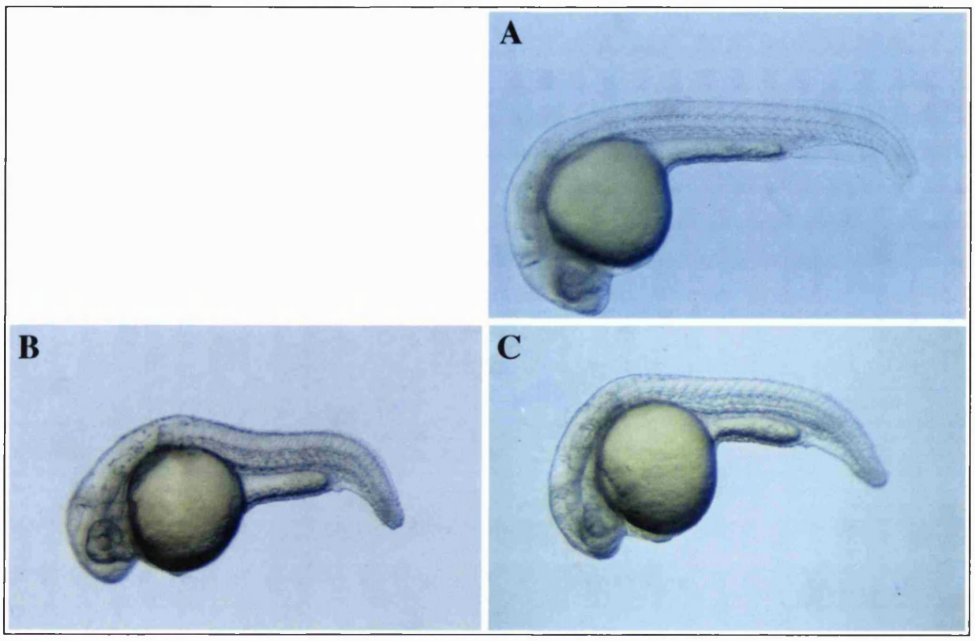

Figure 5.3. *copβ*'-MO injected embryos phenocopy the *dopey* mutation at 32 hpf. At 32 hpf, the notochord of wild-type embryos (A) is completely differentiated, while in *copβ*'-MO (C) and *dopey* embryos (B) it has not differentiated. *copβ'*-MO embryos (C) also phenocopy the body shape of *dopey* mutant embryos (B).

5.1.4 Apoptosis in *dopey*

The similarities between the alleles of *sneezy* and *dopey* are also obvious in terms of abnormal pattern of apoptosis. High levels of apoptosis were found in exactly the same tissues and at the same developmental time points in *sneezy* and *dopey* mutant embryos (Fig.5.4).

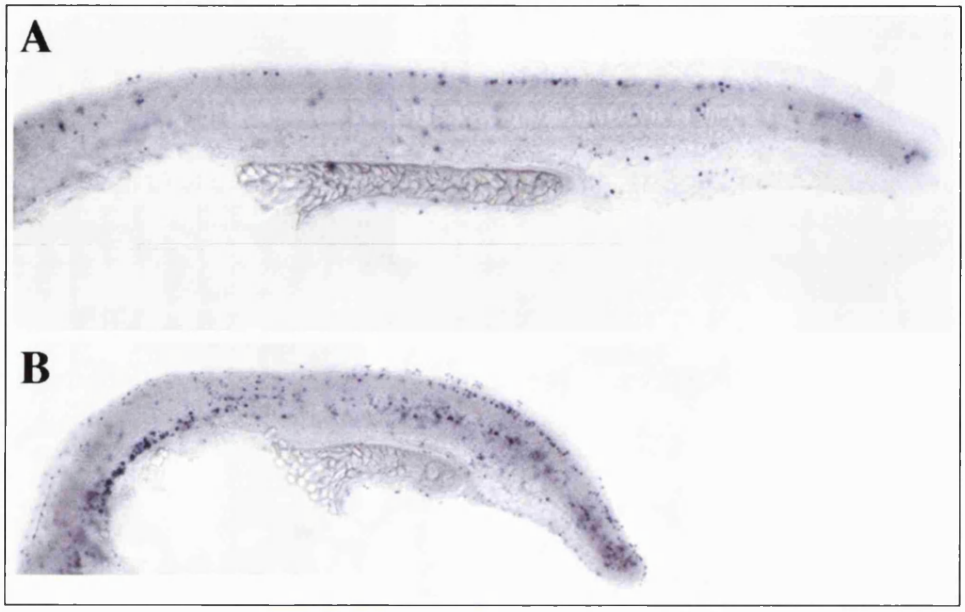

Figure 5.4. *dopey* mutant embryos have abnormally high levels of apoptosis. A TUNEL assay reveals that at 32 hpf, *dopey* mutant embryos (B) show high levels of apoptosis in the notochord, floor plate, posterior dorsal neural tube and tail bud, in comparison with wild-type siblings (A).

5.2 Characterisation of *happy*

5.2.1 Phenotypic characterisation of *happy*

The only phenotypic difference between *happy* and *sneezy* or *dopey* is that the *happy* body shape is slightly less severe than either *sneezy* or dopey, at 24 hpf. At later stages, there are no differences.

5.2.2 A candidate gene for *happy*

There are six alleles of *happy* (plus one, if *mikry* is *happy*) indicating that it may also encode a protein which is probably slightly bigger that one thousand aminoacids. Just as with *dopey*, the largest coatomer subunits represented good candidates. In collaboration with the laboratory of Dr. Geisler, in Tüebingen, the *happy* locus was mapped to linkage group 7, close to the genomic locus of coatomer subunit β (Fig.5.5). In addition, antisense morpholino oligonucleotide against coatomer β are able to phenocopy the *happy* phenotype (Fig.5.6).

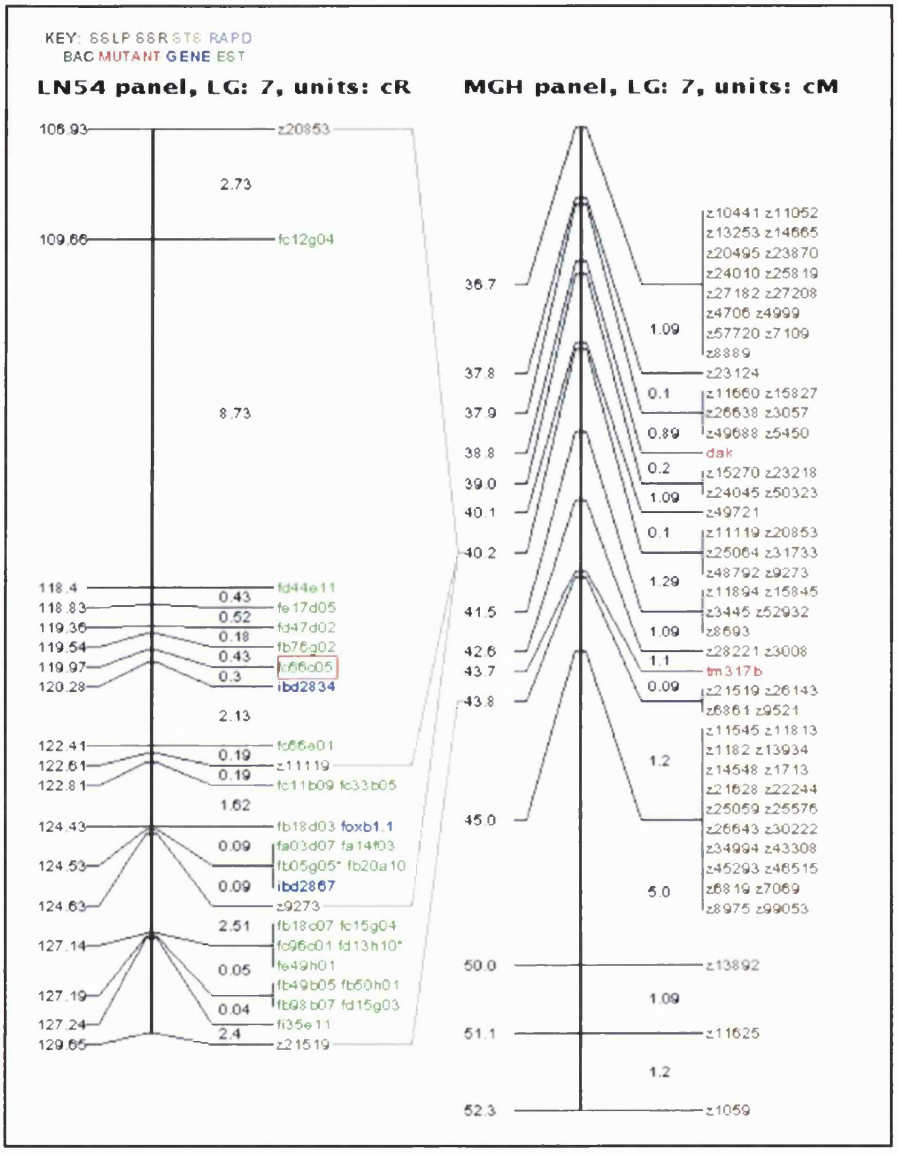

Figure 5.5. *happy* maps. A *copβ* EST, fc66c05, maps to the interval defined by z11119 and z20853, in linkage group 7, which contains the *happy* locus.

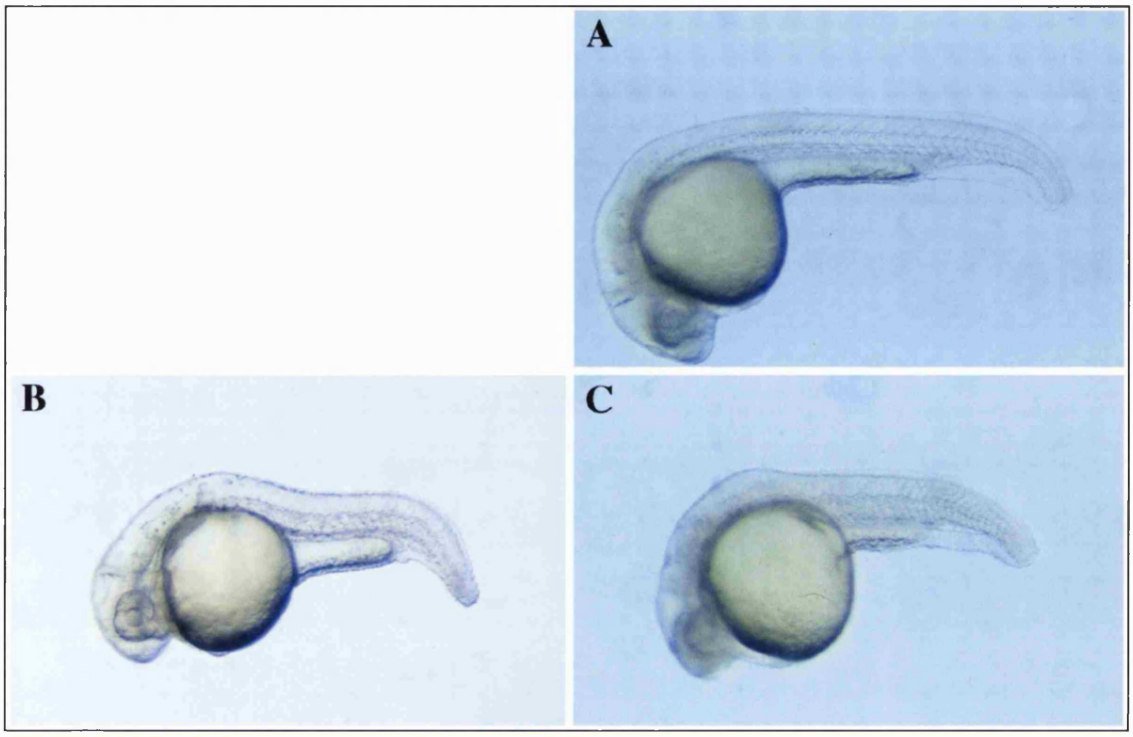

Figure 5.6. *copβ*-MO injected embryos phenocopy the *happy* mutation. At 32 hpf, the notochord of wild-type embryos (A) is fully differentiated, whilst in *copβ*-MO injected (C) and *happy* embryos (B) it has not differentiated. *copβ*-MO injected embryos (C) also phenocopy *happy* mutant embryos' body shape(B).

In conclusion, all the experimental evidence points to coatomer subunit β as the gene mutated in the *happy* mutation. Currently, I am working to obtain cDNA sequence from mutant alleles to identify the *happy* mutation. In addition, I would like to inject RNA into mutants to see if that is sufficient to effect rescue.

Chapter 6 General Discussion

6.1 Notochord differentiation

Analysis of the notochord mutants *sneezy*, *dopey*, *happy*, *sleepy* and *grumpy* by morphological criteria has identified a failure of their notochord cells to differentiate properly. This is supported by the maintenance of expression of early notochord markers in these mutants (Fig.3.1; 5.1). Furthermore, each of these notochord differentiation mutations has abnormally high levels of apoptosis in the notochord.

6.1.1 The role of the perinotochordal basal lamina in notochord development

The notochord is the principal structural element of the vertebrate embryo. Its stiffness arises through the interaction of vacuolated cells and the perinotochordal basal lamina (PBL). As chordamesoderm cells vacuolate, they inflate the surrounding PBL to form a rigid notochord. Therefore the differentiation of the chordamesoderm cells and the formation of the PBL need to be coordinated. Evidence that this coordination is effected by signals from the PBL to chordamesoderm cells comes from the demonstration that the *bashful*, *grumpy* and *sleepy* genes encode Laminin-1 chains, which are structural proteins of the extracellular matrix that also engage in intercellular signalling.

Signals from the PBL could be required for the maintenance of notochord differentiation, induction, or both. With respect to the first possibility, it has been shown in a variety of systems that differentiating cells acquire dependencies on new trophic factors. For example, after being induced to become neurons by bFGF adrenal chromaffin cells become dependent on NGF for survival (Stemple et al., 1988).

Similarly, as chordamesoderm cells begin to differentiate, they may become dependent upon basal lamina derived signals to survive and complete differentiation. Alternatively, basal lamina derived signals may induce differentiation of the chordamesoderm. In the changing environment of the embryo, the factors that supply trophic factors to the chordamesoderm might disappear and the chordamesoderm may undergo apoptosis if it fails to undergo its normal program of differentiation. Of course, it is also conceivable that the PBL is required for both induction and maintenance of notochord differentiation.

If the *bashful*, *grumpy* and *sleepy* mutations arise from a failure in Laminin-1 signalling, it may be possible to rescue these defects with exogenous Laminin-1. Consistent with this, *sleepy* shields transplanted into the ventral side of wild-type sibling embryos give rise to second axes with wild-type notochords (S. Pollard, D. Stemple; in preparation). A modified version of this experiment should be possible using an *in vitro* culture system. Wild-type dorsal shields cultured *in vitro* give rise to tubular structures containing vacuolated cells that resemble differentiated notochord cells (S. Pollard, D. Stemple; personnal communication). Using such an *in vitro* system it would be interesting to culture *sleepy* shields with different concentrations of Laminin-1. If exogenous Laminin-1 can rescue notochord differentiation, then we should be able to obtain notochord -like structures from cultures of *sleepy* shields. We could then determine whether Laminin-1 is necessary for maintenance of notochord differentiation by removing Laminin-1 from the culture media as soon as the first shield cells show signs of notochord-like differentiation. These experiments could help to clarify whether Laminin-1 has a direct role in notochord differentiation and possibly discern whether it is required for induction or maintenance of differentiation.

It would also be interesting to further examine the role of apoptosis in determining notochord mutant phenotypes. If Laminin-1 signalling is required for

maintaining the viability of differentiated cells rather than for induction, this might be uncovered by blocking apoptosis in *sleepy* mutant embryos and rescuing their notochords.

As notochord differentiation requires the PBL, membrane receptors on notochord cells are potential candidates for transducing signals from the PBL. Of particular interest are Laminin receptors, such as integrins and dystroglycan. Several of these receptors have already been identified as zebrafish ESTs. The remaining will be identified in the near future from the genome sequencing project. Using morpholino knock down these receptors, we will be able to inhibit those that are expressed in the notochord until a *sleepy*-like phenotype is obtained, and in this way identify the membrane component(s) of the notochord differentiation signalling mechanism. The identification of the membrane associated components of the notochord signalling pathway will, in turn help us to identify intracellular components and eventually elucidate the complete pathway of notochord differentiation.

6.1.2 The Role role of α-COP in Notochord notochord differentiation

The coatomer subunit α (α-COP) is one of several proteins essential for transport in the early secretory pathway. The half-life of α-COP is approximately 28 hours (Lowe and Kreis, 1996) and in zebrafish embryos, *copa* mRNA is maternally expressed. This maternal component may be responsible for the absence of defects in *sneezy* mutant embryos until 24 hpf.

Zygotic *copa* expression is upregulated in the chordamesoderm, implying that the requirements for α-COP in the chordamesoderm are higher than in other embryonic tissues. This need is likely to arise from a high secretory activity in notochord cells. EM

studies of notochord cells from 32h wild-type embryos reveal slightly swollen ER, which is a characteristic of cells with high secretory activity (Chapter 4).

In *sneezy* mutants, as transport in the early secretory pathway begins to breakdown, components of the PBL and cell membrane receptors should not be efficiently transported. Therefore, notochord defects in *sneezy* mutant embryos may result from the disruption in either formation/maintenance of the PBL or in transport of membrane receptors. Alternatively, since COPI may also be involved in signal transduction pathways, it may be that in *sneezy* mutant embryos, the intracellular differentiation pathway is affected. As an example, cdc42 binds to γ–COP and this association brings cdc42 to the Golgi membrane where cdc42 GTP loading is enhanced. This enhancement may not be possible in *sneezy* mutant embryos, because cdc42 bound to γ-COP might not be brought to the Golgi due to lack of coatomer stability. Therefore the lack of coatomer stability may compromise cdc42 signalling in *sneezy* mutant embryos.

If defects in the PBL or cell membrane are responsible for the failure in differentiation in *sneezy* notochord cells, then knocking out other components of COPI vesicles, COPII vesicles or clathrin vesicles might allow us to discern whether *sneezy* notochord's failure to differentiate is independent of the defects in the PBL or cell membrane. For example, disruption of COPII vesicles would have no effect if the failure to differentiate were independent of transport defects.

To investigate a potential role of cdc42 in differentiation of the notochord, I would first test whether cdc42 is abnormally localised in *sneezy* cells. If so, it would be very interesting to knock out cdc42, ideally only in notochord cells close to the time they differentiate. If cdc42 were directly involved in the differentiation transduction pathway, then the notochord cells would fail to properly differentiate.

6.2 Zebrafish and intracellular transport

The embryological and genetic advantages of zebrafish as a model (see section 1.3) make the zebrafish notochord a good system for studying intracellular transport. The principal advantage of studying intracellular transport in zebrafish, as opposed to yeast, is that zebrafish is a metazoan, allowing the study of factors specific to the protein transport of multicellular organisms, such as ECM factors. In addition, the availability of mutations affecting intracellular transport and the ability to knock out components of transport using morpholinos allows the study of vertebrate intracellular transport *in vivo*. As an example, one of the laminin mutations, *sleepy*, seems to cause a decrease in the secretory function of notochord cells.

One question about protein transport that would be interesting to study in zebrafish, concerns the mechanisms that discern whether cargo is transported through the Golgi in COPI vesicles (fast track transport) or via cisternal maturation (slow track transport). Could size be the criteria for COPI vesicle cargo uptake? Or does COPI selects cargo according to some sort of signal? To study this problem, we could use a protein that is normally transported along the fast track, engineer a concatomer of the protein to significantly increase its size and over-express the construct in embryos. Such a protein should be transported along the fast track if there is no size limitation. If the basis for fast track transport is not size, other modifications of fast track-targeted proteins could be attempted to identify a fast track-specific signal. Reciprocally, we could engineer truncated versions of a protein that is normally transported across cisternae, such as the collagens, to determine if a reduction in size causes a switch to fast track transport.

Another interesting question is which are the mechanisms for cargo segregation in COPI vesicles. It is known that there are at least two distinct populations of COPI vesicles. One type contains mainly secretory cargo and partakes in anterograde transport,

while the other type has KDEL receptors, transports KDEL-tagged cargo proteins and partakes in retrograde transport. It is thought that competing sets of sorting signals act positively and negatively during vesicle budding through a GTPase switch in the COPI coat complex. This switch allows selective uptake into COPI vesicles. One question that arises is whether distinct anterograde or retrograde cargo can be selectively taken up by distinct populations of COPI vesicles? If so, it would be interesting to block secretion or recycling/retention of specific types of cargo. One way to accomplish this would be to engineer mutant coatomer proteins or mutant receptors associated with COPI vesicles to reduce specificity for particular types of cargo. By a combination of morpholino knock out and injection of cRNAs encoding mutant proteins, we would then be able to study the effects of blocking secretion or recycling/retention of specific cargo and by inference elucidate the role of those cargo in development.

6.3 The role of α-COP in development of pigmentation

The melanophore defect in *sneezy* mutants is CNS autonomous (Fig. 4.8; 4.9), suggesting that it may be cell autonomous. Since melanosomes derive from the Golgi complex (Obika and Fukuzawa, 1993) and α-COP is necessary for transport in the early secretory pathway and for integrity of the Golgi complex (as seen in Chapter 4), the melanophore defect autonomy implies that the principal cause for the defect in *sneezy* mutants might be a defect in formation of melanosomes. The study of the expression pattern of genes like *dopachrome tautomerase* (*dct*), which is expressed in premigratory and migratory melanoblasts, will allow us to determine if melanophores which lack pigmentation are present (Kelsh et al., 2000). I suggest that this is what happens in the head and anterior trunk of *sneezy* mutant embryos.

In the posterior dorsal trunk, abnormal levels of apoptosis may represent melanophore precursors that are either unable to delaminate from the neural tube or are otherwise unable to initiate migration. The expression pattern of *dct* and other early neural crest markers combined with microscopy, will shed some light on these questions.

If rostral melanophores are present, another question that could be addressed by analysis of the expression pattern of genes such as *dct*, would be whether they migrate normally. If cdc42 signalling is affected in *sneezy*, I would expect to see some migration defects because cdc42 modulates the actin cytoskeleton, which is required for cell movement. In addition, cell movement is also dependent on membrane proteins such as integrins that function in adhesion. Therefore, it might be that *sneezy* mutant embryos display a variety of melanophore defects depending on their position along the A-P axis: wild-type melanophores that migrate normally (at the most rostral positions); melanophores that have migration defects (in the trunk) and melanophores that are not able to delaminate (in the tail). If this is the case, *sneezy* mutant embryos will become a good system for studying melanophore development.

To conclude, notochord mutants have begun to shed insights into the role of the ECM and intracellular transport in cellular differentiation. Zebrafish in general and notochord mutants specifically should be valuable tools for future research aimed at elucidating molecular details of these processes. Finally, *sneezy* mutants may also help to investigate aspects of melanophore differentiation.

Appendix I Characterisation of *sleepy* and *grumpy*

I.1 Introduction

sleepy and *grumpy* are two other notochord mutations. In *sleepy* and *grumpy* mutant embryos, the notochord cells do not differentiate properly as seen both by morphological analysis (they do not acquire large vacuoles) and by maintenance of expression of early notochord molecular markers.

Although the phenotypes of *sleepy* and *grumpy* mutant embryos are similar to those of *sneezy* and *dopey* mutant embryos, there is a striking difference in that *sleepy* and *grumpy* embryos do not show any pigmentation defect. In addition, while *sleepy* and *grumpy* embryos develop fins, *sneezy* and *dopey* mutant embryos never do. The *grumpy* and *sleepy* mutations also induce CNS defects while none of the *sneezy*, *dopey* or *happy* mutations do.

I.2 *sleepy* locus mapping

To understand the role of the *sleepy* gene product in notochord differentiation, we decided to identify the gene whose function is disrupted in *sleepy* mutant embryos. Linkage group 2 had been identified as the linkage group for the *sleepy* locus. In order to map the mutant locus to a smaller genomic interval, CA repeat markers were used to screen *sleepy*^{m86} mutant embryos. We identified the markers, z11023 and z7632 as the flanking SSLP markers that define the minimal genomic interval containing the *sleepy*

locus, for the available polymorphic CA repeat markers (Fig.I.1). The genetic distances from the *sleepy* locus to z11023 and z7632 were 1.6 cM and 2.2 cM, respectively.

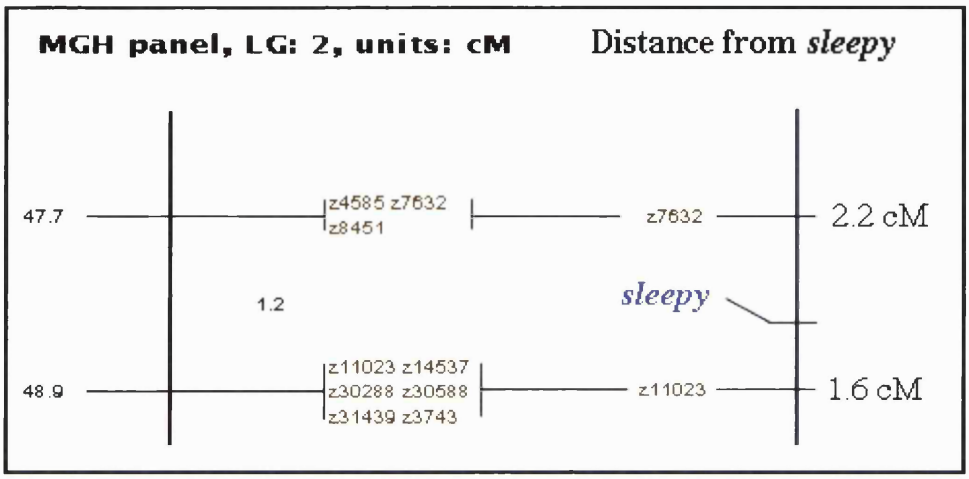

Figure I.1. *sleepy* CA repeat map. The *sleepy* locus is in LG 2, between the markers z11023 and z7632.

The gene *sleepy* has been shown to encode the zebrafish laminin γ1 (Parsons, M.; personal communication). Laminins are extracellular matrix proteins which consist of alpha, beta and gamma chains with molecular masses of 140-400 kDa (Timpl and Brown, 1994). There are at least eight genetically distinct laminin chains that assemble to form at least seven distinct forms of laminin. The best studied laminin isoform, laminin-1 (alpha1, beta1 and gamma1) binds several other matrix components such as perlecan, nidogen, collagen and a few others. This suggests a role for laminin-1 in the organisation of basement membranes. Laminins can also signal through membrane receptors like the integrins and in this way are involved in cell-matrix interactions, which are important for development, tissue homeostasis and morphogenesis.

I.3 Apoptosis in *sleepy* and *grumpy* mutant embryos

The abnormally high levels of apoptosis found in *sneezy* and *dopey* mutant embyos and the similarities between those two mutations and *sleepy* and *grumpy* led me to investigate apoptosis also in the latter mutant embryos.

Using an *in situ* apoptosis detection assay (TUNEL), I found abnormally high levels of apoptosis in the notochord and floor plate of both *sleepy* and *grumpy* mutant embryos. The levels of apoptosis in the tail bud and neural tube were normal (Fig.I.2). As was the case for *dopey* and *sneezy* mutant embryos, the anterior notochord always showed much higher levels of apoptosis than the posterior notochord.

The abnormally high levels of apoptosis in the notochord correlate with the notochord's failure to differentiate.

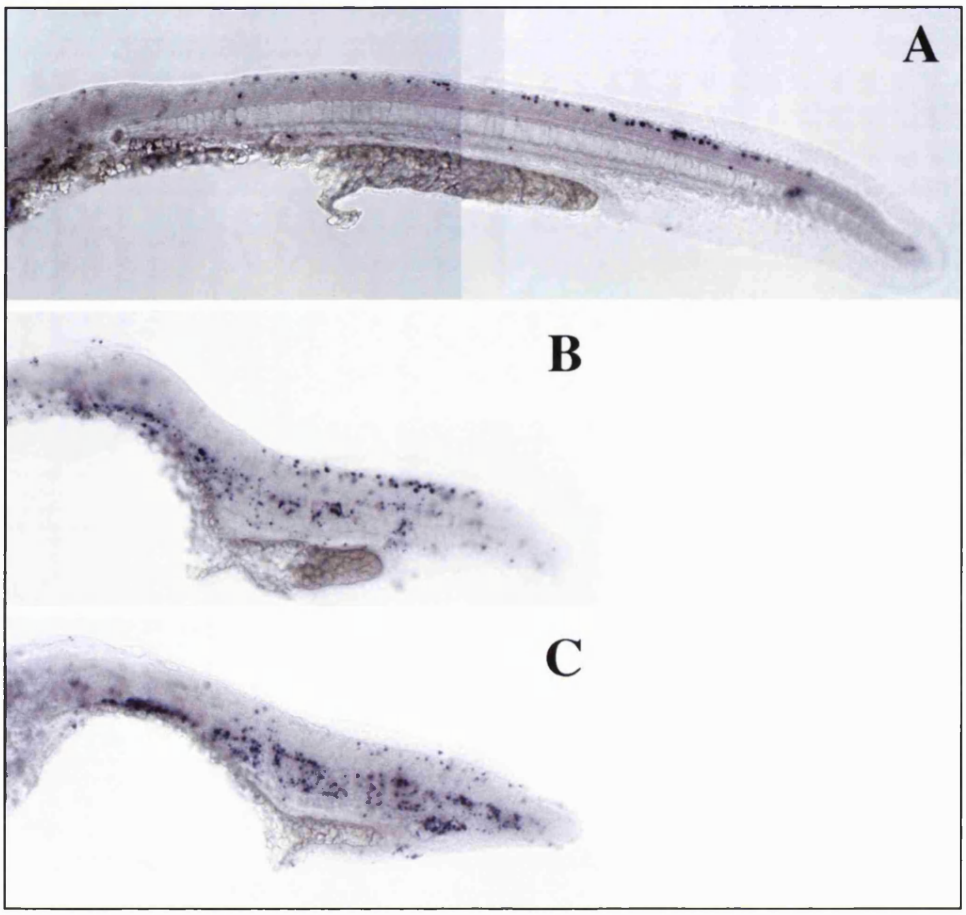

Figure I.2. Abnormally high levels of apoptosis in *sleepy* and *grumpy* mutant embryos. Wild-type (A), *sleepy* (B) and *grumpy* (C) 32 hpf embryos stained for DNA fragmentation, using an *in situ* apoptosis detection assay (TUNEL), show abnormally high levels of apoptosis in the notochord and floorplate of the mutant embryos (B,C).

Appendix II The Zebrafish Anti-Dorsalising Morphogenetic Protein

II.1 Introduction

In zebrafish, work performed by L. Saúde has shown that grafting of tissues adjacent to the shield to the ventral marginal side give rise to an incomplete secondary axis, where the notochord is formed by cells from the graft and surprisingly from cells that derive from ventral cells (Saude et al., 2000). Grafting of the morphological shield to the same coordinates gives rise to a complete secondary axis, where the notochord cells derive exclusively from the grafted tissue. In addition, when the morphological shield is ablated and replaced by a ventral tissue graft, some of the grafted cells become part of notochord derived tissues like notochord, floor plate or hypochord. Fate maps (Solnica-Krezel et al., 1995; Woo et al., 1995) and transplantation experiments (Saúde, L. personal communication) have shown that the ventral tissues are fated to become somitic and blood cells. In chick, the population of floor plate progenitors can be regulated by homeogenetic induction. The extent of floor plate induction was proposed to be limited by the competence of neural plate cells to respond to the inductive signals (Placzek et al., 1993). In zebrafish, analysis of the *cyclops* mutation had also led to the suggestion of homeogenetic induction among the floor plate precursor cells (Hatta et al., 1991).

A proposed model for these results is that the morphological shield secretes a protein that counteracts the lateral shield signal to induce more shield. A good candidate for that function would be the anti-dorsalising morphogenetic protein (ADMP). ADMP is a member of the bone morphogenetic protein (BMP) family, a subfamily of the TGFβ

superfamily. ADMP homologues have been identified in *X.laevis* (Moos et al., 1995) and *G.gallus* (Joubin and Stern, 1999) and shown to repress dorsal fates (in *Xenopus*) and the induction of ectopic node molecular markers by the node inducing centre (in chick). Paradoxically, in both species *admp* is expressed in the dorsal organiser: the blastopore lip in *X.laevis* embryos and the node in *G.gallus* embryos.

II.2 Identification of a zebrafish ADMP homologue

The nucleotide GenBank database contained an expressed sequence tag (EST) for a zebrafish *admp* homologue. This EST corresponded to the RZPD clone MPMGp609I0870, whose 1405 bp insert was sequenced (Fig.II.1) and turned out to have the full cDNA for the *admp* homologue. An open reading frame of 1176 bp was identified (Fig.II.1) and its translation showed a high homology to both *X.laevis* and *G.gallus* ADMP proteins (Fig.II.2; 3). Furthermore, phylogenetic analysis shows that ADMP proteins and BMP3 proteins diverged from a common branch (Fig.II.3) of the TGFβ superfamily.

CCACGCGTCCGCCTGAAAGGTCATCATGTTGTCTGCAATGTTCTTTGCAATGTTGTC
CACAATGATGGGACTCTCTTTCGCCCGGCCCGGGTTTTTTAACGAGCTGGAGGAACATT
TAGCGGTGGAAAGCGAGCCTAAAGTGCGGTCGGAGGCGATCAGGAGGCTTTTGGAGGTG
TTTGGGATGGAAGATCCTCCTGCTGCTTTGGGTCACAAACAGCCTCCTCAGTATATGCT
GGACCTGTACAACACCATCGCTGATGTCGACGGAGTCACCAAAGACCCGACGCTGCTCG
AGGGAAACACGGTCCGGAGCTTCTTCGACAAATTGCACAGTGAACGAATCGAGTATCTC
TTCAACATGTCCACTGTAGCCAAGAGTGAGAAGATCCTGACGGCTGAACTTCACCTGTT
CAAACTCAGACCAAAAACATCAATCGTCTTAAACAGACATCACTTCTGTCAGGTCAGTG
TGTATCAGGTTCTGGACAGCGGCAAAAAAAACGTCTCGCAAGGGAAGAAGCTGCTCTCA
TCCAGACTGGTTCCCATTCACTCTACTGGCTGGGAGGTTTTCACCATCACTCAAGCTGT
GCGCTCGTGGATGTCGGACGAGGGCAGTAATCTGGGTCTGCTGGTCTCAGTCAGGACTC
TCGCAGGCTCTCAGATGGACCTAAAAATGGTGCGTTTCGCATCAGGTCGGGATCATCAT
CACAGCAAACAGCCCATGCTGGTCCTGTTCACTGATGACGGGAGACGAGCTGCTTCTCT
GGAGGCTACAAGTAAAGGTTCAGATGTTTCTCCAGGCAGCCCCAGTCAGCCGCTTCCCA
GTGTCCCGGCCTCCCGGCGTAGCCCTCGCTCTGTGGATTATGACGAGAGAGGAGAAAAG
ATGGCCTGTCAGCGTCAGCCGCTGTACGTTGACTTTGAGGAGATCGGCTGGTCCGGTTG
GATCGTATCTCCCAAAGGATACAATGCGTATCACTGCAAAGGCTCCTGTATATTTCCCT
TGAGCCAGAATATGAGGCCCACGAACCACGCCATCGTCCAGTCCATCATAAACACCCTC
AAACTCAACAAAGGCATTCAGACGCCCTGCTGCGTCCCGGACAAACTCTACAGCATCAG
CCTGCTATACTTTGATGATGACGAGAATGTGGTGCTGAAACAGTATGATGATATGGTGG
CCGGAAGCTGCGGGTGTCGCTGAAAAAAAAAAAAAAAACAGATTTACCTCAGTGTTTAA
TGCAAAATCTGGATAAAATTGTAAATATGTACATAGATAGCCAATATTAATATATGGAG
GAGGCTGAGACGATCCCTTGTAATAAAATGTACATTTTGTAAATTGCATGTCGTGAACT
ATTATGAAGTCTAAATAAATTCTTCCGCCAAAATTT

Figure II.1. ***admp*** **cDNA sequence.** The start codon is in blue, while the stop codon is in red.

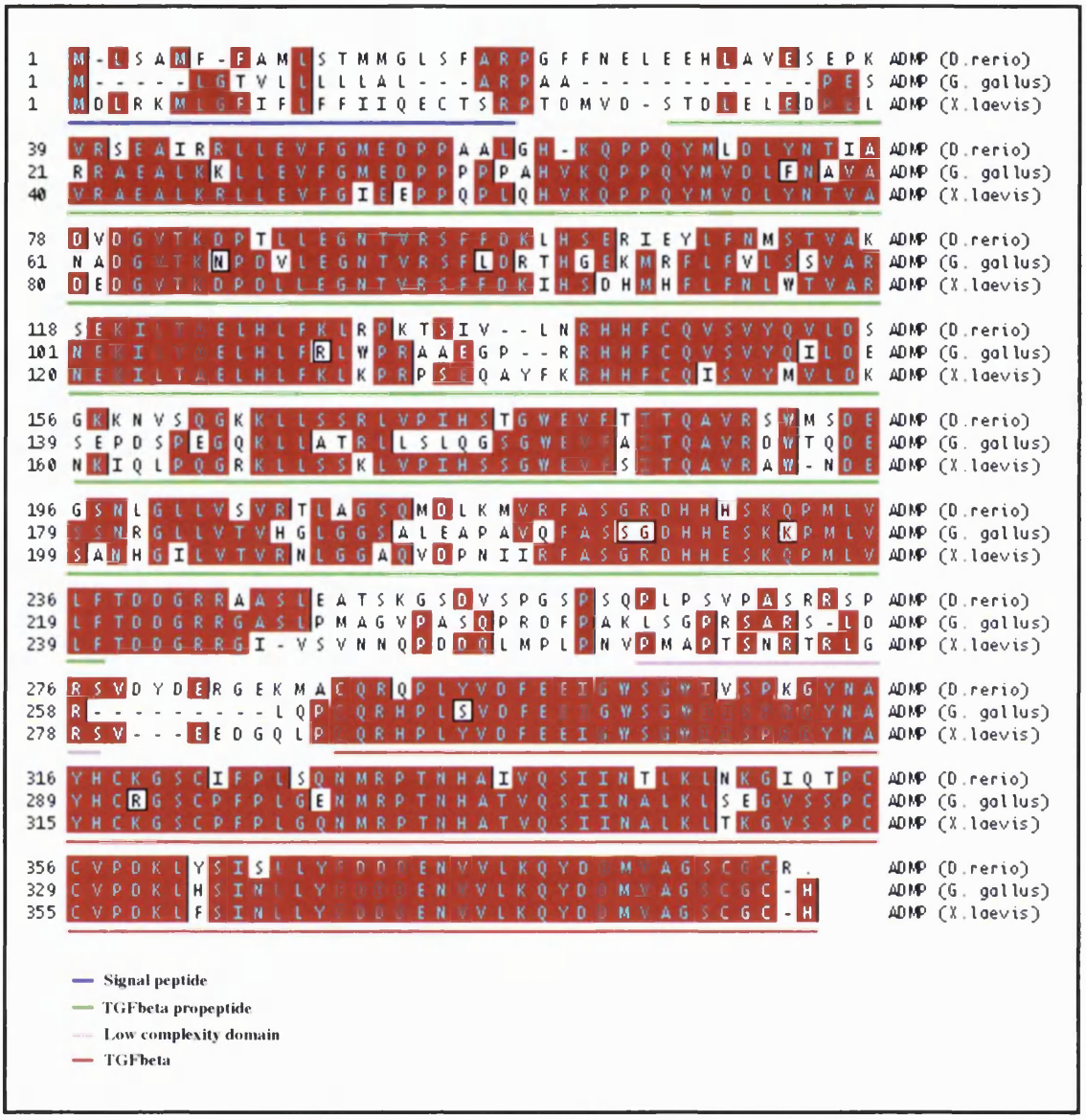

Figure II.2. ADMP proteins alignment. The zebrafish ADMP has three domains: a signal peptide, a TGFβ propeptide and a TGFβ domain. All three ADMP proteins are highly homologous in the mature TGFβ domain.

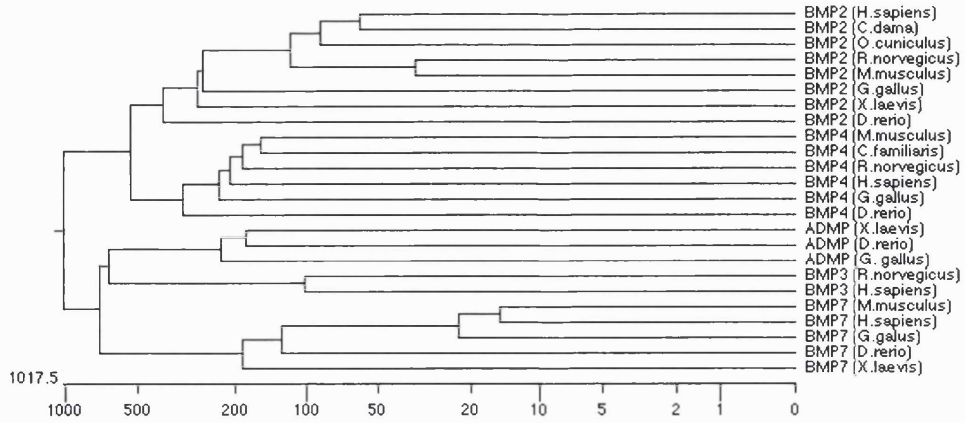

Figure II.3. Zebrafish ADMP phylogenetic tree. The zebrafish protein ADMP is closely related to the other ADMP proteins. ADMP and BMP3 proteins diverge from the same phylogenetic branch.

II.3 *admp* expression pattern

In collaboration with L. Saúde *in situ* hybridisation analysis was performed revealing that *admp* transcription is zygotic and transient. *admp* expression is first detected at shield stage (6 hpf) in the morphological shield (Fig.II.4A-C), apparently in both epiblast and hypoblast. Later at 8 hpf, *admp* is expressed in the nascent axial mesoderm (Fig.II.4D,E). No expression was detected at later stages up to 16 hpf.

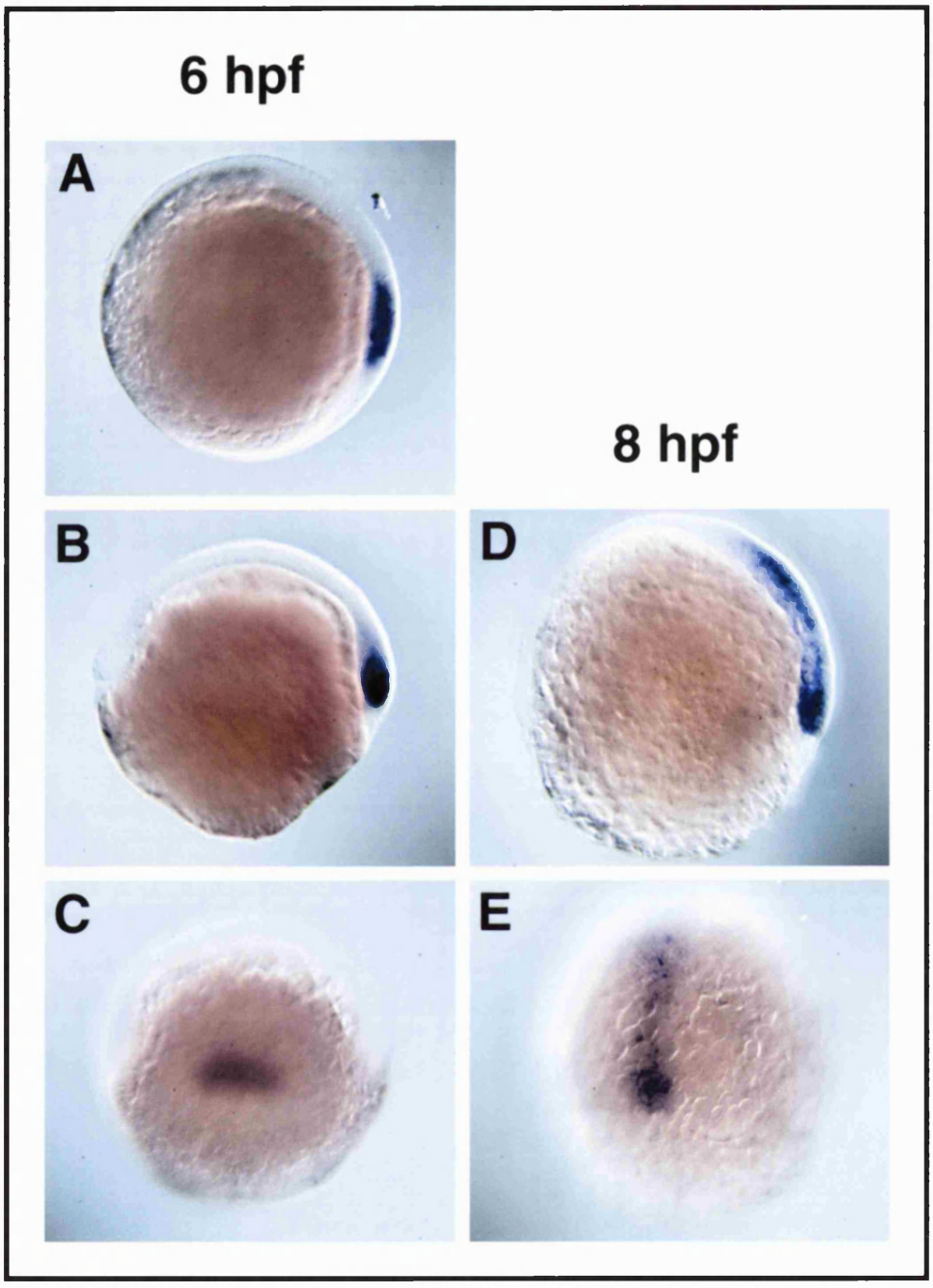

Figure II.4. *admp* expression pattern. Vegetal (A), lateral (B,D) and dorsal (C,E) views of 6 hpf (A-C) and 8 hpf (D,E) wild-type embryos stained for the expression of *admp*.

II.4 Discussion

The expression pattern of the zebrafish *admp* and its high degree of homology to the previously known ADMP proteins make it a strong candidate for the potential shield induction inhibitory signal.

To test the role of ADMP, it would be interesting to inject different concentrations of *admp*.RNA into labelled embryos and then transplant ventral tissues from these into shield ablated unlabelled sibling embryos. If ADMP functions to counteract the lateral shield signal to induce more shield, then I predict that the labelled ventral tissue would not give rise to shield derivative tissues.

It would also be interesting to investigate the consequence of ADMP knock out by morpholino oligonucleotides. Would we obtain embryos with larger shields? Or, would the mechanisms that regulate shield fate compensate for the absence of ADMP? For this purpose morpholino oligonucleotides against *admp* have already been designed.

Appendix III Molecular Characterisation of *masterblind*

III.1 Introduction

Zebrafish embryos which are homozygous for the *masterblind* (*mbl*^{tm213}) mutation exhibit a striking phenotype in which the eyes and telencephalon are reduced or absent and diencephalic fates expand to the front of the brain (Heisenberg et al., 1996; Masai et al., 1997).

The fate changes within the forebrain of *mbl*$^{-/-}$ embryos are reflected in alterations to the expression of genes within the anterior neural plate from gastrulation stages onwards (Heisenberg et al., 2001). In *mbl*$^{-/-}$ embryos, genes expressed in the prospective telencephalon (*anf* and *emx1)* and in the eyes (*rx3*) are reduced or absent by bud stage, whereas genes expressed within the mid/caudal diencephalon (*fkd3 and deltaB*) are expanded anteriorly. In contrast, the expression domains of genes within the prospective midbrain (*pax2.1*) are only mildly altered or show no obvious changes in *mbl*$^{-/-}$ embryos. These results indicate that the anterior forebrain territory adopts posterior forebrain character by late gastrulation stages in *mbl*$^{-/-}$ embryos.

III.2 *masterblind* encodes the zebrafish axin1 protein

To understand the role of the *mbl* gene product in early forebrain patterning, we identified the mutation likely to be responsible for the *mbl*$^{-/-}$ phenotype. Mapping of the *mbl* mutation showed it to be adjacent to the centromeric region of linkage group 3, close to the Wnt scaffolding protein encoding gene, *axin1* (Shimizu et al., 2000). Mice lacking

Axin1 function have axis duplications (Jacobs-Cohen et al., 1984), supporting the conclusion that Axin1 is a negative regulator of Wnt signalling (Zeng et al., 1997). As suppression of Wnt signalling can promote anterior fates (Niehrs, 1999), we tested *axin1* as a candidate for harbouring the *mbl* mutation. Sequencing of the *mbl axin1* allele revealed a leucine to glutamine (L→Q) amino acid exchange at position 399 within the Gsk3 binding domain of Axin1 (Fig. III.1) raising the possibility that altered Axin1 function could be responsible for the $mbl^{-/-}$ phenotype. Mutations at the same or nearby sites in human Axin have been identified in cells from colon cancers and *in vitro* assays have shown that such mutations can reduce binding of Axin to Gsk3 (Webster et al., 2000).

axin1 RNA is maternally provided and ubiquitously expressed throughout early development. The expression of *axin1* is not noticeably changed in $mbl^{-/-}$ mutant embryos. Axin1 is therefore likely to be present throughout the embryo at stages when Mbl function is required (Heisenberg et al., 2001).

To test if altered Axin1 function is indeed responsible for the $mbl^{-/-}$ phenotype, $mbl^{-/-}$ embryos were microinjected with wild-type Axin1 RNA. This efficiently rescues early neural plate patterning and restores eyes and telencephalic structures at later stages (Heisenberg et al., 2001). In addition, injection of equivalent or 10 times higher levels of *mbl axin1* RNA into $mbl^{-/-}$ embryos did not rescue the $mbl^{-/-}$ phenotype. The mutation within Axin1 is therefore likely to be responsible for the fate transformations within the anterior neural plate of $mbl^{-/-}$ embryos.

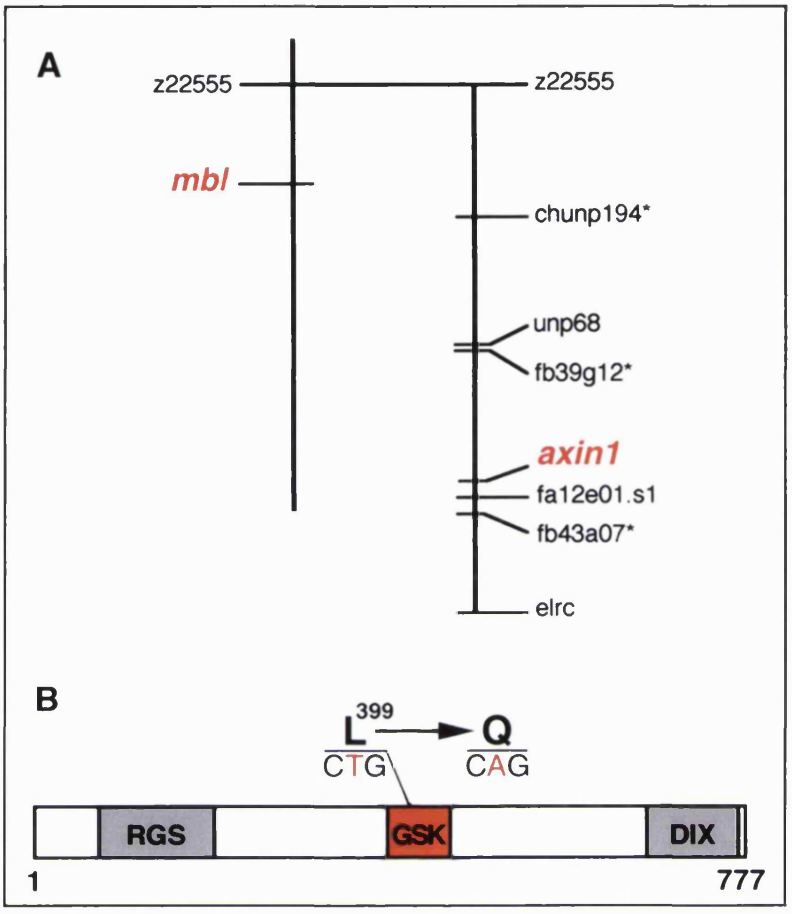

Figure III.1. *mbl*$^{-/-}$ embryos harbour a mutation in the *axin1* gene. (A) Mapping of *mbl* on linkage group 3 close to *axin1* on the corresponding region of a radiation hybrid map. (B) Schematic representation of the Axin1 protein showing the amino acid exchange (L^{399}→Q) and underlying point mutation (T→A) within the predicted Gsk3 binding site in the *mbl* Axin1 allele. Adapted from Heisenberg et al.,2001.

III.3 The zebrafish axin1 functions in early dorsoventral patterning

Mice lacking Axin1 function have multiple axes (Zeng et al., 1997) whereas *mbl*$^{-/-}$ fish embryos exhibit normal early dorsoventral patterning of mesodermal structures. This difference could be due to the presence of maternally provided Axin1 in *mbl*$^{-/-}$ embryos.

To test this model, I microinjected antisense oligonucleotide morpholinos against *axin1* into wild-type embryos. 50% of embryos injected with *axin1* morpholinos (n=205), were dorsalised as shown by the expanded expression of *pax2.1*, *flh* and *gsc* at bud stage (Fig. III.2). Furthermore, microinjection of higher doses of *axin1* morpholinos lead to expansion of *flh* expression. Therefore, in fish as in mice, Axin1 has an early role in dorsoventral patterning but this activity is not affected in zygotic *mbl*$^{-/-}$ embryos.

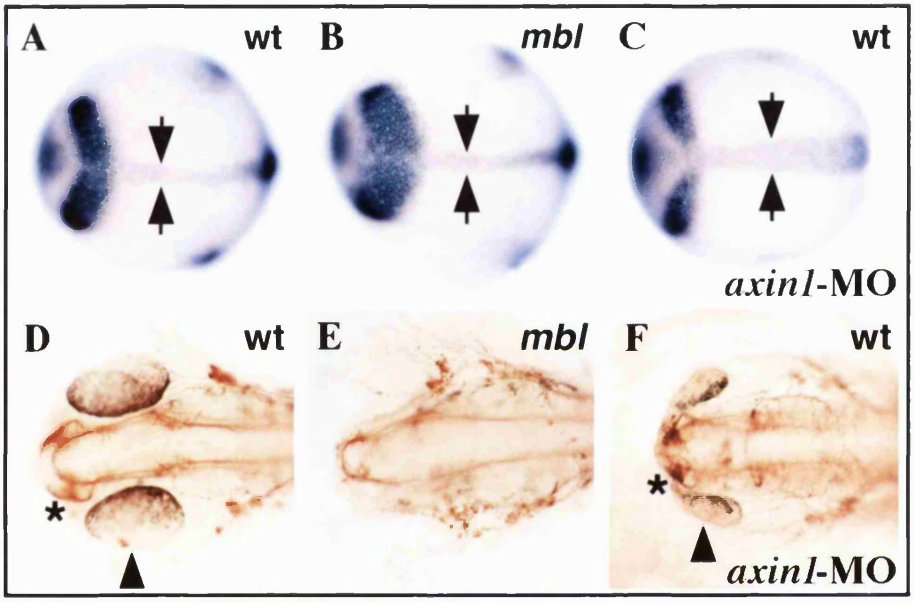

Figure III.2. Injection of *axin1* morpholinos partially phenocopies the *mbl* phenotype. Dorsal views of neural plates and brains of wild-type (A,D), *mbl*$^{-/-}$ (B,E) and wild-type embryos injected with *axin1*-MO antisense RNA (C,F) stained for the expression of *flh* and *pax2.1* at bud stage (A-C) or stained with α-acetylated tubulin antibody at pharyngula stage (D-F). In (C), the wildtype bud stage embryo injected with *axin1*-MO has a broader notochord (arrows in (A) to (C) point to the width of the notochord) indicative of dorsalisation. In (F), the wildtype pharyngula stage embryo injected with *axin1*-MO shows eyes of reduced size (arrowhead).

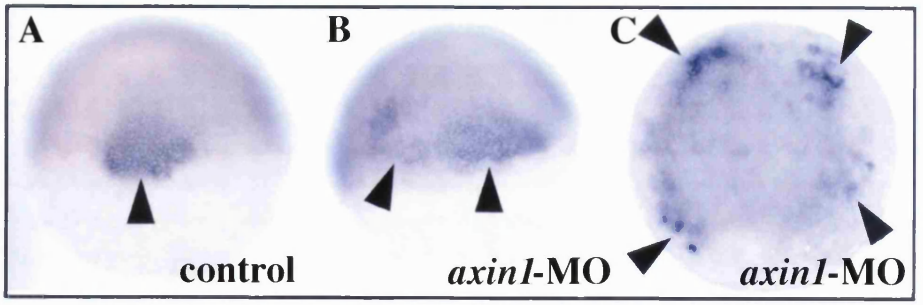

Figure III.3. Injection of *axin1* morpholinos leads to widespread dorsalisation. Dorsal (A,B) and animal pole (C) views of a wild-type embryo and embryos injected with *axin1* morpholino antisense oligonucleotides (B,C) stained for the expression of *flh* (a marker of organiser tissue, arrowheads) at shield stage. (A) is an uninjected wild-type control embryo showing a single expression domain of *flh* within the dorsal organiser region. In (B), the injected embryo shows expansion of *flh* expression on the dorsal side of the embryo. In (C), the injected embryo has multiple sites of *flh* expression indicative of widespread dorsalisation.

III.4 Antisense morpholino oligos phenocopy the *masterblind* mutation

Microinjection of antisense oligonucleotide morpholinos against *axin1* into wild-type embryos is able to phenocopy the *masterblind* mutation (Fig. III.2). About 45% of morpholino injected embryos had smaller eyes and anteriorly enlarged trigeminal ganglia resembling a mild $mbl^{-/-}$ phenotype. The stronger $mbl^{-/-}$ phenotype was not possible to obtain using this method because it is not possible to eliminate all the zygotic Axin1 protein function without affecting the maternal contribution. Microinjection of higher doses of *axin1* morpholinos lead to dorsalisation which impaired the gastrulation movements and resulted in death around the tail bud stages.

III.5 Discussion

Misexpression studies have suggested that suppression of Wnt signalling is required for induction of the vertebrate head (Niehrs, 1999). Direct genetic evidence supporting this conclusion has come from the finding that the *headless* (*hdl*) zebrafish mutation abolishes the repressor function of Tcf3, a transcriptional modulator of Wnt signalling (Kim et al., 2000). Although the evidence implicating the Wnt pathway in head development is strong, it remains to be determined where, when and how Wnt signalling must be suppressed to promote head formation.

Levels of Wnt signalling can be negatively regulated through the activity of a variety of extracellular proteins that include members of the Cerberus, Dickkopf and Sfrp families (Niehrs, 1999). In addition, several intracellular components of the Wnt signalling pathway can modulate the degree to which Wnt target genes are activated or repressed (Brown and Moon, 1998; Wodarz and Nusse, 1998). The protein kinase Gsk3 phosphorylates ß-catenin, targeting it for degradation (Aberle et al., 1997; Ikeda et al., 1998; Kishida et al., 1999), thereby limiting the amount of ß-catenin available to activate Wnt target genes. Gsk3 functions in multi-component complexes, one of which appears to include APC, Axin and additional proteins (Kim et al., 2000). Within this complex, Axin is believed to function as a scaffolding protein that enables Gsk3 to efficiently co-localise with and thereby phosphorylate ß-catenin (Ikeda et al., 1998; Kishida et al., 1999). Therefore the eventual transcription of Wnt signal target genes can be modulated in many ways and at several different positions in the Wnt signal transduction pathway.

Our studies reveal a novel role for Axin1 in the regional subdivision of prospective forebrain territories. We propose a model in which Wnt signalling must be suppressed to allow the development of telencephalic and optic fates and that if this fails to occur, prospective forebrain cells adopt a more caudal diencephalic identity. In support of this model, *headless/tcf3* mutant embryos show expansion of midbrain (or midbrain/hindbrain boundary) fates at the expense of forebrain fates (Kim et al., 2000).

In conclusion, thresholds of Wnt activity may specify different posterior to anterior fates within the neural plate in a manner analogous to that proposed for graded Bmp

activity in the allocation of fates along the dorsoventral axis of the neural plate (Barth et al., 1999; Nguyen et al., 2000).

References

Aberle, H., Bauer, A., Stappert, J., Kispert, A., and Kemler, R. (1997). beta-catenin is a target for the ubiquitin-proteasome pathway. Embo J *16*, 3797-804.

Aniento, F., Gu, F., Parton, R. G., and Gruenberg, J. (1996). An endosomal beta COP is involved in the pH-dependent formation of transport vesicles destined for late endosomes. J Cell Biol *133*, 29-41.

Antonny, B., Huber, I., Paris, S., Chabre, M., and Cassel, D. (1997). Activation of ADP-ribosylation factor 1 GTPase-activating protein by phosphatidylcholine-derived diacylglycerols. J Biol Chem *272*, 30848-51.

Aoe, T., Cukierman, E., Lee, A., Cassel, D., Peters, P. J., and Hsu, V. W. (1997). The KDEL receptor, ERD2, regulates intracellular traffic by recruiting a GTPase-activating protein for ARF1. Embo J *16*, 7305-16.

Appel, B., Fritz, A., Westerfield, M., Grunwald, D. J., Eisen, J. S., and Riley, B. B. (1999). Delta-mediated specification of midline cell fates in zebrafish embryos. Curr Biol *9*, 247-56.

Asakura,A., and Tapscott, S. J. (1998). Apoptosis of epaxial myotome in Danforth's short-tail (Sd) mice in somites that form following notochord degeneration. Dev Biol *203*, 276-89.

Bannykh, S. I., Nishimura, N., and Balch, W. E. (1998). Getting into the Golgi. Trends Cell Biol *8*, 21-5.

Barde, Y. A. (1989). Trophic factors and neuronal survival. Neuron *2*, 1525-34.

Barlowe, C., Orci, L., Yeung, T., Hosobuchi, M., Hamamoto, S., Salama, N., Rexach, M. F., Ravazzola, M., Amherdt, M., and Schekman, R. (1994). COPII: a membrane coat formed by Sec proteins that drive vesicle budding from the endoplasmic reticulum. Cell *77*, 895-907.

Barresi, M. J., Stickney, H. L., and Devoto, S. H. (2000). The zebrafish slow-muscle-omitted gene product is required for Hedgehog signal transduction and the development of slow muscle identity. Development *127*, 2189-99.

Barth, K. A., Kishimoto, Y., Rohr, K. B., Seydler, C., Schulte-Merker, S., and Wilson, S. W. (1999). Bmp activity establishes a gradient of positional information throughout the entire neural plate. Development *126*, 4977-87.

Beattie, C. E., Hatta, K., Halpern, M. E., Liu, H., Eisen, J. S., and Kimmel, C. B. (1997). Temporal separation in the specification of primary and secondary motoneurons in zebrafish. Dev Biol *187*, 171-82.

Beck, K. A., Buchanan, J. A., Malhotra, V., and Nelson, W. J. (1994). Golgi spectrin: identification of an erythroid beta-spectrin homolog associated with the Golgi complex. J Cell Biol *127*, 707-23.

Beck, K. A., Buchanan, J. A., and Nelson, W. J. (1997). Golgi membrane skeleton: identification, localization and oligomerization of a 195 kDa ankyrin isoform associated with the Golgi complex. J Cell Sci *110*, 1239-49.

Beck, K. A., and Nelson, W. J. (1996). The spectrin-based membrane skeleton as a membrane protein-sorting machine. Am J Physiol *270*, C1263-70.

Bennett, V., and Gilligan, D. M. (1993). The spectrin-based membrane skeleton and micron-scale organization of the plasma membrane. Annu Rev Cell Biol *9*, 27-66.

Beraud-Dufour, S., Paris, S., Chabre, M., and Antonny, B. (1999). Dual interaction of ADP ribosylation factor 1 with Sec7 domain and with lipid membranes during catalysis of guanine nucleotide exchange. J Biol Chem *274*, 37629-36.

Biemar, F., Argenton, F., Schmidtke, R., Epperlein, S., Peers, B., and Driever, W. (2001). Pancreas development in zebrafish: early dispersed appearance of endocrine hormone expressing cells and their convergence to form the definitive islet. Dev Biol *230*, 189-203.

Blagden, C. S., Currie, P. D., Ingham, P. W., and Hughes, S. M. (1997). Notochord induction of zebrafish slow muscle mediated by Sonic hedgehog. Genes Dev *11*, 2163-75.

Bobak, D. A., Nightingale, M. S., Murtagh, J. J., Price, S. R., Moss, J., and Vaughan, M. (1989). Molecular cloning, characterization, and expression of human ADP- ribosylation factors: two guanine nucleotide-dependent activators of cholera toxin. Proc Natl Acad Sci U S A *86*, 6101-5.

Bonfanti, L., Mironov, A. A., Jr., Martinez-Menarguez, J. A., Martella, O., Fusella, A., Baldassarre, M., Buccione, R., Geuze, H. J., Mironov, A. A., and Luini, A. (1998). Procollagen traverses the Golgi stack without leaving the lumen of cisternae: evidence for cisternal maturation. Cell *95*, 993-1003.

Borycki, A. G., Brunk, B., Tajbakhsh, S., Buckingham, M., Chiang, C., and Emerson, C. P., Jr. (1999). Sonic hedgehog controls epaxial muscle determination through Myf5 activation. Development *126*, 4053-63.

Bovolenta, P., and Dodd, J. (1991). Perturbation of neuronal differentiation and axon guidance in the spinal cord of mouse embryos lacking a floor plate: analysis of Danforth's short-tail mutation. Development *113*, 625-39.

Bowers, P. N., Brueckner, M., and Yost, H. J. (1996). The genetics of left-right development and heterotaxia. Semin Perinatol *20*, 577-88.

Brand, M., Heisenberg, C. P., Warga, R. M., Pelegri, F., Karlstrom, R. O., Beuchle, D., Picker, A., Jiang, Y. J., Furutani-Seiki, M., van Eeden, F. J., Granato, M., Haffter, P., Hammerschmidt, M., Kane, D. A., Kelsh, R. N., Mullins, M. C., Odenthal, J., and Nusslein-Volhard, C. (1996). Mutations affecting development of the midline and general body shape during zebrafish embryogenesis. Development *123*, 129-42.

Brand-Saberi, B., Ebensperger, C., Wilting, J., Balling, R., and Christ, B. (1993). The ventralizing effect of the notochord on somite differentiation in chick embryos. Anat Embryol (Berl) *188*, 239-45.

Bremser, M., Nickel, W., Schweikert, M., Ravazzola, M., Amherdt, M., Hughes, C. A., Sollner, T. H., Rothman, J. E., and Wieland, F. T. (1999). Coupling of coat assembly and vesicle budding to packaging of putative cargo receptors. Cell *96*, 495-506.

Briscoe, J., and Ericson, J. (1999). The specification of neuronal identity by graded Sonic Hedgehog signalling. Semin Cell Dev Biol *10*, 353-62.

Brown, H. A., Gutowski, S., Moomaw, C. R., Slaughter, C., and Sternweis, P. C. (1993). ADP-ribosylation factor, a small GTP-dependent regulatory protein, stimulates phospholipase D activity. Cell *75*, 1137-44.

Brown, J. D., and Moon, R. T. (1998). Wnt signaling: why is everything so negative? Curr Opin Cell Biol *10*, 182-7.

Brownlie, A., Donovan, A., Pratt, S. J., Paw, B. H., Oates, A. C., Brugnara, C., Witkowska, H. E., Sassa, S., and Zon, L. I. (1998). Positional cloning of the zebrafish sauternes gene: a model for congenital sideroblastic anaemia. Nat Genet *20*, 244-50.

Burkhardt, J. K., Echeverri, C. J., Nilsson, T., and Vallee, R. B. (1997). Overexpression of the dynamitin (p50) subunit of the dynactin complex disrupts dynein-dependent maintenance of membrane organelle distribution. J Cell Biol *139*, 469-84.

Chiang, C., Litingtung, Y., Lee, E., Young, K. E., Corden, J. L., Westphal, H., and Beachy, P. A. (1996). Cyclopia and defective axial patterning in mice lacking Sonic hedgehog gene function. Nature *383*, 407-13.

Chow, V. T., and Quek, H. H. (1997). Alpha coat protein COPA (HEP-COP): presence of an Alu repeat in cDNA and identity of the amino terminus to xenin. Ann Hum Genet *61*, 369-73.

Christ, B., and Ordahl, C. P. (1995). Early stages of chick somite development. Anat Embryol (Berl) *191*, 381-96.

Christ, B., and Wilting, J. (1992). From somites to vertebral column. Anat Anz *174*, 23-32.

Cleaver, O., and Krieg, P. A. (1998). VEGF mediates angioblast migration during development of the dorsal aorta in Xenopus. Development *125*, 3905-14.

Cleaver, O., Seufert, D. W., and Krieg, P. A. (2000). Endoderm patterning by the notochord: development of the hypochord in Xenopus. Development *127*, 869-79.

Cockcroft, S., Thomas, G. M., Fensome, A., Geny, B., Cunningham, E., Gout, I., Hiles, I., Totty, N. F., Truong, O., and Hsuan, J. J. (1994). Phospholipase D: a downstream effector of ARF in granulocytes. Science *263*, 523-6.

Colamarino, S. A., and Tessier-Lavigne, M. (1995). The axonal chemoattractant netrin-1 is also a chemorepellent for trochlear motor axons. Cell *81*, 621-9.

Colamarino, S. A., and Tessier-Lavigne, M. (1995). The role of the floor plate in axon guidance. Annu Rev Neurosci *18*, 497-529.

Cole, N. B., Sciaky, N., Marotta, A., Song, J., and Lippincott-Schwartz, J. (1996). Golgi dispersal during microtubule disruption: regeneration of Golgi stacks at peripheral endoplasmic reticulum exit sites. Mol Biol Cell *7*, 631-50.

Cosson, P., Lefkir, Y., Demolliere, C., and Letourneur, F. (1998). New COP1-binding motifs involved in ER retrieval. Embo J *17*, 6863-70.

Cosson, P., and Letourneur, F. (1997). Coatomer (COPI)-coated vesicles: role in intracellular transport and protein sorting. Curr Opin Cell Biol *9*, 484-7.

Cosson, P., and Letourneur, F. (1994). Coatomer interaction with di-lysine endoplasmic reticulum retention motifs. Science *263*, 1629-31.

Coucouvanis, E., and Martin, G. R. (1995). Signals for death and survival: a two-step mechanism for cavitation in the vertebrate embryo. Cell *83*, 279-87.

Currie, P. D., and Ingham, P. W. (1996). Induction of a specific muscle cell type by a hedgehog-like protein in zebrafish. Nature *382*, 452-5.

Daga, R. R., Thode, G., and Amores, A. (1996). Chromosome complement, C-banding, Ag-NOR and replication banding in the zebrafish Danio rerio. Chromosome Res *4*, 29-32.

Danos, M. C., and Yost, H. J. (1995). Linkage of cardiac left-right asymmetry and dorsal-anterior development in Xenopus. Development *121*, 1467-74.

Danos, M. C., and Yost, H. J. (1996). Role of notochord in specification of cardiac left-right orientation in zebrafish and Xenopus. Dev Biol *177*, 96-103.

Daro, E., Sheff, D., Gomez, M., Kreis, T., and Mellman, I. (1997). Inhibition of endosome function in CHO cells bearing a temperature- sensitive defect in the coatomer (COPI) component epsilon-COP. J Cell Biol *139*, 1747-59.

De Matteis, M. A., and Morrow, J. S. (1998). The role of ankyrin and spectrin in membrane transport and domain formation. Curr Opin Cell Biol *10*, 542-9.

De Matteis, M. A., Santini, G., Kahn, R. A., Di Tullio, G., and Luini, A. (1993). Receptor and protein kinase C-mediated regulation of ARF binding to the Golgi complex. Nature *364*, 818-21.

Denetclaw, W. F., Jr., Christ, B., and Ordahl, C. P. (1997). Location and growth of epaxial myotome precursor cells. Development *124*, 1601-10.

Devarajan, P., Stabach, P. R., De Matteis, M. A., and Morrow, J. S. (1997). Na,K-ATPase transport from endoplasmic reticulum to Golgi requires the Golgi spectrin-ankyrin G119 skeleton in Madin Darby canine kidney cells. Proc Natl Acad Sci U S A *94*, 10711-6.

Devarajan, P., Stabach, P. R., Mann, A. S., Ardito, T., Kashgarian, M., and Morrow, J. S. (1996). Identification of a small cytoplasmic ankyrin (AnkG119) in the kidney and muscle that binds beta I sigma spectrin and associates with the Golgi apparatus. J Cell Biol *133*, 819-30.

Devoto, S. H., Melancon, E., Eisen, J. S., and Westerfield, M. (1996). Identification of separate slow and fast muscle precursor cells in vivo, prior to somite formation. Development *122*, 3371-80.

Dietrich, S., Schubert, F. R., Healy, C., Sharpe, P. T., and Lumsden, A. (1998). Specification of the hypaxial musculature. Development *125*, 2235-49.

Dietrich, S., Schubert, F. R., Gruss, P., and Lumsden, A. (1999). The role of the notochord for epaxial myotome formation in the mouse. Cell Mol Biol (Noisy-le-grand) *45*, 601-16.

Ding, Q., Motoyama, J., Gasca, S., Mo, R., Sasaki, H., Rossant, J., and Hui, C. C. (1998). Diminished Sonic hedgehog signaling and lack of floor plate differentiation in Gli2 mutant mice. Development *125*, 2533-43.

Dockter, J. L. (2000). Sclerotome induction and differentiation. Curr Top Dev Biol *48*, 77-127.

Donaldson, J. G., Cassel, D., Kahn, R. A., and Klausner, R. D. (1992). ADP-ribosylation factor, a small GTP-binding protein, is required for binding of the coatomer protein beta-COP to Golgi membranes. Proc Natl Acad Sci U S A *89*, 6408-12.

Donaldson, J. G., Finazzi, D., and Klausner, R. D. (1992). Brefeldin A inhibits Golgi membrane-catalysed exchange of guanine nucleotide onto ARF protein. Nature *360*, 350-2.

Driever, W., Solnica-Krezel, L., Schier, A. F., Neuhauss, S. C., Malicki, J., Stemple, D. L., Stainier, D. Y., Zwartkruis, F., Abdelilah, S., Rangini, Z., Belak, J., and Boggs, C. (1996). A genetic screen for mutations affecting embryogenesis in zebrafish. Development *123*, 37-46.

Drubin, D. G., and Nelson, W. J. (1996). Origins of cell polarity. Cell *84*, 335-44.

Du, S. J., Devoto, S. H., Westerfield, M., and Moon, R. T. (1997). Positive and negative regulation of muscle cell identity by members of the hedgehog and TGF-beta gene families. J Cell Biol *139*, 145-56.

Duden, R., Griffiths, G., Frank, R., Argos, P., and Kreis, T. E. (1991). Beta-COP, a 110 kd protein associated with non-clathrin-coated vesicles and the Golgi complex, shows homology to beta-adaptin. Cell *64*, 649-65.

Echeverri, C. J., Paschal, B. M., Vaughan, K. T., and Vallee, R. B. (1996). Molecular characterization of the 50-kD subunit of dynactin reveals function for the complex in chromosome alignment and spindle organization during mitosis. J Cell Biol *132*, 617-33.

Ekker, S. C. (2000). Morphants: a new systematic vertebrate functional genomics approach. Yeast *17*, 302-306.

Ekker, S. C., Ungar, A. R., Greenstein, P., von Kessler, D. P., Porter, J. A., Moon, R. T., and Beachy, P. A. (1995). Patterning activities of vertebrate hedgehog proteins in the developing eye and brain. Curr Biol *5*, 944-55.

Ericson, J., Briscoe, J., Rashbass, P., van Heyningen, V., and Jessell, T. M. (1997). Graded sonic hedgehog signaling and the specification of cell fate in the ventral neural tube. Cold Spring Harb Symp Quant Biol *62*, 451-66.

Eriksson, J., and Lofberg, J. (2000). Development of the hypochord and dorsal aorta in the zebrafish embryo (Danio rerio). J Morphol *244*, 167-76.

Eugster, A., Frigerio, G., Dale, M., and Duden, R. (2000). COP I domains required for coatomer integrity, and novel interactions with ARF and ARF-GAP. Embo J *19*, 3905-17.

Fan, C. M., and Tessier-Lavigne, M. (1994). Patterning of mammalian somites by surface ectoderm and notochord: evidence for sclerotome induction by a hedgehog homolog. Cell *79*, 1175-86.

Faulstich, D., Auerbach, S., Orci, L., Ravazzola, M., Wegchingel, S., Lottspeich, F., Stenbeck, G., Harter, C., Wieland, F. T., and Tschochner, H. (1996). Architecture of coatomer: molecular characterization of delta-COP and protein interactions within the complex. J Cell Biol *135*, 53-61.

Fekany, K., Yamanaka, Y., Leung, T., Sirotkin, H. I., Topczewski, J., Gates, M. A., Hibi, M., Renucci, A., Stemple, D., Radbill, A., Schier, A. F., Driever, W., Hirano, T., Talbot, W. S., and Solnica-Krezel, L. (1999). The zebrafish bozozok locus encodes Dharma, a homeodomain protein essential for induction of gastrula organizer and dorsoanterior embryonic structures. Development *126*, 1427-38.

Fiedler, K., Veit, M., Stamnes, M. A., and Rothman, J. E. (1996). Bimodal interaction of coatomer with the p24 family of putative cargo receptors. Science *273*, 1396-9.

Finazzi, D., Cassel, D., Donaldson, J. G., and Klausner, R. D. (1994). Aluminum fluoride acts on the reversibility of ARF1-dependent coat protein binding to Golgi membranes. J Biol Chem *269*, 13325-30.

Fouquet, B., Weinstein, B. M., Serluca, F. C., and Fishman, M. C. (1997). Vessel patterning in the embryo of the zebrafish: guidance by notochord. Dev Biol *183*, 37-48.

Fraser, S., Keynes, R., and Lumsden, A. (1990). Segmentation in the chick embryo hindbrain is defined by cell lineage restrictions. Nature *344*, 431-5.

Gaynor, E. C., Graham, T. R., and Emr, S. D. (1998). COPI in ER/Golgi and intra-Golgi transport: do yeast COPI mutants point the way? Biochim Biophys Acta *1404*, 33-51.

Girod, A., Storrie, B., Simpson, J. C., Johannes, L., Goud, B., Roberts, L. M., Lord, J. M., Nilsson, T., and Pepperkok, R. (1999). Evidence for a COP-I-independent transport route from the Golgi complex to the endoplasmic reticulum. Nat Cell Biol *1*, 423-30.

Glick, B. S., Elston, T., and Oster, G. (1997). A cisternal maturation mechanism can explain the asymmetry of the Golgi stack. FEBS Lett *414*, 177-81.

Glucksman, A. (1951). Cell deaths in normal vertebrate ontogeny. Biol. Rev. *26*.

Godi, A., Santone, I., Pertile, P., Devarajan, P., Stabach, P. R., Morrow, J. S., Di Tullio, G., Polishchuk, R., Petrucci, T. C., Luini, A., and De Matteis, M. A. (1998). ADP ribosylation factor regulates spectrin binding to the Golgi complex. Proc Natl Acad Sci U S A *95*, 8607-12.

Goff, D. J., Galvin, K., Katz, H., Westerfield, M., Lander, E. S., and Tabin, C. J. (1992). Identification of polymorphic simple sequence repeats in the genome of the zebrafish. Genomics *14*, 200-2.

Goldberg, J. (2000). Decoding of sorting signals by coatomer through a GTPase switch in the COPI coat complex. Cell *100*, 671-9.

Goldberg, J. (1999). Structural and functional analysis of the ARF1-ARFGAP complex reveals a role for coatomer in GTP hydrolysis. Cell *96*, 893-902.

Goldstein, A. M., and Fishman, M. C. (1998). Notochord regulates cardiac lineage in zebrafish embryos. Dev Biol *201*, 247-52.

Good, P. J. (1995). A conserved family of elav-like genes in vertebrates. Proc Natl Acad Sci U S A *92*, 4557-61.

Goulding, M., Lumsden, A., and Paquette, A. J. (1994). Regulation of Pax-3 expression in the dermomyotome and its role in muscle development. Development *120*, 957-71.

Goulding, M. D., Lumsden, A., and Gruss, P. (1993). Signals from the notochord and floor plate regulate the region-specific expression of two Pax genes in the developing spinal cord. Development *117*, 1001-16.

Gu, F., Aniento, F., Parton, R. G., and Gruenberg, J. (1997). Functional dissection of COP-I subunits in the biogenesis of multivesicular endosomes. J Cell Biol *139*, 1183-95.

Guo, Q., Vasile, E., and Krieger, M. (1994). Disruptions in Golgi structure and membrane traffic in a conditional lethal mammalian cell mutant are corrected by epsilon-COP. J Cell Biol *125*, 1213-24.

Haffter, P., Granato, M., Brand, M., Mullins, M. C., Hammerschmidt, M., Kane, D. A., Odenthal, J., van Eeden, F. J., Jiang, Y. J., Heisenberg, C. P., Kelsh, R. N., Furutani-Seiki, M., Vogelsang, E., Beuchle, D., Schach, U., Fabian, C., and Nusslein-Volhard, C. (1996). The identification of genes with unique and essential functions in the development of the zebrafish, Danio rerio. Development *123*, 1-36.

Halpern, M. E., Hatta, K., Amacher, S. L., Talbot, W. S., Yan, Y. L., Thisse, B., Thisse, C., Postlethwait, J. H., and Kimmel, C. B. (1997). Genetic interactions in zebrafish midline development. Dev Biol *187*, 154-70.

Halpern, M. E., Ho, R. K., Walker, C., and Kimmel, C. B. (1993). Induction of muscle pioneers and floor plate is distinguished by the zebrafish no tail mutation. Cell *75*, 99-111.

Hammerschmidt, M., Bitgood, M. J., and McMahon, A. P. (1996). Protein kinase A is a common negative regulator of Hedgehog signaling in the vertebrate embryo. Genes Dev *10*, 647-58.

Hammerschmidt, M., and McMahon, A. P. (1998). The effect of pertussis toxin on zebrafish development: a possible role for inhibitory G-proteins in hedgehog signaling. Dev Biol *194*, 166-71.

Hara-Kuge, S., Kuge, O., Orci, L., Amherdt, M., Ravazzola, M., Wieland, F. T., and Rothman, J. E. (1994). En bloc incorporation of coatomer subunits during the assembly of COP- coated vesicles. J Cell Biol *124*, 883-92.

Hatta, K., Kimmel, C. B., Ho, R. K., and Walker, C. (1991). The cyclops mutation blocks specification of the floor plate of the zebrafish central nervous system. Nature *350*, 339-41.

Hauri, H. P., Kappeler, F., Andersson, H., and Appenzeller, C. (2000). ERGIC-53 and traffic in the secretory pathway. J Cell Sci *113*, 587-96.

Hay, J. C., Klumperman, J., Oorschot, V., Steegmaier, M., Kuo, C. S., and Scheller, R. H. (1998). Localization, dynamics, and protein interactions reveal distinct roles for ER and Golgi SNAREs. J Cell Biol *141*, 1489-502.

Hebrok, M., Kim, S. K., and Melton, D. A. (1998). Notochord repression of endodermal Sonic hedgehog permits pancreas development. Genes Dev *12*, 1705-13.

Hegde, R. S., and Lingappa, V. R. (1997). Membrane protein biogenesis: regulated complexity at the endoplasmic reticulum. Cell *91*, 575-82.

Heisenberg, C.-P., Houart, C., Take-uchi, M., Rauch, G.-J., Young, Y., Coutinho, P., Masai, I., Caneparo, L., Concha, M. L., Geisler, R., Dale, T. C., Wilson, S. W., and Stemple, D. (2001). A mutation in the Gsk3-binding domain of zebrafish Masterblind/Axin1 leads to a fate transformation of telencephalon and eyes to diencephalon. Genes Dev *In print.*

Heisenberg, C. P., Brand, M., Jiang, Y. J., Warga, R. M., Beuchle, D., van Eeden, F. J., Furutani-Seiki, M., Granato, M., Haffter, P., Hammerschmidt, M., Kane, D. A., Kelsh, R. N., Mullins, M. C., Odenthal, J., and Nusslein-Volhard, C. (1996). Genes involved in forebrain development in the zebrafish, Danio rerio. Development *123*, 191-203.

Helms, J. B., Palmer, D. J., and Rothman, J. E. (1993). Two distinct populations of ARF bound to Golgi membranes. J Cell Biol *121*, 751-60.

Helms, J. B., and Rothman, J. E. (1992). Inhibition by brefeldin A of a Golgi membrane enzyme that catalyses exchange of guanine nucleotide bound to ARF. Nature *360*, 352-4.

Ho, W. C., Allan, V. J., van Meer, G., Berger, E. G., and Kreis, T. E. (1989). Reclustering of scattered Golgi elements occurs along microtubules. Eur J Cell Biol *48*, 250-63.

Hollenbeck, P. J. (1993). Phosphorylation of neuronal kinesin heavy and light chains in vivo. J Neurochem *60*, 2265-75.

Holleran, E. A., Karki, S., and Holzbaur, E. L. (1998). The role of the dynactin complex in intracellular motility. Int Rev Cytol *182*, 69-109.

Holleran, E. A., Tokito, M. K., Karki, S., and Holzbaur, E. L. (1996). Centractin (ARP1) associates with spectrin revealing a potential mechanism to link dynactin to intracellular organelles. J Cell Biol *135*, 1815-29.

Holzbaur, E. L., and Vallee, R. B. (1994). DYNEINS: molecular structure and cellular function. Annu Rev Cell Biol *10*, 339-72.

Huang, R., Zhi, Q., Schmidt, C., Wilting, J., Brand-Saberi, B., and Christ, B. (2000). Sclerotomal origin of the ribs. Development *127*, 527-32.

Hudson, R. T., and Draper, R. K. (1997). Interaction of coatomer with aminoglycoside antibiotics: evidence that coatomer has at least two dilysine binding sites. Mol Biol Cell *8*, 1901-10.

Hukriede, N. A., Joly, L., Tsang, M., Miles, J., Tellis, P., Epstein, J. A., Barbazuk, W. B., Li, F. N., Paw, B., Postlethwait, J. H., Hudson, T. J., Zon, L. I., McPherson, J. D., Chevrette, M., Dawid, I. B., Johnson, S. L., and Ekker, M. (1999). Radiation hybrid mapping of the zebrafish genome. Proc Natl Acad Sci U S A *96*, 9745-50.

Ikeda, S., Kishida, S., Yamamoto, H., Murai, H., Koyama, S., and Kikuchi, A. (1998). Axin, a negative regulator of the Wnt signaling pathway, forms a complex with GSK-3beta and beta-catenin and promotes GSK-3beta- dependent phosphorylation of beta-catenin. Embo J *17*, 1371-84.

Jacobs-Cohen, R. J., Spiegelman, M., Cookingham, J. C., and Bennett, D. (1984). Knobbly, a new dominant mutation in the mouse that affects embryonic ectoderm organization. Genet Res *43*, 43-50.

Jacobsen, M. D., Weil, M., and Raff, M. C. (1996). Role of Ced-3/ICE-family proteases in staurosporine-induced programmed cell death. J Cell Biol *133*, 1041-51.

Johnson, D. I. (1999). Cdc42: An essential Rho-type GTPase controlling eukaryotic cell polarity. Microbiol Mol Biol Rev *63*, 54-105.

Johnson, K. J., Hall, E. S., and Boekelheide, K. (1996). Kinesin localizes to the trans-Golgi network regardless of microtubule organization. Eur J Cell Biol *69*, 276-87.

Johnson, S. L., Gates, M. A., Johnson, M., Talbot, W. S., Horne, S., Baik, K., Rude, S., Wong, J. R., and Postlethwait, J. H. (1996). Centromere-linkage analysis and consolidation of the zebrafish genetic map. Genetics *142*, 1277-88.

Joubin, K., and Stern, C. D. (1999). Molecular interactions continuously define the organizer during the cell movements of gastrulation. Cell *98*, 559-71.

Kahn, R. A., and Gilman, A. G. (1986). The protein cofactor necessary for ADP-ribosylation of Gs by cholera toxin is itself a GTP binding protein. J Biol Chem *261*, 7906-11.

Karlstrom, R. O., Talbot, W. S., and Schier, A. F. (1999). Comparative synteny cloning of zebrafish you-too: mutations in the Hedgehog target gli2 affect ventral forebrain patterning. Genes Dev *13*, 388-93.

Kelly, P. D., Chu, F., Woods, I. G., Ngo-Hazelett, P., Cardozo, T., Huang, H., Kimm, F., Liao, L., Yan, Y. L., Zhou, Y., Johnson, S. L., Abagyan, R., Schier, A. F., Postlethwait, J. H., and Talbot, W. S. (2000). Genetic linkage mapping of zebrafish genes and ESTs. Genome Res *10*, 558-67.

Kelsh, R. N., Brand, M., Jiang, Y. J., Heisenberg, C. P., Lin, S., Haffter, P., Odenthal, J., Mullins, M. C., van Eeden, F. J., Furutani-Seiki, M., Granato, M., Hammerschmidt, M., Kane, D. A., Warga, R. M., Beuchle, D., Vogelsang, L., and Nusslein-Volhard, C. (1996). Zebrafish pigmentation mutations and the processes of neural crest development. Development *123*, 369-89.

Kelsh, R. N., Schmid, B., and Eisen, J. S. (2000). Genetic analysis of melanophore development in zebrafish embryos. Dev Biol *225*, 277-93.

Kerr, J. F., Harmon, B., and Searle, J. (1974). An electron-microscope study of cell deletion in the anuran tadpole tail during spontaneous metamorphosis with special reference to apoptosis of striated muscle fibers. J Cell Sci *14*, 571-85.

Kerr, J. F., Wyllie, A. H., and Currie, A. R. (1972). Apoptosis: a basic biological phenomenon with wide-ranging implications in tissue kinetics. Br J Cancer *26*, 239-57.

Keynes, R., Tannahill, D., Morgenstern, D. A., Johnson, A. R., Cook, G. M., and Pini, A. (1997). Surround repulsion of spinal sensory axons in higher vertebrate embryos. Neuron *18*, 889-97.

Kim, C. H., Oda, T., Itoh, M., Jiang, D., Artinger, K. B., Chandrasekharappa, S. C., Driever, W., and Chitnis, A. B. (2000). Repressor activity of Headless/Tcf3 is essential for vertebrate head formation. Nature *407*, 913-6.

Kim, S. K., Hebrok, M., and Melton, D. A. (1997). Notochord to endoderm signaling is required for pancreas development. Development *124*, 4243-52.

Kimmel, C. B., Ballard, W. W., Kimmel, S. R., Ullmann, B., and Schilling, T. F. (1995). Stages of embryonic development of the zebrafish. Dev Dyn *203*, 253-310.

Kishida, M., Koyama, S., Kishida, S., Matsubara, K., Nakashima, S., Higano, K., Takada, R., Takada, S., and Kikuchi, A. (1999). Axin prevents Wnt-3a-induced accumulation of beta-catenin. Oncogene *18*, 979-85.

Klessinger, S., and Christ, B. (1996). Axial structures control laterality in the distribution pattern of endothelial cells. Anat Embryol (Berl) *193*, 319-30.

Knapik, E. W., Goodman, A., Atkinson, O. S., Roberts, C. T., Shiozawa, M., Sim, C. U., Weksler-Zangen, S., Trolliet, M. R., Futrell, C., Innes, B. A., Koike, G., McLaughlin, M. G., Pierre, L., Simon, J. S., Vilallonga, E., Roy, M., Chiang, P. W., Fishman, M. C., Driever, W., and Jacob, H. J. (1996). A reference cross DNA panel for zebrafish (Danio rerio) anchored with simple sequence length polymorphisms. Development *123*, 451-60.

Kooy, J., Toh, B. H., Pettitt, J. M., Erlich, R., and Gleeson, P. A. (1992). Human autoantibodies as reagents to conserved Golgi components. Characterization of a peripheral, 230-kDa compartment-specific Golgi protein. J Biol Chem *267*, 20255-63.

Krauss, S., Concordet, J. P., and Ingham, P. W. (1993). A functionally conserved homolog of the Drosophila segment polarity gene hh is expressed in tissues with polarizing activity in zebrafish embryos. Cell *75*, 1431-44.

Krauss, S., Johansen, T., Korzh, V., and Fjose, A. (1991). Expression of the zebrafish paired box gene pax[zf-b] during early neurogenesis. Development *113*, 1193-206.

Kuge, O., Hara-Kuge, S., Orci, L., Ravazzola, M., Amherdt, M., Tanigawa, G., Wieland, F. T., and Rothman, J. E. (1993). zeta-COP, a subunit of coatomer, is required for COP-coated vesicle assembly. J Cell Biol *123*, 1727-34.

Kumar, J., Yu, H., and Sheetz, M. P. (1995). Kinectin, an essential anchor for kinesin-driven vesicle motility. Science *267*, 1834-7.

Kwok, C., Korn, R. M., Davis, M. E., Burt, D. W., Critcher, R., McCarthy, L., Paw, B. H., Zon, L. I., Goodfellow, P. N., and Schmitt, K. (1998). Characterization of whole genome radiation hybrid mapping resources for non-mammalian vertebrates. Nucleic Acids Res *26*, 3562-6.

Le Douarin, N. M., and Halpern, M. E. (2000). Discussion point. Origin and specification of the neural tube floor plate: insights from the chick and zebrafish. Curr Opin Neurobiol *10*, 23-30.

Letourneur, F., Gaynor, E. C., Hennecke, S., Demolliere, C., Duden, R., Emr, S. D., Riezman, H., and Cosson, P. (1994). Coatomer is essential for retrieval of dilysine-tagged proteins to the endoplasmic reticulum. Cell *79*, 1199-207.

Levi-Montalcini, R. (1987). The nerve growth factor 35 years later. Science *237*, 1154-62.

Levin, M., Roberts, D. J., Holmes, L. B., and Tabin, C. (1996). Laterality defects in conjoined twins. Nature *384*, 321.

Lewis, K. E., Currie, P. D., Roy, S., Schauerte, H., Haffter, P., and Ingham, P. W. (1999). Control of muscle cell-type specification in the zebrafish embryo by Hedgehog signalling. Dev Biol *216*, 469-80.

Lewis, M. J., and Pelham, H. R. (1992). Ligand-induced redistribution of a human KDEL receptor from the Golgi complex to the endoplasmic reticulum. Cell *68*, 353-64.

Linstedt, A. D., Foguet, M., Renz, M., Seelig, H. P., Glick, B. S., and Hauri, H. P. (1995). A C-terminally-anchored Golgi protein is inserted into the endoplasmic reticulum and then transported to the Golgi apparatus. Proc Natl Acad Sci U S A *92*, 5102-5.

Linstedt, A. D., and Hauri, H. P. (1993). Giantin, a novel conserved Golgi membrane protein containing a cytoplasmic domain of at least 350 kDa. Mol Biol Cell *4*, 679-93.

Lippincott-Schwartz, J. (1998). Cytoskeletal proteins and Golgi dynamics. Curr Opin Cell Biol *10*, 52-9.

Lippincott-Schwartz, J., Cole, N. B., Marotta, A., Conrad, P. A., and Bloom, G. S. (1995). Kinesin is the motor for microtubule-mediated Golgi-to-ER membrane traffic. J Cell Biol *128*, 293-306.

Lister, J. A., Robertson, C. P., Lepage, T., Johnson, S. L., and Raible, D. W. (1999). nacre encodes a zebrafish microphthalmia-related protein that regulates neural-crest-derived pigment cell fate. Development *126*, 3757-67.

Lofberg, J., and Collazo, A. (1997). Hypochord, an enigmatic embryonic structure: study of the axolotl embryo. J Morphol *232*, 57-66.

Lohr, J. L., Danos, M. C., and Yost, H. J. (1997). Left-right asymmetry of a nodal-related gene is regulated by dorsoanterior midline structures during Xenopus development. Development *124*, 1465-72.

Lowe, M., and Kreis, T. E. (1995). In vitro assembly and disassembly of coatomer. J Biol Chem *270*, 31364-71.

Lowe, M., and Kreis, T. E. (1996). In vivo assembly of coatomer, the COP-I coat precursor. J Biol Chem *271*, 30725-30.

Luby-Phelps, K., Castle, P. E., Taylor, D. L., and Lanni, F. (1987). Hindered diffusion of inert tracer particles in the cytoplasm of mouse 3T3 cells. Proc Natl Acad Sci U S A *84*, 4910-3.

Maier, C. E., and Miller, R. H. (1997). Notochord is essential for oligodendrocyte development in Xenopus spinal cord. J Neurosci Res *47*, 361-71.

Manifava, M., Thuring, J. W., Lim, Z. Y., Packman, L., Holmes, A. B., and Ktistakis, N. T. (2000). Differential binding of traffic-related proteins to phosphatidic acid- or phosphatidylinositol (4,5) bisphosphate-coupled affinity reagents. J Biol Chem.

Mansour, S. J., Skaug, J., Zhao, X. H., Giordano, J., Scherer, S. W., and Melancon, P. (1999). p200 ARF-GEP1: a Golgi-localized guanine nucleotide exchange protein whose Sec7 domain is targeted by the drug brefeldin A. Proc Natl Acad Sci U S A *96*, 7968-73.

Marcelle, C., Stark, M. R., and Bronner-Fraser, M. (1997). Coordinate actions of BMPs, Wnts, Shh and noggin mediate patterning of the dorsal somite. Development *124*, 3955-63.

Marks, D. L., Larkin, J. M., and McNiven, M. A. (1994). Association of kinesin with the Golgi apparatus in rat hepatocytes. J Cell Sci *107*, 2417-26.

Masai, I., Heisenberg, C. P., Barth, K. A., Macdonald, R., Adamek, S., and Wilson, S. W. (1997). floating head and masterblind regulate neuronal patterning in the roof of the forebrain. Neuron *18*, 43-57.

Masuda, T., Okado, N., and Shiga, T. (2000). The involvement of axonin-1/SC2 in mediating notochord-derived chemorepulsive activities for dorsal root ganglion neurites. Dev Biol *224*, 112-21.

Matise, M. P., Epstein, D. J., Park, H. L., Platt, K. A., and Joyner, A. L. (1998). Gli2 is required for induction of floor plate and adjacent cells, but not most ventral neurons in the mouse central nervous system. Development *125*, 2759-70.

McCallum, S. J., Erickson, J. W., and Cerione, R. A. (1998). Characterization of the association of the actin-binding protein, IQGAP, and activated Cdc42 with Golgi membranes. J Biol Chem *273*, 22537-44.

Mellman, I., and Simons, K. (1992). The Golgi complex: in vitro veritas? Cell *68*, 829-40.

Melloy, P. G., Ewart, J. L., Cohen, M. F., Desmond, M. E., Kuehn, M. R., and Lo, C. W. (1998). No turning, a mouse mutation causing left-right and axial patterning defects. Dev Biol *193*, 77-89.

Metzler, M., Gertz, A., Sarkar, M., Schachter, H., Schrader, J. W., and Marth, J. D. (1994). Complex asparagine-linked oligosaccharides are required for morphogenic events during post-implantation development. Embo J *13*, 2056-65.

Milligan, C. E., Prevette, D., Yaginuma, H., Homma, S., Cardwell, C., Fritz, L. C., Tomaselli, K. J., Oppenheim, R. W., and Schwartz, L. M. (1995). Peptide inhibitors of the ICE protease family arrest programmed cell death of motoneurons in vivo and in vitro. Neuron *15*, 385-93.

Moos, M., Jr., Wang, S., and Krinks, M. (1995). Anti-dorsalizing morphogenetic protein is a novel TGF-beta homolog expressed in the Spemann organizer. Development *121*, 4293-301.

Nagahama, M., Orci, L., Ravazzola, M., Amherdt, M., Lacomis, L., Tempst, P., Rothman, J. E., and Sollner, T. H. (1996). A v-SNARE implicated in intra-Golgi transport. J Cell Biol *133*, 507-16.

Nakamoto, K., and Shiga, T. (1998). Tissues exhibiting inhibitory [correction of inhibiory] and repulsive activities during the initial stages of neurite outgrowth from the dorsal root ganglion in the chick embryo. Dev Biol *202*, 304-14.

Nakamura, N., Lowe, M., Levine, T. P., Rabouille, C., and Warren, G. (1997). The vesicle docking protein p115 binds GM130, a cis-Golgi matrix protein, in a mitotically regulated manner. Cell *89*, 445-55.

Nakamura, N., Rabouille, C., Watson, R., Nilsson, T., Hui, N., Slusarewicz, P., Kreis, T. E., and Warren, G. (1995). Characterization of a cis-Golgi matrix protein, GM130. J Cell Biol *131*, 1715-26.

Nascone, N., and Mercola, M. (1997). Organizer induction determines left-right asymmetry in Xenopus. Dev Biol *189*, 68-78.

Nasevicius, A., and Ekker, S. C. (2000). Effective targeted gene 'knockdown' in zebrafish. Nat Genet *26*, 216-20.

Nelson, D. S., Alvarez, C., Gao, Y. S., Garcia-Mata, R., Fialkowski, E., and Sztul, E. (1998). The membrane transport factor TAP/p115 cycles between the Golgi and earlier secretory compartments and contains distinct domains required for its localization and function. J Cell Biol *143*, 319-31.

Nguyen, V. H., Trout, J., Connors, S. A., Andermann, P., Weinberg, E., and Mullins, M. C. (2000). Dorsal and intermediate neuronal cell types of the spinal cord are established by a BMP signaling pathway. Development *127*, 1209-20.

Nickel, W., and Wieland, F. T. (1997). Biogenesis of COPI-coated transport vesicles. FEBS Lett *413*, 395-400.

Niehrs, C. (1999). Head in the WNT: the molecular nature of Spemann's head organizer. Trends Genet *15*, 314-9.

Nuoffer, C., and Balch, W. E. (1994). GTPases: multifunctional molecular switches regulating vesicular traffic. Annu Rev Biochem *63*, 949-90.

Obika, M., and Fukuzawa, T. (1993). Cytoskeletal architecture of dermal chromatophores of the freshwater teleost Oryzias latipes. Pigment Cell Res *6*, 417-22.

Odenthal, J., Haffter, P., Vogelsang, E., Brand, M., van Eeden, F. J., Furutani-Seiki, M., Granato, M., Hammerschmidt, M., Heisenberg, C. P., Jiang, Y. J., Kane, D. A., Kelsh, R. N., Mullins, M. C., Warga, R. M., Allende, M. L., Weinberg, E. S., and Nusslein-Volhard, C. (1996). Mutations affecting the formation of the notochord in the zebrafish, Danio rerio. Development *123*, 103-15.

Odenthal, J., Rossnagel, K., Haffter, P., Kelsh, R. N., Vogelsang, E., Brand, M., van Eeden, F. J., Furutani-Seiki, M., Granato, M., Hammerschmidt, M., Heisenberg, C. P., Jiang, Y. J., Kane, D. A., Mullins, M. C., and Nusslein-Volhard, C. (1996). Mutations affecting xanthophore pigmentation in the zebrafish, Danio rerio. Development *123*, 391-8.

Odenthal, J., van Eeden, F. J., Haffter, P., Ingham, P. W., and Nusslein-Volhard, C. (2000). Two distinct cell populations in the floor plate of the zebrafish are induced by different pathways. Dev Biol *219*, 350-63.

Olivera-Martinez, I., Coltey, M., Dhouailly, D., and Pourquie, O. (2000). Mediolateral somitic origin of ribs and dermis determined by quail- chick chimeras. Development *127*, 4611-7.

Oppenheim, R. W. (1991). Cell death during development of the nervous system. Annu Rev Neurosci *14*, 453-501.
Oppenheimer, J. M. (1936). Transplantation experiments on developing teleosts

(Fundulus and Perca). *J.Exp.Zool. 72*, 247-269.

Orci, L., Amherdt, M., Ravazzola, M., Perrelet, A., and Rothman, J. E. (2000). Exclusion of golgi residents from transport vesicles budding from Golgi cisternae in intact cells. J Cell Biol *150*, 1263-70.

Orci, L., Glick, B. S., and Rothman, J. E. (1986). A new type of coated vesicular carrier that appears not to contain clathrin: its possible role in protein transport within the Golgi stack. Cell *46*, 171-84.

Orci, L., Perrelet, A., and Rothman, J. E. (1998). Vesicles on strings: morphological evidence for processive transport within the Golgi stack. Proc Natl Acad Sci U S A *95*, 2279-83.

Orci, L., Ravazzola, M., Volchuk, A., Engel, T., Gmachl, M., Amherdt, M., Perrelet, A., Sollner, T. H., and Rothman, J. E. (2000). Anterograde flow of cargo across the golgi stack potentially mediated via bidirectional "percolating" COPI vesicles. Proc Natl Acad Sci U S A *97*, 10400-5.

Orci, L., Stamnes, M., Ravazzola, M., Amherdt, M., Perrelet, A., Sollner, T. H., and Rothman, J. E. (1997). Bidirectional transport by distinct populations of COPI-coated vesicles. Cell *90*, 335-49.

Ostermann, J., Orci, L., Tani, K., Amherdt, M., Ravazzola, M., Elazar, Z., and Rothman, J. E. (1993). Stepwise assembly of functionally active transport vesicles. Cell *75*, 1015-25.

Palmer, D. J., Helms, J. B., Beckers, C. J., Orci, L., and Rothman, J. E. (1993). Binding of coatomer to Golgi membranes requires ADP-ribosylation factor. J Biol Chem *268*, 12083-9.

Parichy, D. M., Mellgren, E. M., Rawls, J. F., Lopes, S. S., Kelsh, R. N., and Johnson, S. L. (2000). Mutational analysis of endothelin receptor b1 (rose) during neural crest and pigment pattern development in the zebrafish danio rerio [In Process Citation]. Dev Biol *227*, 294-306.

Parichy, D. M., Ransom, D. G., Paw, B., Zon, L. I., and Johnson, S. L. (2000). An orthologue of the kit-related gene fms is required for development of neural crest-derived xanthophores and a subpopulation of adult melanocytes in the zebrafish, Danio rerio. Development *127*, 3031-44.

Parichy, D. M., Rawls, J. F., Pratt, S. J., Whitfield, T. T., and Johnson, S. L. (1999). Zebrafish sparse corresponds to an orthologue of c-kit and is required for the morphogenesis of a subpopulation of melanocytes, but is not essential for hematopoiesis or primordial germ cell development. Development *126*, 3425-36.

Paschal, B. M., Holzbaur, E. L., Pfister, K. K., Clark, S., Meyer, D. I., and Vallee, R. B. (1993). Characterization of a 50-kDa polypeptide in cytoplasmic dynein preparations reveals a complex with p150GLUED and a novel actin. J Biol Chem *268*, 15318-23.

Pavel, J., Harter, C., and Wieland, F. T. (1998). Reversible dissociation of coatomer: functional characterization of a beta/delta-coat protein subcomplex. Proc Natl Acad Sci U S A *95*, 2140-5.

Peng, Z. G., Calvert, I., Clark, J., Helman, L., Kahn, R., and Kung, H. F. (1989). Molecular cloning, sequence analysis and mRNA expression of human ADP-ribosylation factor. Biofactors *2*, 45-9.

Pettway, Z., Domowicz, M., Schwartz, N. B., and Bronner-Fraser, M. (1996). Age-dependent inhibition of neural crest migration by the notochord correlates with alterations in the S103L chondroitin sulfate proteoglycan. Exp Cell Res *225*, 195-206.

Pettway, Z., Guillory, G., and Bronner-Fraser, M. (1990). Absence of neural crest cells from the region surrounding implanted notochords in situ. Dev Biol *142*, 335-45.

Peyroche, A., Antonny, B., Robineau, S., Acker, J., Cherfils, J., and Jackson, C. L. (1999). Brefeldin A acts to stabilize an abortive ARF-GDP-Sec7 domain protein complex: involvement of specific residues of the Sec7 domain. Mol Cell *3*, 275-85.

Pfanner, N., Orci, L., Glick, B. S., Amherdt, M., Arden, S. R., Malhotra, V., and Rothman, J. E. (1989). Fatty acyl-coenzyme A is required for budding of transport vesicles from Golgi cisternae. Cell *59*, 95-102.

Pfeffer, S. R. (1999). Transport-vesicle targeting: tethers before SNAREs. Nat Cell Biol *1*, E17-22.

Placzek, M., Dodd, J., and Jessell, T. M. (2000). Discussion point. The case for floor plate induction by the notochord. Curr Opin Neurobiol *10*, 15-22.

Placzek, M., Jessell, T. M., and Dodd, J. (1993). Induction of floor plate differentiation by contact-dependent, homeogenetic signals. Development *117*, 205-18.

Placzek, M., Tessier-Lavigne, M., Yamada, T., Jessell, T., and Dodd, J. (1990). Mesodermal control of neural cell identity: floor plate induction by the notochord. Science *250*, 985-8.

Placzek, M., Yamada, T., Tessier-Lavigne, M., Jessell, T., and Dodd, J. (1991). Control of dorsoventral pattern in vertebrate neural development: induction and polarizing properties of the floor plate. Development *Suppl*, 105-22.

Poncet, C., Soula, C., Trousse, F., Kan, P., Hirsinger, E., Pourquie, O., Duprat, A. M., and Cochard, P. (1996). Induction of oligodendrocyte progenitors in the trunk neural tube by ventralizing signals: effects of notochord and floor plate grafts, and of sonic hedgehog. Mech Dev *60*, 13-32.

Postlethwait, J. H., Johnson, S. L., Midson, C. N., Talbot, W. S., Gates, M., Ballinger, E. W., Africa, D., Andrews, R., Carl, T., Eisen, J. S., and et al. (1994). A genetic linkage map for the zebrafish. Science *264*, 699-703.

Postlethwait, J. H., and Talbot, W. S. (1997). Zebrafish genomics: from mutants to genes. Trends Genet *13*, 183-90.

Postlethwait, J. H., Yan, Y. L., Gates, M. A., Horne, S., Amores, A., Brownlie, A., Donovan, A., Egan, E. S., Force, A., Gong, Z., Goutel, C., Fritz, A., Kelsh, R., Knapik, E., Liao, E., Paw, B., Ransom, D., Singer, A., Thomson, M., Abduljabbar, T. S., Yelick,

P., Beier, D., Joly, J. S., Larhammar, D., Rosa, F., and et al. (1998). Vertebrate genome evolution and the zebrafish gene map. Nat Genet *18*, 345-9.

Pourquie, O., Coltey, M., Teillet, M. A., Ordahl, C., and Le Douarin, N. M. (1993). Control of dorsoventral patterning of somitic derivatives by notochord and floor plate. Proc Natl Acad Sci U S A *90*, 5242-6.

Presley, J. F., Cole, N. B., Schroer, T. A., Hirschberg, K., Zaal, K. J., and Lippincott-Schwartz, J. (1997). ER-to-Golgi transport visualized in living cells. Nature *389*, 81-5.

Pringle, N. P., Yu, W. P., Guthrie, S., Roelink, H., Lumsden, A., Peterson, A. C., and Richardson, W. D. (1996). Determination of neuroepithelial cell fate: induction of the oligodendrocyte lineage by ventral midline cells and sonic hedgehog. Dev Biol *177*, 30-42.

Randazzo, P. A., Yang, Y. C., Rulka, C., and Kahn, R. A. (1993). Activation of ADP-ribosylation factor by Golgi membranes. Evidence for a brefeldin A- and protease-sensitive activating factor on Golgi membranes. J Biol Chem *268*, 9555-63.

Rapoport, T. A., Jungnickel, B., and Kutay, U. (1996). Protein transport across the eukaryotic endoplasmic reticulum and bacterial inner membranes. Annu Rev Biochem *65*, 271-303.

Rassart, E., Bedirian, A., Do Carmo, S., Guinard, O., Sirois, J., Terrisse, L., and Milne, R. (2000). Apolipoprotein D. Biochim Biophys Acta *1482*, 185-98.

Rebagliati, M. R., Toyama, R., Haffter, P., and Dawid, I. B. (1998). cyclops encodes a nodal-related factor involved in midline signaling. Proc Natl Acad Sci U S A *95*, 9932-7.

Reinhard, C., Harter, C., Bremser, M., Brugger, B., Sohn, K., Helms, J. B., and Wieland, F. (1999). Receptor-induced polymerization of coatomer. Proc Natl Acad Sci U S A *96*, 1224-8.

Ring, C., Hassell, J., and Halfter, W. (1996). Expression pattern of collagen IX and potential role in the segmentation of the peripheral nervous system. Dev Biol *180*, 41-53.

Rogalski, A. A., Bergmann, J. E., and Singer, S. J. (1984). Effect of microtubule assembly status on the intracellular processing and surface expression of an integral protein of the plasma membrane. J Cell Biol *99*, 1101-9.

Rothman, J. E., and Wieland, F.T. (1996). Protein Sorting by Transport Vesicles. Science *272*, 227-262.

Ruiz i Altaba, A. (1996). Coexpression of HNF-3 beta and Isl-1/2 and mixed distribution of ventral cell types in the early neural tube. Int J Dev Biol *40*, 1081-8.

Sacksteder, K. A., Jones, J. M., South, S. T., Li, X., Liu, Y., and Gould, S. J. (2000). PEX19 binds multiple peroxisomal membrane proteins, is predominantly cytoplasmic, and is required for peroxisome membrane synthesis. J Cell Biol *148*, 931-44.

Sampath, K., Rubinstein, A. L., Cheng, A. M., Liang, J. O., Fekany, K., Solnica-Krezel, L., Korzh, V., Halpern, M. E., and Wright, C. V. (1998). Induction of the zebrafish ventral brain and floorplate requires cyclops/nodal signalling. Nature *395*, 185-9.

Saraste, J., and Kuismanen, E. (1992). Pathways of protein sorting and membrane traffic between the rough endoplasmic reticulum and the Golgi complex. Semin Cell Biol *3*, 343-55.

Saude, L., Woolley, K., Martin, P., Driever, W., and Stemple, D. L. (2000). Axis-inducing activities and cell fates of the zebrafish organizer. Development *127*, 3407-17.

Scales, S. J., Gomez, M., and Kreis, T. E. (2000). Coat proteins regulating membrane traffic. Int Rev Cytol *195*, 67-144.

Scales, S. J., Pepperkok, R., and Kreis, T. E. (1997). Visualization of ER-to-Golgi transport in living cells reveals a sequential mode of action for COPII and COPI. Cell *90*, 1137-48.

Schauerte, H. E., van Eeden, F. J., Fricke, C., Odenthal, J., Strahle, U., and Haffter, P. (1998). Sonic hedgehog is not required for the induction of medial floor plate cells in the zebrafish. Development *125*, 2983-93.

Schekman, R., and Orci, L. (1996). Coat proteins and vesicle budding. Science *271*, 1526-33.

Scheller, R. H. (1995). Membrane trafficking in the presynaptic nerve terminal. Neuron *14*, 893-7.

Schimmoller, F., Simon, I., and Pfeffer, S. R. (1998). Rab GTPases, directors of vesicle docking. J Biol Chem *273*, 22161-4.

Schoenwolf, G. C., Bortier, H., and Vakaet, L. (1989). Fate mapping the avian neural plate with quail/chick chimeras: origin of prospective median wedge cells. J Exp Zool *249*, 271-8.

Schreeb, K. H., Groth, G., Sachsse, W., and Freundt, K. J. (1993). The karyotype of the zebrafish (Brachydanio rerio). J Exp Anim Sci *36*, 27-31.

Schroer, T. A. (1996). Structure and function of dynactin. Semin Cell Develop Biol *7*, 321-328.

Schulte-Merker, S., Hammerschmidt, M., Beuchle, D., Cho, K. W., De Robertis, E. M., and Nusslein-Volhard, C. (1994). Expression of zebrafish goosecoid and no tail gene products in wild- type and mutant no tail embryos. Development *120*, 843-52.

Schulte-Merker, S., van Eeden, F. J., Halpern, M. E., Kimmel, C. B., and Nusslein-Volhard, C. (1994). no tail (ntl) is the zebrafish homologue of the mouse T (Brachyury) gene. Development *120*, 1009-15.

Sciaky, N., Presley, J., Smith, C., Zaal, K. J., Cole, N., Moreira, J. E., Terasaki, M., Siggia, E., and Lippincott-Schwartz, J. (1997). Golgi tubule traffic and the effects of brefeldin A visualized in living cells. J Cell Biol *139*, 1137-55.

Seelig, H. P., Schranz, P., Schroter, H., Wiemann, C., Griffiths, G., and Renz, M. (1994). Molecular genetic analyses of a 376-kilodalton Golgi complex membrane protein (giantin). Mol Cell Biol *14*, 2564-76.

Serafini, T., Orci, L., Amherdt, M., Brunner, M., Kahn, R. A., and Rothman, J. E. (1991). ADP-ribosylation factor is a subunit of the coat of Golgi-derived COP- coated vesicles: a novel role for a GTP-binding protein. Cell *67*, 239-53.

Serbedzija, G. N., Chen, J. N., and Fishman, M. C. (1998). Regulation in the heart field of zebrafish. Development *125*, 1095-101.

Shimizu, T., Yamanaka, Y., Ryu, S. L., Hashimoto, H., Yabe, T., Hirata, T., Bae, Y. K., Hibi, M., and Hirano, T. (2000). Cooperative roles of Bozozok/Dharma and Nodal-related proteins in the formation of the dorsal organizer in zebrafish. Mech Dev *91*, 293-303.

Sirotkin, H. I., Gates, M. A., Kelly, P. D., Schier, A. F., and Talbot, W. S. (2000). Fast1 is required for the development of dorsal axial structures in zebrafish. Curr Biol *10*, 1051-4.

Sohn, K., Orci, L., Ravazzola, M., Amherdt, M., Bremser, M., Lottspeich, F., Fiedler, K., Helms, J. B., and Wieland, F. T. (1996). A major transmembrane protein of Golgi-derived COPI-coated vesicles involved in coatomer binding. J Cell Biol *135*, 1239-48.

Solnica-Krezel, L., Stemple, D. L., and Driever, W. (1995). Transparent things: cell fates and cell movements during early embryogenesis of zebrafish. Bioessays *17*, 931-9.

Sonnichsen, B., Lowe, M., Levine, T., Jamsa, E., Dirac-Svejstrup, B., and Warren, G. (1998). A role for giantin in docking COPI vesicles to Golgi membranes. J Cell Biol *140*, 1013-21.

Sonnichsen, B., Watson, R., Clausen, H., Misteli, T., and Warren, G. (1996). Sorting by COP I-coated vesicles under interphase and mitotic conditions. J Cell Biol *134*, 1411-25.

Stemple, D. L., Mahanthappa, N. K., and Anderson, D. J. (1988). Basic FGF induces neuronal differentiation, cell division, and NGF dependence in chromaffin cells: a sequence of events in sympathetic development. Neuron *1*, 517-25.

Stemple, D. L., Solnica-Krezel, L., Zwartkruis, F., Neuhauss, S. C., Schier, A. F., Malicki, J., Stainier, D. Y., Abdelilah, S., Rangini, Z., Mountcastle-Shah, E., and Driever, W. (1996). Mutations affecting development of the notochord in zebrafish. Development *123*, 117-28.

Stenbeck, G., Harter, C., Brecht, A., Herrmann, D., Lottspeich, F., Orci, L., and Wieland, F. T. (1993). beta'-COP, a novel subunit of coatomer. Embo J *12*, 2841-5.

Stern, C. D., Artinger, K. B., and Bronner-Fraser, M. (1991). Tissue interactions affecting the migration and differentiation of neural crest cells in the chick embryo. Development *113*, 207-16.

Stickney, H. L., Barresi, M. J., and Devoto, S. H. (2000). Somite development in zebrafish. Dev Dyn *219*, 287-303.

Stockdale, F. E., Nikovits, W., Jr., and Christ, B. (2000). Molecular and cellular biology of avian somite development. Dev Dyn *219*, 304-21.

Strahle, U., Blader, P., and Ingham, P. W. (1996). Expression of axial and sonic hedgehog in wildtype and midline defective zebrafish embryos. Int J Dev Biol *40*, 929-40.

Strahle, U., Jesuthasan, S., Blader, P., Garcia-Villalba, P., Hatta, K., and Ingham, P. W. (1997). one-eyed pinhead is required for development of the ventral midline of the zebrafish (Danio rerio) neural tube. Genes Funct *1*, 131-48.

Streisinger, G., Singer, F., Walker, C., Knauber, D., and Dower, N. (1986). Segregation analyses and gene-centromere distances in zebrafish. Genetics *112*, 311-9.

Szafer, E., Pick, E., Rotman, M., Zuck, S., Huber, I., and Cassel, D. (2000). Role of coatomer and phospholipids in GTPase-activating protein- dependent hydrolysis of GTP by ADP-ribosylation factor-1. J Biol Chem *275*, 23615-9.

Talbot, W. S., Trevarrow, B., Halpern, M. E., Melby, A. E., Farr, G., Postlethwait, J. H., Jowett, T., Kimmel, C. B., and Kimelman, D. (1995). A homeobox gene essential for zebrafish notochord development. Nature *378*, 150-7.

Tanigawa, G., Orci, L., Amherdt, M., Ravazzola, M., Helms, J. B., and Rothman, J. E. (1993). Hydrolysis of bound GTP by ARF protein triggers uncoating of Golgi- derived COP-coated vesicles. J Cell Biol *123*, 1365-71.

Teillet, M. A., Lapointe, F., and Le Douarin, N. M. (1998). The relationships between notochord and floor plate in vertebrate development revisited. Proc Natl Acad Sci U S A *95*, 11733-8.

Teillet, M. A., Watanabe, Y., Jeffs, P., Duprez, D., Lapointe, F., and Le Douarin, N. M. (1998). Sonic hedgehog is required for survival of both myogenic and chondrogenic somitic lineages. Development *125*, 2019-30.

Thisse, C., Thisse, B., Schilling, T. F., and Postlethwait, J. H. (1993). Structure of the zebrafish snail1 gene and its expression in wild-type, spadetail and no tail mutant embryos. Development *119*, 1203-15.

Thyberg, J., and Moskalewski, S. (1985). Microtubules and the organization of the Golgi complex. Exp Cell Res *159*, 1-16.

Timpl, R., and Brown, J. C. (1994). The laminins. Matrix Biol. *14*, 275-81.

Vaisberg, E. A., Grissom, P. M., and McIntosh, J. R. (1996). Mammalian cells express three distinct dynein heavy chains that are localized to different cytoplasmic organelles. J Cell Biol *133*, 831-42.

van Straaten, H. W., and Hekking, J. W. (1991). Development of floor plate, neurons and axonal outgrowth pattern in the early spinal cord of the notochord-deficient chick embryo. Anat Embryol *184*, 55-63.

van Straaten, H. W., Hekking, J. W., Wiertz-Hoessels, E. J., Thors, F., and Drukker, J. (1988). Effect of the notochord on the differentiation of a floor plate area in the neural tube of the chick embryo. Anat Embryol *177*, 317-24.

Vaughan, K. T., and Vallee, R. B. (1995). Cytoplasmic dynein binds dynactin through a direct interaction between the intermediate chains and p150Glued. J Cell Biol *131*, 1507-16.

Volchuk, A., Amherdt, M., Ravazzola, M., Brugger, B., Rivera, V. M., Clackson, T., Perrelet, A., Sollner, T. H., Rothman, J. E., and Orci, L. (2000). Megavesicles implicated in the rapid transport of intracisternal aggregates across the Golgi stack. Cell *102*, 335-48.

Waterman-Storer, C. M., Karki, S., and Holzbaur, E. L. (1995). The p150Glued component of the dynactin complex binds to both microtubules and the actin-related protein centractin (Arp-1). Proc Natl Acad Sci U S A *92*, 1634-8.

Waters, M. G., Clary, D. O., and Rothman, J. E. (1992). A novel 115-kD peripheral membrane protein is required for intercisternal transport in the Golgi stack. J Cell Biol *118*, 1015-26.

Waters, M. G., Serafini, T., and Rothman, J. E. (1991). 'Coatomer': a cytosolic protein complex containing subunits of non- clathrin-coated Golgi transport vesicles. Nature *349*, 248-51.

Webster, M. T., Rozycka, M., Sara, E., Davis, E., Smalley, M., Young, N., Dale, T. C., and Wooster, R. (2000). Sequence variants of the axin gene in breast, colon, and other cancers: an analysis of mutations that interfere with GSK3 binding. Genes Chromosomes Cancer *28*, 443-53.

White, J., Johannes, L., Mallard, F., Girod, A., Grill, S., Reinsch, S., Keller, P., Tzschaschel, B., Echard, A., Goud, B., and Stelzer, E. H. (1999). Rab6 coordinates a novel Golgi to ER retrograde transport pathway in live cells. J Cell Biol *147*, 743-60.

Whitney, J. A., Gomez, M., Sheff, D., Kreis, T. E., and Mellman, I. (1995). Cytoplasmic coat proteins involved in endosome function. Cell *83*, 703-13.

Wiertz-Hoessels, E. L., Hara, K., Hekking, J. W., van Straaten, H. W., Thors, F., and Drukker, J. (1987). Differentiation of gut endoderm in dependence of the notochord. Anat Embryol *176*, 337-43.

Wittke, S., Dunnwald, M., and Johnsson, N. (2000). Sec62p, a component of the endoplasmic reticulum protein translocation machinery, contains multiple binding sites for the Sec-complex. Mol Biol Cell *11*, 3859-71.

Wodarz, A., and Nusse, R. (1998). Mechanisms of Wnt signaling in development. Annu Rev Cell Dev Biol *14*, 59-88.

Woo, K., Shih, J., and Fraser, S. E. (1995). Fate maps of the zebrafish embryo. Curr Opin Genet Dev *5*, 439-43.

Wu, W. J., Erickson, J. W., Lin, R., and Cerione, R. A. (2000). The gamma-subunit of the coatomer complex binds Cdc42 to mediate transformation. Nature *405*, 800-4.

Yamada, T., Placzek, M., Tanaka, H., Dodd, J., and Jessell, T. M. (1991). Control of cell pattern in the developing nervous system: polarizing activity of the floor plate and notochord. Cell *64*, 635-47.

Yan, Y. L., Hatta, K., Riggleman, B., and Postlethwait, J. H. (1995). Expression of a type II collagen gene in the zebrafish embryonic axis. Dev Dyn *203*, 363-76.

Yost, H. J. (1990). Inhibition of proteoglycan synthesis eliminates left-right asymmetry in Xenopus laevis cardiac looping. Development *110*, 865-74.

Yost, H. J. (1992). Regulation of vertebrate left-right asymmetries by extracellular matrix. Nature *357*, 158-61.

Zeng, L., Fagotto, F., Zhang, T., Hsu, W., Vasicek, T. J., Perry, W. L., 3rd, Lee, J. J., Tilghman, S. M., Gumbiner, B. M., and Costantini, F. (1997). The mouse Fused locus encodes Axin, an inhibitor of the Wnt signaling pathway that regulates embryonic axis formation. Cell *90*, 181-92.

Zhang, J., Talbot, W. S., and Schier, A. F. (1998). Positional cloning identifies zebrafish one-eyed pinhead as a permissive EGF-related ligand required during gastrulation. Cell *92*, 241-51.

Zhao, L., Helms, J. B., Brugger, B., Harter, C., Martoglio, B., Graf, R., Brunner, J., and Wieland, F. T. (1997). Direct and GTP-dependent interaction of ADP ribosylation factor 1 with coatomer subunit beta. Proc Natl Acad Sci U S A *94*, 4418-23.

Zhao, L., Helms, J. B., Brunner, J., and Wieland, F. T. (1999). GTP-dependent binding of ADP-ribosylation factor to coatomer in close proximity to the binding site for dilysine retrieval motifs and p23. J Biol Chem *274*, 14198-203.

Zheng, Y., Glaven, J. A., Wu, W. J., and Cerione, R. A. (1996). Phosphatidylinositol 4,5-bisphosphate provides an alternative to guanine nucleotide exchange factors by stimulating the dissociation of GDP from Cdc42Hs. J Biol Chem *271*, 23815-9.